



**CALIFORNIA  
ENERGY COMMISSION**



Energy Research and Development Division

## **FINAL PROJECT REPORT**

# **Climate Appropriate Innovations for Variable Refrigerant Flow Systems**

**Integrated Indirect Evaporative Cooling Adaptive  
Controls and Advanced Refrigerants**

**Gavin Newsom, Governor  
April 2021 | CEC-500-2021-028**

**PREPARED BY:**

**Primary Authors:**

Omar Siddiqui<sup>1</sup>

Mukesh Khattar, Ph.D.<sup>1</sup>

Ryan Berg<sup>1</sup>

Ram Narayanamurthy<sup>1</sup>

Nelson Dichter<sup>2</sup>

Edwin Huestis<sup>3</sup>

<sup>1</sup>Electric Power Research Institute

3420 Hillview Ave., Palo Alto, CA 94304 (<http://www.epri.com>)

<sup>2</sup>University of California, Davis

1 Shields Ave., Davis, CA 95616 ([www.ucdavis.edu](http://www.ucdavis.edu))

<sup>3</sup>Pacific Gas and Electric Company, Applied Technology Services

3400 Crow Canyon Road, San Ramon, CA 94583 ([www.pge.com](http://www.pge.com))

**Contract Number:** EPC-15-004

**PREPARED FOR:**

California Energy Commission

Bradley Meister, Ph.D., P.E.

**Project Manager**

Virginia Lew

**Office Manager**

**ENERGY EFFICIENCY RESEARCH OFFICE**

Laurie ten Hope

**Deputy Director**

**ENERGY RESEARCH AND DEVELOPMENT DIVISION**

Drew Bohan

**Executive Director**

**DISCLAIMER**

This report was prepared as the result of work sponsored by the California Energy Commission. It does not necessarily represent the views of the Energy Commission, its employees or the State of California. The Energy Commission, the State of California, its employees, contractors and subcontractors make no warranty, express or implied, and assume no legal liability for the information in this report; nor does any party represent that the uses of this information will not infringe upon privately owned rights. This report has not been approved or disapproved by the California Energy Commission nor has the California Energy Commission passed upon the accuracy or adequacy of the information in this report.

## **ACKNOWLEDGEMENTS**

The project team would like to thank the California Energy Commission Contract Agreement Manager Bradley Meister, for his guidance and assistance throughout this project. The Electric Power Research Institute recognizes and appreciates the contributions of major project subcontractors: the University of California, Davis Western Cooling Efficiency Center (Nelson Dichter and Jose Garcia), and Pacific Gas and Electric Company's Advanced Technology Services laboratory (Edwin Huestis, Yi Qu, and Michael Daukoru). The team extends special thanks to its demonstration partners for their cooperation throughout the planning, installation, and commissioning phases at their respective sites.

This report is dedicated to the memory of Mukesh Khattar, a dear Electric Power Research Institute colleague who passed away on February 13, 2020. Mukesh was a technical expert in heating, ventilation, and air-conditioning systems who contributed immensely to this project and was admired and beloved by his colleagues.

## PREFACE

The California Energy Commission's (CEC) Energy Research and Development Division supports energy research and development programs to spur innovation in energy efficiency, renewable energy and advanced clean generation, energy-related environmental protection, energy transmission and distribution and transportation.

In 2012, the Electric Program Investment Charge (EPIC) was established by the California Public Utilities Commission to fund public investments in research to create and advance new energy solutions, foster regional innovation and bring ideas from the lab to the marketplace. The CEC and the state's three largest investor-owned utilities—Pacific Gas and Electric Company, San Diego Gas & Electric Company and Southern California Edison Company—were selected to administer the EPIC funds and advance novel technologies, tools, and strategies that provide benefits to their electric ratepayers.

The CEC is committed to ensuring public participation in its research and development programs that promote greater reliability, lower costs, and increase safety for the California electric ratepayer and include:

- Providing societal benefits.
- Reducing greenhouse gas emission in the electricity sector at the lowest possible cost.
- Supporting California's loading order to meet energy needs first with energy efficiency and demand response, next with renewable energy (distributed generation and utility scale), and finally with clean, conventional electricity supply.
- Supporting low-emission vehicles and transportation.
- Providing economic development.
- Using ratepayer funds efficiently.

*Climate Appropriate Innovations for Variable Refrigerant Flow* is the final report for the Climate Appropriate Innovations for Variable Refrigerant Flow Systems project (Contract Number: EPC 15-004) conducted by the Electric Power Research Institute with support from the University of California, Davis and Pacific Gas and Electric Company. The information from this project contributes to the Energy Research and Development Division's EPIC Program.

For more information about the Energy Research and Development Division, please visit the CEC's research website ([www.energy.ca.gov/research/](http://www.energy.ca.gov/research/)) or contact ERDD@energy.ca.gov.

# ABSTRACT

This project demonstrated the application of a hybrid space conditioning system that integrates variable refrigerant flow with indirect evaporative cooling as a more energy-efficient alternative to the rooftop units prevalent in small- to medium-sized commercial buildings throughout California. While variable refrigerant flow has been demonstrated as an energy-efficient space conditioning technology, one of its inherent challenges is limited ventilation capacity. This hybrid configuration uses indirect evaporative cooling as a dedicated outside air system to satisfy ventilation requirements, eliminate outside air loads during cooling, and reduce heating loads as an air-air heat exchanger.

Field demonstrations at three California sites sought to validate energy savings relative to modeled baseline performance, as well as peak load reduction, demand responsiveness, and maintained or enhanced occupant comfort.

A key advancement of this project was the development of an integrated system controller that optimizes operation of the combined variable refrigerant flow and indirect evaporative cooling configuration through zonal occupancy sensing and learned building behavior. Control sequence algorithms were based on governing logic informed by adaptive capabilities and response to inputs such as ambient weather conditions, humidity control, occupancy, and occupant comfort preferences.

This project also advanced modeling of variable refrigerant flow, indirect evaporated cooling, and hybrid variable refrigerant flow-indirect evaporative cooling systems by adding associated modules to the EnergyPlus building simulation software. This modeling work, which was calibrated with results from the field demonstrations, has developed and refined EnergyPlus for future modeling of these emerging space conditioning technologies and configurations.

Finally, this project featured laboratory testing of three leading natural refrigerants – propane, carbon dioxide, and ammonia – as sustainable, low global warming potential alternatives to traditional refrigerants. Novel heat pump and chiller equipment featuring these natural refrigerants were tested in three different laboratories, demonstrating energy-efficient performance coupled with low global warming potential.

**Keywords:** Variable refrigerant flow, indirect evaporative cooling, natural refrigerants, low global warming potential refrigerants, climate-appropriate heating, ventilation, and air conditioning.

Please use the following citation for this report:

Siddiqui, Omar, Mukesh Khattar, Ram Narayanamurthy, Ryan Berg, Edwin Huestis, and Nelson Dichter. 2021. *Climate Appropriate Innovations for Variable Refrigerant Flow Systems*. California Energy Commission. Publication Number: CEC-500-2021-028.



# TABLE OF CONTENTS

	Page
ACKNOWLEDGEMENTS.....	i
PREFACE .....	ii
ABSTRACT .....	iii
EXECUTIVE SUMMARY .....	1
Introduction.....	1
Project Purpose.....	2
Project Approach.....	2
Project Results.....	3
Demonstration of Variable Refrigerant Flow Plus Indirect Evaporative Cooling Hybrid System .....	3
Testing of Natural Refrigerant Systems .....	3
Technology Transfer (Advancing Research to Market) .....	4
Benefits to California’s Ratepayers and Environment.....	4
Conclusions.....	5
CHAPTER 1: Introduction .....	7
Background .....	7
Project Objective.....	8
CHAPTER 2: Project Approach .....	10
Approach: Variable Refrigerant Flow Plus Indirect Evaporative Cooling Hybrid System Demonstration .....	10
Technical Barriers.....	11
Nontechnical Barriers.....	11
Approach: Laboratory Testing of Natural Refrigerants.....	12
Technical Barriers.....	12
Nontechnical Barriers.....	13
CHAPTER 3: Modeling .....	14
Modeling Method.....	14
Modeling Results for Western Cooling Efficiency Center Site.....	15
Modeling Results for Del Taco Site .....	23
Modeling Results for Energy Innovation Center Site.....	27
Model Calibration .....	27
Calibration Process .....	27

Calibration Results.....	28
Improving Future Modeling of Integrated Variable Refrigerant Flow+Indirect Evaporative Cooling Systems.....	30
Ducting.....	30
Ventilation .....	30
Evaporative Cooling.....	30
Variable Refrigerant Flow .....	30
Calibration Tools.....	31
Runtime Errors.....	31
CHAPTER 4: Field Demonstration of Variable Refrigerant Flow Indirect Evaporative Cooling Systems .....	32
Site Selection .....	32
Western Cooling Efficiency Center Site.....	33
Del Taco Site.....	34
Energy Innovation Center Site.....	35
Controller Development .....	37
Economizer-Only Mode to Provide “Free-Cooling” .....	38
Indirect Evaporative Cooling Mode.....	38
Variable Refrigerant Flow Only Mode .....	39
Variable Refrigerant Flow + Indirect Evaporative Cooling Mode .....	39
Western Cooling Efficiency Center Site.....	42
Instrumentation and Baseline Measurement.....	42
Installation and Commissioning Process .....	45
Field Results.....	47
Del Taco Site .....	51
Baseline Determination .....	51
Process Description .....	51
Field Results.....	54
Energy Innovation Center Site.....	59
Baseline Determination .....	59
Process Description .....	60
Field Results.....	61
CHAPTER 5: Laboratory Testing of Alternative Refrigerants .....	62
Background .....	62
Bundgaard Propane (R290) Chiller .....	63
Equipment Information .....	63



Testing Plan .....	66
Testing Results.....	74
Supplemental Modeling.....	77
Results .....	83
CTS Custom Carbon Dioxide (R744) Heat Pump .....	86
Equipment Information .....	86
Testing Plan .....	90
Testing Results.....	92
Ammonia (R717) Heat Pump.....	95
Conclusions and Recommended Next Steps .....	101
CHAPTER 6: Knowledge Transfer Activities .....	102
Variable Refrigerant Flow + Indirect Evaporative Cooling Demonstration .....	102
Natural Refrigerant Testing .....	103
CHAPTER 7: Conclusions and Recommendations.....	104
Variable Refrigerant Flow + Indirect Evaporative Cooling Demonstration .....	104
Natural Refrigerant Testing .....	104
LIST OF ACRONYMS.....	108

## **LIST OF FIGURES**

	Page
Figure 1: Modeled Annual Electricity Consumption of Systems at Western Cooling Efficiency Center Site .....	15
Figure 2: Modeled Summer Peak Demand of Systems at Western Cooling Efficiency Center Site .....	16
Figure 3: Modeled Annual Demand Profile of Systems at Western Cooling Efficiency Center Site (Watts) .....	17
Figure 4: Modeled Electric Heating Consumption per California Climate Zone.....	18
Figure 5: Modeled Unmet Set Point Heating Hours per California Climate Zone .....	19
Figure 6: Modeled Cooling Electricity Use in 16 California Climate Zones.....	20
Figure 7: Modeled Unmet Set Point Cooling Hours per California Climate Zone.....	20
Figure 8: Modeled Annual Electricity Use per Heating, Ventilation, and Air Conditioning System per Climate Zone .....	21
Figure 9: Modeled Variable Refrigerant Flow + Indirect Evaporative Cooling Annual Energy and Water Savings per Climate Zone .....	22

Figure 10: Variable Refrigerant Flow + Indirect Evaporative Cooling Energy Savings by Climate Zone, Normalized by Water Use .....	22
Figure 11: Modeled Share of Energy Savings from Indirect Evaporative Cooling Economizing	23
Figure 12: Del Taco Simulated Annual Energy Use by Climate Zone .....	24
Figure 13: Del Taco Monthly Energy Use for Climate Zone 3 .....	25
Figure 14: Del Taco Carbon Impact of Avoided Gas Use by Climate Zone .....	25
Figure 15: Del Taco Unmet Cooling Hours by Setpoint, Indirect Evaporative Cooling Only ....	26
Figure 16: Model Calibration Results, Electricity Consumption – Del Taco Site .....	29
Figure 17: Rendering of Western Cooling Efficiency Center Exterior .....	33
Figure 18: Aliso Viejo Del Taco .....	35
Figure 19: Rooftop Views Del Taco Treatment (left) and Control (right) Sites .....	35
Figure 20: Energy Innovation Center Street Facing View .....	36
Figure 21: Energy Innovation Center Conditioned Zones for Variable Refrigerant Flow Retrofit.....	36
Figure 22: Incumbent Heating, Ventilation, and Air Conditioning Equipment at Energy Innovation Center, Building Automation View .....	37
Figure 23: Indirect Evaporative Cooler Schematic Diagram .....	39
Figure 24: Control System Architecture .....	40
Figure 25: Automatic Demand Response Control Architecture .....	41
Figure 26: Open Standards Communications for Control of Components.....	42
Figure 27: Indirect Evaporative Cooling Insulated Supply Flex Duct During Construction .....	46
Figure 28: Completed Indirect Evaporative Cooling Supply and Exhaust Connections .....	46
Figure 29: Completed Indirect Evaporative Cooling Inlet Ducting .....	47
Figure 30: Outdoor Dry-Bulb Temperature on Similar Days.....	48
Figure 31: Power Draw on Similar Days, Pre-Retrofit and Post-Retrofit .....	49
Figure 32: Total Heating, Ventilation, and Air Conditioning Energy Consumption on Similar Days .....	50
Figure 33: Variable Refrigerant Flow and Indirect Evaporative Cooling Units Installed on Roof of Del Taco.....	52
Figure 34: Data Monitoring Layout at Del Taco Treatment Site .....	53
Figure 35: Data Monitoring Layout at Del Taco Control Site .....	54
Figure 36: Monthly Cumulative Heating, Ventilation, and Air Conditioning Energy Use, Del Taco Sites .....	55

Figure 37: Del Taco Cooling Season Average Daily Heating, Ventilation, and Air Conditioning Demand Profile .....	56
Figure 38: Del Taco Summer Peak Day Heating, Ventilation, and Air Conditioning Demand Profile .....	57
Figure 39: Del Taco Heating Season Average Daily Demand Profile .....	58
Figure 40: Del Taco Winter Peak Day Heating, Ventilation, and Air Conditioning Demand Profile .....	59
Figure 41: Energy Innovation Center Variable Refrigerant Flow Installation Diagram .....	60
Figure 42: Hydronic Heat Pump Cooling (Left) and Heating (Right) Mode .....	64
Figure 43: ClimaCheck Portable Performance Analyzer and Online Platform .....	65
Figure 44: Bundgaard R290 Chiller Piping and Instrumentation Diagram .....	66
Figure 45: Bundgaard R290 Chiller Cooling Mode Factory Acceptance Test of Coefficient of Performance Values .....	67
Figure 46: Bundgaard R290 Chiller Factory Acceptance Testing Cooling Mode Test Capacity Values .....	67
Figure 47: Schematic Layout for Testing Propane Refrigerant System .....	68
Figure 48: Chilled Water Feeding Condenser Side Hydronic Tempering System .....	69
Figure 49: Condenser Side Hydronic Instrumentation Schematic .....	70
Figure 50: Evaporator Side Hydronic Instrumentation Schematic.....	70
Figure 51: Coefficient of Performance and Liquid Refrigerant Temperature for Cooling Mode Tests .....	75
Figure 52: Coefficient of Performance and Vapor Refrigerant Temperature for Heating Mode Tests .....	76
Figure 53: Flow Cycles in Secondary Loop Bundgaard Refrigeration Unit .....	78
Figure 54: Example of p-h Diagram in an R290 Refrigeration System .....	79
Figure 55: Components in R290 Refrigeration System .....	79
Figure 56: Compressor Capacity Performance Map.....	81
Figure 57: Compressor Power Performance Map .....	81
Figure 58: Compressor EER Performance Map .....	82
Figure 59: Condenser Specifications .....	82
Figure 60: Evaporator Specifications.....	83
Figure 61: Capacity as Function of Outdoor Temperature .....	85
Figure 62: Efficiency as a Function of Outdoor Temperature .....	86
Figure 63: Carbon Dioxide Heat Pump and Air Flow Diagram .....	87

Figure 64: Diagram of Carbon Dioxide Heat Pump Component Locations.....	88
Figure 65: Carbon Dioxide Heat Pump Schematic and Instrumentation Locations.....	89
Figure 66: Carbon Dioxide Heat Pump Testing Facility Setup .....	90
Figure 67: Heat Rejection Chamber.....	90
Figure 68: Heat Load Chamber .....	91
Figure 69: Pressure/Enthalpy Diagram (Left) and Performance Diagram (Right).....	93
Figure 70: Cooling Conditions Test Results .....	93
Figure 71: Comparison to Other Commercially Ready R410A Systems .....	95
Figure 72: Mayekawa Sierra System at EPRI Knoxville Labs.....	96
Figure 74: Secondary Loop Configuration, Ammonia Chiller, and Carbon Dioxide Working Fluid .....	97
Figure 75: Outdoor System Fully Installed .....	97
Figure 76: Cooling Capacity vs. Time at Approximately 75°F Ambient Temperature .....	99
Figure 77: Cooling Capacity vs. Time at Approximately 86.5°F Ambient Temperature .....	100
Figure 78: Cooling Capacity & Outdoor Temperature vs. Time (High Ambient).....	100

## LIST OF TABLES

	Page
Table 1: Model Parameters.....	15
Table 2: Parameter Values for Final Generic Building Simulations.....	18
Table 3: Calibrated Modeling Parameters.....	28
Table 4: Comparison of Calibrated Model Results to Experimental Results .....	28
Table 5: Summary of Variable Refrigerant Flow + Indirect Evaporative Cooling Demonstration Sites .....	32
Table 6: Mapping of Indirect Evaporative Cooling Units to Conditioning Zones .....	37
Table 7: Total Heating, Ventilation, and Air Conditioning Energy Consumption on Similar Days .....	50
Table 8: Monthly Cumulative Energy Savings for Del Taco Site .....	55
Table 9: Bundgaard R290 Chiller Specifications.....	63
Table 10: Bill of Material in Bundgaard R290 Chiller Piping and Instrumentation Diagram .....	66
Table 11: Hydronic Heat Pump Cooling and Heating Testing Conditions .....	71
Table 12: Advanced Technology Performance Laboratory Testing Instrument List.....	72

Table 13: Bundgaard Hydronic Heat Pump Laboratory Test Results.....	74
Table 14: Measurement Uncertainty of Applied Technology Services Laboratory Test Results	76
Table 16: Bundgaard Propane System, Performance Data .....	85
Table 16: Comparison of Propane System and Simulated R410A VRF System .....	86
Table 17: List of Carbon Dioxide Heat Pump Components.....	87
Table 18: List of Sensors .....	89
Table 19: Cooling Mode Testing Conditions.....	91
Table 20: Heating Mode Testing Conditions .....	91
Table 21: System Optimization Testing Results for Cooling and Heating .....	94
Table 22: Traditional versus Ammonia/Carbon Dioxide Refrigerant Systems .....	98
Table 23: Summary of Refrigerant Testing Results .....	101
Table 24: Summary of Refrigerant Testing Results .....	105



# EXECUTIVE SUMMARY

## Introduction

Small- and medium-sized commercial buildings in California, such as office buildings, retail establishments, restaurants, and schools, are predominantly air-conditioned with packaged rooftop units. These ubiquitous rooftop units are economical and familiar for heating, ventilation, and air-conditioning (HVAC) contractors to install. However, they are inherently inefficient, suffering from significant thermal losses through leaks from ducts and cabinets, poor distribution efficacy, and low peak performance. Replacing rooftop units with more efficient space conditioning technology represents a significant opportunity for energy efficiency to help California make progress toward the goal of Senate Bill 350 (de León, Chapter 547, Statutes of 2015) to double end-use energy savings, relative to a 2015 baseline, by 2030.

Fortunately, more energy-efficient space conditioning alternatives exist on the market. Variable refrigerant flow, a type of ductless heat pump technology that flows refrigerant to indoor heat exchange units rather than blowing conditioned air through ducts, offers a particularly novel approach to achieving a high degree of energy efficiency. Indirect evaporative cooling offers an even more energy-efficient solution since it operates without using a compressor, instead passing outside air through a heat exchanger that evaporates water to cool indoor air circulated through ductwork. However, both technologies are inhibited by inherent technical limitations. Variable refrigerant flow has limited ventilation capacity, while indirect evaporative cooling has limited cooling capacity to address peak cooling demand of buildings.

Recognizing that their limitations are complementary, a hybrid solution that features the two technologies working in concert is a potentially compelling solution for energy savings. In theory, indirect evaporative cooling can provide highly energy-efficient cooling during major portions of the year, with variable refrigerant flow being activated to efficiently satisfy higher cooling demands during the warmer summer periods. Extrapolating prior tests and applications of variable refrigerant flow and indirect evaporative cooling systems separately, replacing packaged rooftop units with a combined variable refrigerant flow plus indirect evaporative cooling approach has an assumed potential to reduce energy use in these small and medium commercial segments by 30 percent to 50 percent. Rooftop units have an average economic useful life of 15 years, meaning that about one-fifteenth of building rooftop units will naturally turn over each year, representing a retrofit opportunity, not including potential early replacements of equipment.

While variable refrigerant flow plus indirect evaporative cooling is an elegant solution in theory, there has been no prior field demonstration of this technology pairing to validate energy savings, payback, and other customer benefits. Given the higher initial cost of a variable refrigerant flow plus indirect evaporative cooling combination relative to rooftop units, and the lack of familiarity among local HVAC contractors with installing and commissioning such systems, which involves a higher degree of complexity, it is doubtful that the market would start adopting this technology on its own without external intervention.

Another significant California policy goal is to reduce the use of refrigerants with high global warming potential. Therefore, conversion to HVAC systems using alternative low global warming potential refrigerants is an important component to achieving California's climate

policy objectives and aligns with California Assembly Bill 3232 (Friedman, Chapter 373, Statutes of 2018), Senate Bill 1477 (Stern, Chapter 378, Statutes of 2018), and the United States Environmental Protection Agency's mandate to phase out hydro-chlorofluorocarbons.

An added consideration is the use of natural refrigerants, which exist in nature and do not have to be synthetically produced. Although some natural refrigerants have been used in niche market applications for decades, their use is virtually absent in packaged air-conditioning systems. This conversion requires extensive testing to identify suitable refrigerants on the basis of global warming potential, thermodynamic properties that drive energy efficiency performance, compatibility with existing equipment, and safety issues such as corrosion, toxicity, and flammability.

## **Project Purpose**

The project's overall objective was — through field demonstration, laboratory testing, and energy simulation modeling — to advance technologies that can help California achieve its policy goals for energy efficiency, building decarbonization, and greenhouse gas reduction. Specifically, this project sought to demonstrate the application of a hybrid space conditioning system that integrates variable refrigerant flow with indirect evaporative cooling as a more energy-efficient alternative to rooftop units prevalent in small- to medium-sized commercial buildings throughout California. This hybrid configuration uses indirect evaporative cooling as a dedicated outside air system to satisfy ventilation requirements, eliminate outside air loads during cooling, and reduce heating loads as an air-air heat exchanger.

Field demonstrations at three sites — a multipurpose office building in Northern California; a quick-serve restaurant, Del Taco, in Southern California; and a multi-purpose office building in San Diego — sought to validate energy savings relative to modeled baseline performance of rooftop units, as well as peak load reduction, demand responsiveness, and maintained or enhanced occupant comfort.

A key advancement of this project was the development of an integrated system controller that optimizes operation of the combined variable refrigerant flow plus indirect evaporative cooling configuration through zonal occupancy sensing and learned building behavior.

This project also advanced modeling of variable refrigerant flow, indirect evaporative cooling, and hybrid variable refrigerant flow plus indirect evaporative cooling systems by adding associated modules to the EnergyPlus building simulation software. This modeling work will enable more accurate estimates of the energy saving effects of variable refrigerant flow, indirect evaporative cooling, and variable refrigerant flow plus indirect evaporative cooling in other buildings throughout California's diverse climate zones.

Finally, this project conducted laboratory testing to assess trade-offs between performance and environmental effects of three leading natural refrigerants — propane, carbon dioxide, and ammonia — as sustainable, low global warming potential alternatives to traditional refrigerants.

## **Project Approach**

The core project team consisted of the Electric Power Research Institute and two major subcontractors: the University of California, Davis Western Cooling Efficiency Center and Pacific Gas and Electric Company's Applied Technology Services center. Another subcontractor,



MelRok, developed the controller unit based on governing logic furnished by the core project team. Qualified contractors installed and commissioned the technologies at each site.

The variable refrigerant flow plus indirect evaporative cooling research aspect of the project, as well as the alternative refrigerant component research aspect, each applied a series of steps to model, demonstrate, test, document, and analyze the potential energy-saving and mitigation potential of global warming, respectively, overcoming technical and non-technical obstacles in each aspect of the research.

## **Project Results**

### **Demonstration of Variable Refrigerant Flow Plus Indirect Evaporative Cooling Hybrid System**

Overall, the demonstrations validated the energy savings and demand reduction impact of the variable refrigerant flow plus indirect evaporative cooling hybrid system as an alternative to rooftop unit systems or to variable refrigerant flow systems alone.

The Del Taco results showed significant energy savings and peak demand reduction. Over the course of a six-month period spanning September 2019 through February 2020, the Del Taco treatment site with the variable refrigerant flow plus indirect evaporative cooling system yielded average monthly energy savings of approximately 32.4 percent compared to the rooftop unit control site. On the summer peak day during this period, the demonstration system resulted in energy savings of 20.0 percent, including a 14.7 percent reduction in peak demand during the 1:00 pm hour. During the winter peak day, the variable refrigerant flow in heating mode resulted in 45 percent energy savings compared to the control site heating system. The pre-retrofit configuration was a roof top unit system and the post-retrofit configuration was variable refrigerant flow plus indirect evaporative cooling.

The Northern California office building demonstration yielded an average energy savings of 18.7 percent beyond the previous operation of a variable refrigerant flow system on similar days across a variety of ambient temperatures during the cooling season. The pre-retrofit configuration was variable refrigerant flow only, and the post-retrofit configuration was variable refrigerant flow plus indirect evaporative cooling.

The nature of the Southern California office site demonstration was different from the other two in that the operative objective was not energy savings but rather enhancing occupant comfort and increasing utilization of the space during periods of high temperature and high indoor occupancy. Despite circumstances inhibiting full measurement of the energy savings impact, the variable refrigerant flow plus indirect evaporative cooling system performed as commissioned and met all qualitative measures of comfort.

Further deployments in other California climate zones and in different types of commercial buildings would provide even greater insight into the energy savings potential of this unique hybrid configuration.

### **Testing of Natural Refrigerant Systems**

The refrigerant testing component of the project offered a range of results that validate that the use of low global warming potential refrigerants, particularly natural refrigerants of propane, carbon dioxide, and ammonia, does not adversely compromise system performance

and efficiency compared to more common, higher global warming potential, synthetic refrigerants.

Test results demonstrated that equipment operating on low global warming potential natural refrigerants exhibits performance and efficiency commensurate with traditional synthetic refrigerants. This suggests that converting to low global warming potential refrigerants does not compromise energy efficiency and performance efficacy.

The natural refrigerants tested in this project, as well as R32, can be suitable for variable refrigerant flow systems. These alternate refrigerants cannot be used as a drop-in replacement for R410A but rather in systems (variable refrigerant flow or otherwise) for which they are specifically designed.

## **Technology Transfer (Advancing Research to Market)**

The results from this project will be widely shared following the release of this report through presentations and papers at such industry outreach events as the American Council for an Energy-Efficient Economy Building Summer Study, Emerging Technologies Summit, California Emerging Technology Coordination Council, Utility Energy Forum, and meetings of the California Institute for Energy and Environment, Western Cooling Efficiency Center, and New Buildings Institute, as well as through articles in the trade press for HVAC technology. Electric Power Research Institute plans to conduct similar demonstration projects in California with a greater variety of appropriate commercial buildings in different climate zones, in conjunction with utilities and other partners. The company also intends to work with utility partners to replicate this type of technology demonstration around the country.

By selecting a quick-serve chain restaurant, Del Taco, as one of the demonstration sites, the results are directly replicable and scalable to the other 580-plus Del Taco restaurants in California. This represents an immediate and sizable “warm market” for this technology.

By extension, other quick-serve restaurant chains represent an additional addressable market. According to a 2020 market research report by Ibis World, there are nearly 90,000 restaurants in California, with approximately one-third in the fast food or quick-serve segment. Outreach to industry trade organizations such as the California Restaurant Association can help transfer the knowledge and experience of this research.

Enhancements to the EnergyPlus building energy simulation tool developed by the project have been communicated to the United States Department of Energy.

The research results will be promulgated through papers and presentations at industry conferences, as well as through articles in the trade press for energy research and HVAC technology.

## **Benefits to California’s Ratepayers and Environment**

The project directly benefits California ratepayers by demonstrating that a combined variable refrigerant flow plus indirect evaporative cooling approach has the potential to reduce energy consumption in small- and medium-sized commercial buildings by 20 percent to 32 percent as a replacement for the less energy-efficient packaged rooftop units ubiquitous to this market. This project demonstrated that the hybrid system can reduce demand on a peak summer hour by 15 percent. The energy savings reduces emissions of carbon and other pollutants and also

improves occupant comfort. The overall system cost can be competitive to rooftop replacement when the two systems are right sized using optimized economizer operation.

In addition, laboratory testing results of the three natural refrigerants (propane, carbon dioxide, and ammonia) demonstrated efficiencies in cooling mode commensurate with traditional synthetic refrigerants and suggest that converting to natural refrigerants with low global warming potential does not compromise energy efficiency and performance efficacy. This significant finding can encourage further tests and scaled deployments of natural refrigerant systems to help meet California's greenhouse gas reduction goals.

The research has benefited numerous stakeholders.

Del Taco has expressed interest in expanding the technology to other locations. Because of COVID the dining areas have been closed, which has reduced the near-term urgency to implement at other locations. Del Taco is pleased with the operations of the Aliso Viejo location. The site consistently maintains comfortable kitchen temperatures and the system has not required any service calls. The HVAC contractor also plans to discuss this hybrid HVAC configuration with other fast food accounts, including a notable pizza chain.

A key market influencer with this type of system is the HVAC contractor, who can serve as the system integrator. The team sees an important step as the continual education transfer to the HVAC contractor/installer community.

This project developed modules that had previously not existed in EnergyPlus: (1) multi-zone variable refrigerant flow; (2) variable refrigerant flow plus dedicated outside air system; and (3) indirect evaporative cooling as part of a dedicated outside air system solution. The project team communicated and transferred these innovations to the EnergyPlus community through such organizations as Big Ladder (an industry trainer for EnergyPlus), the National Renewable Energy Laboratory and Lawrence Berkeley National Laboratory. The latest version of EnergyPlus (v9.4) reflects some of these enhancements. EnergyPlus v9.4 is available for the HVAC/building community to use for Title 24 compliance calculations. These enhancements in EnergyPlus can influence future iterations of Title 24, insofar as the energy savings performance of variable refrigerant flow plus indirect evaporative cooling can be explicitly included. This can allow for aesthetic tradeoffs preferred by builders and customers such as greater window to wall ratio.

Information on alternative refrigerants has been shared in public forums, industry conferences and Electric Power Research Institute meetings and will lead to future installations using refrigerants with lower global warming.

Energy policy makers and regulators in California and throughout the United States can better understand the potential role of this hybrid system in achieving climate goal objectives. Utilities can inform similar demonstrations, scaled field deployments, and customer incentive programs to help attain prescribed energy efficiency goals. And the results can also bolster the confidence of HVAC contractors to offer these solutions to customers.

## **Conclusions**

By providing a unique research and demonstration opportunity to bridge disjointed silos within the building industry, this research sets the stage for further demonstrations at small- and medium-sized commercial buildings throughout California.



# CHAPTER 1:

## Introduction

---

### Background

Small- and medium-sized commercial buildings in California are predominantly air-conditioned with packaged rooftop units (RTUs). Economical and familiar for heating, ventilation, and air-conditioning (HVAC) contractors to install, RTUs are ubiquitous for small- and medium-size office buildings, retail establishments, restaurants, and schools throughout the state. However, RTUs are inherently inefficient, suffering from significant thermal losses through leaks from ducts and cabinets, poor distribution efficacy, and low peak performance. Replacing RTUs with more efficient space conditioning technology represents a significant opportunity for energy efficiency to help California make progress toward the ambitious goal directed in Senate Bill 350 (De León, Chapter 547, Statutes of 2015) to double end-use energy savings, relative to a 2015 baseline, by 2030.

Fortunately, more energy-efficient space conditioning alternatives exist on the market, including heat pumps and indirect evaporative cooling (IEC). Variable refrigerant flow (VRF), a type of ductless heat pump technology that flows refrigerant to indoor heat exchange units, rather than blowing conditioned air through ducts, offers a particularly novel approach to achieving a high degree of energy efficiency. IEC offers an even more energy-efficient solution since it operates without using a compressor, instead passing outside air through a heat exchanger that evaporates water to cool indoor air circulated through ductwork. However, VRF and IEC are each inhibited by inherent technical limitations. VRF has limited ventilation capacity, while IEC has limited cooling capacity to address peak cooling demand of buildings.

Recognizing that the limitations of VRF and IEC are complementary, a hybrid solution that features VRF and IEC working in concert is a potentially compelling solution for energy savings. In theory, IEC can provide highly energy-efficient cooling during major portions of the year, with VRF being activated to efficiently satisfy higher cooling demands during the warmer summer periods. Extrapolating prior tests and applications of VRF and IEC systems separately, replacing packaged RTUs with a combined VRF+IEC approach has an assumed potential to reduce energy use in these small- and medium-sized commercial segments by 30 percent to 50 percent. For perspective, a 40 percent reduction in energy use for these building segments represents 2,800 gigawatt-hours (GWh) of energy savings or about 5 percent of electricity use in commercial buildings in California.<sup>1</sup> A commensurate reduction in peak demand would be 2 gigawatts (GW), or about 4 percent of total California peak demand. Not only is this energy savings opportunity vast, it is also immediately addressable. RTUs have an average economic useful life of 15 years, meaning that about one-fifteenth of building RTUs will naturally turn over each year. Each instance of turnover represents a retrofit opportunity, not including potential early replacements of equipment.

While VRF+IEC is an elegant solution in theory, there has been no prior field demonstration of this technology pairing to validate energy savings, payback, and other customer benefits.

---

<sup>1</sup> California Energy Commission. "California Commercial End-Use Survey." CEC-400-2006-005. March 2006.

Given the higher initial cost of a VRF+IEC combination relative to RTUs, and the lack of familiarity among local HVAC contractors with installing and commissioning such systems, which involves a higher degree of complexity, it is doubtful that the market would start adopting this technology on its own without external intervention. Demonstrating the performance of this technology in actual commercial buildings can inform building owners, HVAC contractors, and other market actors and thereby accelerate market adoption. Accordingly, allocating funds from California ratepayers to demonstrate this technology in the field is a prudent investment.

Another significant California policy goal is to reduce the use of refrigerants with high global warming potential (GWP). Leakage of synthetic refrigerants into the atmosphere, including hydrochlorofluorocarbons widely used in HVAC and refrigeration systems, is known to have high GWP. California Assembly Bill 3232 (Friedman, Chapter 373, Statutes of 2018) requires the California Energy Commission (CEC), in consultation with the California Public Utilities Commission, California Air Resources Board, and the California Independent System Operator, to assess by January 1, 2021 the potential to reduce greenhouse gases (GHG) in buildings by 40 percent below 1990 levels by 2030. In addition, California Senate Bill 1477 (Stern, Chapter 378, Statutes of 2018) allocates funding for building decarbonization programs. The United States Environmental Protection Agency (USEPA) mandates a phase-out of hydrochlorofluorocarbons, including the common refrigerants R-22 and R-142b, due to their ozone-depleting attributes. Although their production and import are banned starting in 2020, continued use of existing stockpiles can continue through 2030.<sup>2</sup>

Conversion to HVAC systems using alternative low-GWP refrigerants is therefore an important component to achieving these California policy objectives. An added consideration is the use of natural refrigerants, which exist in nature and do not have to be synthetically produced. Although some natural refrigerants have been used in niche market applications for decades, their use is virtually absent in packaged air-conditioning systems. However, this conversion requires extensive testing to identify suitable refrigerants on the basis of GWP, thermodynamic properties that drive energy efficiency performance, compatibility with existing equipment, and safety issues such as corrosion, toxicity, and flammability. Laboratory testing of low-GWP, natural refrigerant HVAC systems warrants California ratepayer funding to inform policy makers, HVAC equipment manufacturers, and contractors, and thereby accelerate market adoption and use.

## **Project Objective**

This project sought to demonstrate the application of a hybrid space conditioning system that integrates VRF with IEC as a more energy-efficient alternative to RTUs prevalent in small- to medium-sized commercial buildings throughout California. While VRF has been demonstrated as an energy-efficient space conditioning technology, one of its inherent challenges is limited ventilation capacity. This hybrid configuration uses IEC as a dedicated outside air system (DOAS) to satisfy ventilation requirements, eliminate outside air loads during cooling, and reduce heating loads as an air-air heat exchanger.

---

<sup>2</sup> U.S. Environmental Protection Agency. <https://www.epa.gov/ods-phaseout>.

Field demonstrations at three sites — a multi-purpose office building in Northern California (Pacific Gas and Electric Company [PG&E] territory), a quick-serve restaurant in Southern California (Southern California Edison [SCE] territory), and a multi-purpose office building in San Diego (San Diego Gas & Electric Company [SDG&E] territory) — sought to validate energy savings relative to modeled baseline performance of RTUs, as well as peak load reduction, demand responsiveness, and maintained or enhanced occupant comfort.

A key advancement of this project was the development of an integrated system controller that optimizes operation of the combined VRF+IEC configuration through zonal occupancy sensing and learned building behavior. Control sequence algorithms were based on governing logic informed by adaptive capabilities and response to inputs such as ambient weather conditions, humidity control, occupancy, and occupant comfort preferences.

This project also advanced modeling of VRF, IEC, and hybrid VRF+IEC systems by adding associated modules to the EnergyPlus building simulation software. This modeling work, which was calibrated with results from the field demonstrations, has developed and refined EnergyPlus for future modeling of these emerging space conditioning technologies and configurations. This will enable more accurate estimates of the energy savings effects of VRF, IEC, and VRF+IEC in other buildings throughout California's diverse climate zones.

Finally, this project conducted laboratory testing of three leading natural refrigerants — propane, carbon dioxide, and ammonia — as sustainable, low-GWP alternatives to traditional refrigerants. Novel heat pump and chiller equipment featuring these natural refrigerants were tested in three different laboratories, demonstrating energy-efficient performance coupled with low-GWP properties. The objective of these tests was to assess the trade-offs between performance and environmental effect as well as to document other important considerations such as safety.

The project's overall objective was — through field demonstration, laboratory testing, and energy simulation modeling — to advance technologies that can help California achieve its policy goals for energy efficiency, building decarbonization, and GHG reduction. These project objectives offer multifold benefits to California residents and businesses, including reduced energy bills, reduced carbon emissions to address climate change, and reduced emission of air pollutants to improve air quality. Accordingly, this project merited ratepayer funding.

The results of this research can benefit numerous stakeholders in addition to California residents and businesses. Energy policy makers and regulators, both in California and throughout the United States, can gain a better understanding of the potential role that VRF+IEC and natural refrigerants can play in achieving government policy objectives. Utilities can learn from these results to inform similar demonstrations, scaled field deployments, and customer incentive programs to help attain prescribed energy efficiency goals. These results can also bolster the confidence of HVAC contractors to offer these solutions to customers.

The research results will be promulgated through papers and presentations at industry conferences, as well as through articles in the trade press for energy research and HVAC technology.

# CHAPTER 2:

## Project Approach

---

This chapter describes the approach taken for both aspects of the project — the demonstration of the VRF+IEC hybrid system and laboratory testing of three natural refrigerants, each operating in a different HVAC system.

### **Approach: Variable Refrigerant Flow Plus Indirect Evaporative Cooling Hybrid System Demonstration**

The core project team consisted of the Electric Power Research Institute (EPRI) and two major subcontractors: the University of California, Davis' Western Cooling Efficiency Center (WCEC) and PG&E's Applied Technology Services center. EPRI provided project management and led two field demonstration sites. Since WCEC's own building on the campus of UC Davis was selected as a demonstration site, WCEC was responsible for managing its demonstration site, and it also led the modeling work. PG&E conducted testing of one of the alternative refrigerant units — a propane chiller — at its laboratory facilities. Another subcontractor, MelRok, developed the controller unit based on governing logic furnished by the core project team.

The demonstration sites were:

- WCEC multi-purpose office building and laboratory space located on the campus of UC Davis, managed by WCEC.
- Del Taco quick-service restaurant located in Aliso Viejo, California, managed by EPRI.
- Del Taco quick-service restaurant located in Irvine, California, serving as an experimental control site to the Aliso Viejo site, managed by EPRI.
- The San Diego Gas & Electric (SDG&E) Energy Innovation Center (EIC) located in San Diego, California, managed by EPRI.

Qualified contractors installed and commissioned the technologies at each site, including SH Mechanical at the Davis site, Aire-Rite for the Del Taco treatment site, and Jackson & Blanc for the San Diego site.

The VRF+IEC research in this project applied the following steps:

- Modeled the energy savings potential of a VRF+IEC hybrid system under a variety of California climate zones
- Scouted viable sites in each of the three investor-owned utility (IOU) service territories with a diversity of building types and incumbent HVAC technologies
- Developed a baseline monitoring and data collection plan for each demonstration treatment site
- Installed and commissioned VRF+IEC hybrid systems at the demonstration sites
- Collected and analyzed data from the demonstration sites
- Calibrated building energy models based on field data
- Documented results



## **Technical Barriers**

A key technical challenge was developing a stand-alone controller for the VRF + IEC hybrid system. This challenge was compounded by the fact that all commercial VRF systems employ proprietary control systems. This involved first developing a control schema based on governing logic on how the system should function in various modes — economizer-only, IEC, VRF, or simultaneous VRF and IEC operation. The next step was converting governing logic into corresponding control algorithms and developing a cloud-based architecture and communications platform to provide overlaying controls for both a VRF and IEC system. The researchers addressed this challenge by identifying and securing a controls vendor, MelRok, with the requisite expertise to build a controller using generic hardware and applying the BACnet data communication protocol to extract data and send control signals to the VRF system.

For the Del Taco site, the research team realized post-installation that the VRF unit had not been commissioned with BACnet connectivity. As a result, the team had to procure and install a compatible BACnet gateway device to enable control and data transfer.

Another technical challenge was modeling the performance of a VRF+IEC hybrid system. Current building energy simulation models had not been able to accurately represent the “as-is” implementation of VRF and IEC technologies separately, let alone operating in conjunction with one another. This project developed new modules for VRF and IEC systems within the EnergyPlus tool to simulate their energy use in the context of whole-building performance.

## **Nontechnical Barriers**

The project team encountered non-technical barriers as well. Unexpected site issues can compromise aspects of any field demonstration. In this case, for example, the original demonstration site in the SCE territory, an office building in Mission Viejo, that had been committed to the project for more than two years dropped out due to an unrelated legal dispute between the site owners and a third party. The team had already collected more than two years’ worth of baseline data, and despite months of attempts to salvage the situation had to quickly improvise to secure another appropriate site.

Fortunately, the researchers were able to quickly pivot to a Del Taco restaurant in Aliso Viejo that was being serviced by the designated local HVAC contractor and was due for a significant HVAC retrofit. In retrospect, shifting to a restaurant site allowed the team to expand the diversity of demonstration venues to assess the VRF+IEC technology in a setting that is, in theory, inherently conducive due to its distinct zones (kitchen versus customer area) and high ventilation needs. However, the change to the Del Taco site occurred at too late a juncture in the project to allow for a years’ worth of baseline data monitoring, as had been the original plan to compare pre-retrofit (baseline) to post-retrofit energy consumption. Accordingly, the researchers shifted the experimental design to a side-by-side control and treatment approach by simultaneously monitoring an identical Del Taco location in nearby Irvine as a control site to the Aliso Viejo treatment site.

Broadly speaking, the inertia of market forces poses barriers to any new technology. VRF and IEC systems are relatively expensive since they are not yet produced at a scale to drive costs lower. Most contractors and design engineers are not familiar with the design needs, operating conditions, and control considerations for VRF or IEC systems separately, let alone together.

The experienced gained from this project can inform future installations, reducing their complexity and size requirements and thereby reducing costs.

The uptake of innovative energy-efficient HVAC systems depends on the interaction and interdependence of a complex network of market actors in the building industry. Service technicians and contractors influence customer purchase decisions with their input and recommendations about technology choices. Design engineers are drawn to familiar technology solutions and strategies advocated by their go-to distributors. Although policy changes such as efficiency mandates can quickly shift industry practices, policy making is a slow process that is challenged to address all contingencies. Incentive and rebate programs offer some positive pressure for the adoption of efficiency measures, but even programs that offer obvious return on investment can have little effect when other challenges to implementation remain in place. VRF and IEC technologies are both plodding their way toward broader application but are hindered by a reluctance to change from traditional practices, by cost challenges and by general lack of awareness and professional understanding for the technologies.

## **Approach: Laboratory Testing of Natural Refrigerants**

The alternative refrigerant component of this research project applied the following steps:

- Investigated alternative refrigerants most appropriate for laboratory testing, based on mitigation of GWP, energy efficiency, and safety
- Selected three natural refrigerants — propane, carbon dioxide, and ammonia — based on the mitigation of GWP, energy efficiency, and safety
- Developed testing protocols
- Scouted, procured or otherwise secured, and shipped heat pump or chiller units using these natural refrigerants to laboratory facilities
- Installed and commissioned alternate refrigerant units at three laboratory locations
- Conducted evaluation tests consistent with protocols
- Collected and analyzed data
- Documented results

## **Technical Barriers**

The primary technical barrier to laboratory testing of alternate refrigerants was planning and designing flexible testing configurations appropriate for different applications. For example, for a non-VRF application, a single loop configuration is appropriate since the refrigerant conditions air that is circulated through ducts. For a VRF set up, a secondary pump loop configuration is suitable to measure system performance while ensuring safety, due to the potential health and safety concerns related to toxicity. This entailed working with laboratory partners and contractors to configure tests with ancillary equipment to allow testing of HVAC equipment using the alternate, natural refrigerant in the primary loop and a heat exchanger to condition a separate working fluid in a secondary loop to transfer cooling or heating to indoor fan coil units in a VRF application.

## **Nontechnical Barriers**

The major barrier for natural refrigerant testing was identifying and procuring, or otherwise securing, suitable equipment for demonstration. The project team learned that packaged HVAC systems operating on natural refrigerants are not commercially available in the United States. Accordingly, the team directed its focus to Europe and Asia in a search for suitable equipment operating on alternate, natural refrigerants. Even in those regions of the world, use of natural refrigerants is typically relegated to niche applications of large refrigeration equipment. The project team scoured worldwide for HVAC systems operating on propane, carbon dioxide, or ammonia that would be feasible and appropriate for laboratory testing.

After months of extensive review, the researchers sourced a water-cooled heat pump manufactured by a Danish company, Bundgaard Refrigeration, that uses propane as a refrigerant. Due diligence required months of correspondence to confirm equipment specifications and readiness for lab testing in the United States. This process included travelling to Denmark to assess the equipment in preliminary factory tests prior to shipment. The team then had to arrange international shipment from Denmark for delivery to the San Francisco Bay Area for testing, which required complex logistical planning, a significant test of the resourcefulness and resiliency of the project team.

Recognizing that the value of this project would increase with the number of different refrigerants assessed, the project team sought additional equipment to test and facilities in which to test them. After considerable evaluation, the team identified a carbon dioxide heat pump designed and configured by a leading HVAC research group at the University of Illinois, Champaign-Urbana. Working in close coordination with researchers there, the project team commissioned testing of this carbon dioxide heat pump at their lab in Illinois, following consistent test protocols.

To round out the refrigerant testing portfolio, the project team directed attention to acquiring ammonia refrigerant equipment to complement the propane and carbon dioxide systems. Auspiciously, simultaneous to this project, EPRI's thermal laboratories in Knoxville, Tennessee had arranged the first test of an ammonia refrigerant chiller in North America, manufactured by Mayekawa of Japan. The project team coordinated with the EPRI research team in Knoxville, where the testing was conducted, to ensure that test results would inform the overall project mission.

# CHAPTER 3:

## Modeling

---

This chapter describes the approach used in this project to model the performance of baseline RTU systems and the integrated VRF+IEC system for multiple sites.

### Modeling Method

- Overcoming challenges to model VRF
- Creating new modules in EnergyPlus for VRF + dedicated outside air system (DOAS)

This research project is aimed at documenting the performance of two California climate appropriate HVAC systems and evaluating the electrical demand and energy reductions associated with installing the systems. The researchers created and refined a calibrated building energy model to prove the accuracy of the modeling methods. A standard model was then used to extend the proven modeling methods to the stock of existing commercial buildings in California. Finally, the electric demand, energy, and water effects of different HVAC technologies throughout California were predicted using the final models.

The building energy modeling was performed with EnergyPlus. EnergyPlus is a modeling software that is commonly used to analyze HVAC cooling and heating loads and HVAC-related electrical energy consumption in buildings. The software can be used to study the effects of various energy efficiency measures and technologies. Since EnergyPlus does not include modules to simulate several of the strategies and technologies investigated for this project, the researchers used the energy management system feature to model these strategies and technologies. Although some of the energy management system models do not completely capture the behavior of the real systems, the annual effect of the errors is expected to be low.

An EnergyPlus model was calibrated using field measurements of capacity, electrical energy use, and zone temperatures. The researchers then used the calibrated model to simulate three other HVAC systems that could be used in the same building. The report compares the electrical energy use, electrical demand, and water use associated with the installation of the four HVAC technology packages, which are:

- 1) Roof top units (RTUs) with vapor-compression cooling, electric resistance heating, and ductwork for air distribution; this is considered the baseline technology since it is the prevalent incumbent equipment for small- and medium-sized buildings
- 2) Variable air volume (VAV) system with a central air handling and cooling system and zone-level electric reheat coils
- 3) VRF system with a dedicated ventilation system
- 4) VRF system with a DOAS that incorporates IEC

## Modeling Results for Western Cooling Efficiency Center Site

The researchers updated the site model after the calibration study to reflect schedule changes that occurred after the calibration period and before the retrofit study. The stack effect flow through the ventilation chase was eliminated since it was a unique observation at the field test site. Furthermore, a permanent fix was implemented in the building to eliminate stack effect in the ventilation chase. The parameter values used in the final models are tabulated in Table 1.

**Table 1: Model Parameters**

Parameter	Value
Schedule	7 a.m. to 7 p.m.
Electric Gains / Lighting Gains	12 W/m <sup>2</sup> * / 2.54 W/m <sup>2</sup>
People	18.58 people/m <sup>2</sup>
Winter Set Point	75°F (24°C)
Summer Set Point	72°F (22°C)
Exterior Wall Construction R-Value	1.4 hr-ft <sup>2</sup> -°F/BTU**

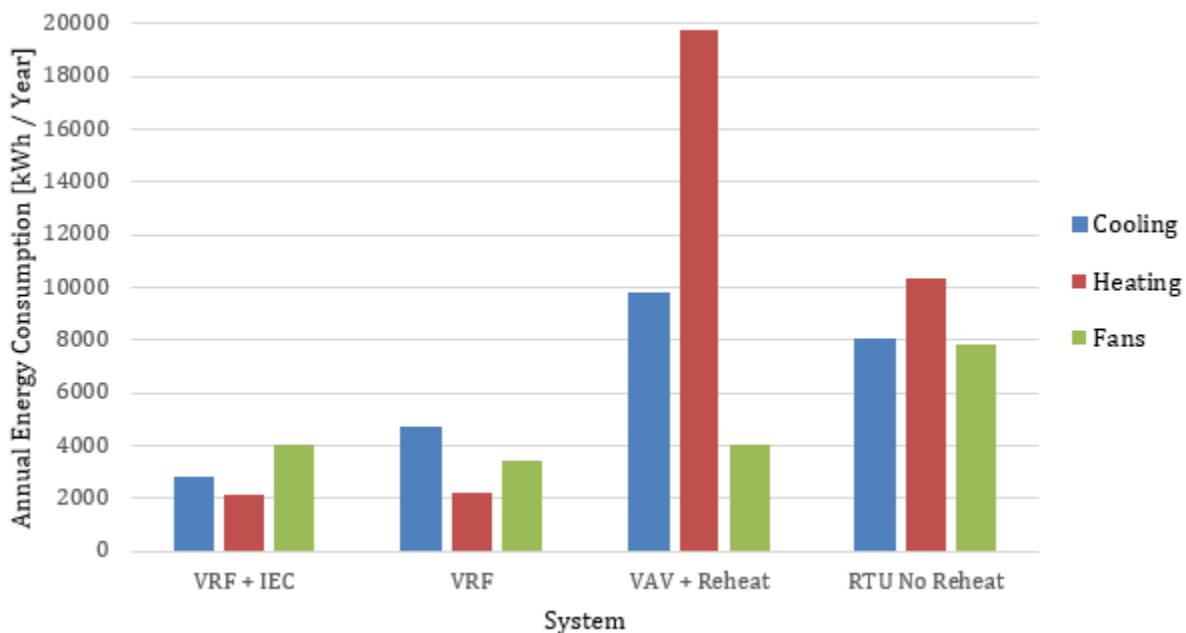
\*watts per square meter

\*\*British thermal units

Source: Electric Power Research Institute

Figure 1 illustrates the annual modeled electrical energy consumption by end use for each of the HVAC systems.

**Figure 1: Modeled Annual Electricity Consumption of Systems at Western Cooling Efficiency Center Site**

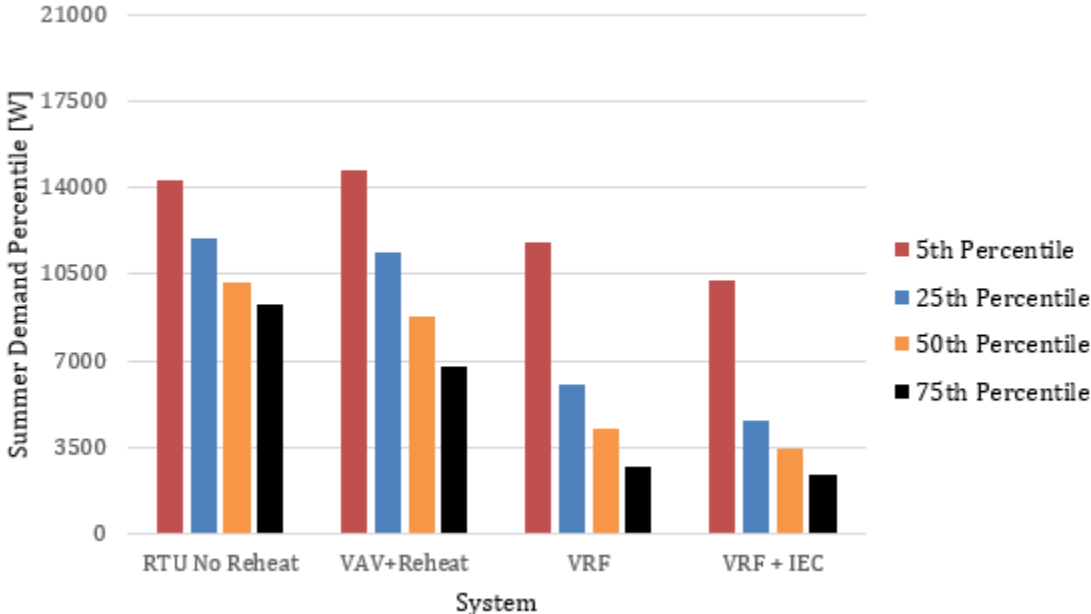


Source: Electric Power Research Institute

Between the baseline systems, the VAV uses more energy, but also meets the set points more frequently than the RTU system. Although the focus is not on the baseline systems, it is important to note that the VAV system performs with a higher efficiency than the RTU system, which is expected. The results show that the VRF systems have significantly lower electrical energy use due to cooling and heating than either the RTU or the VAV systems. Fan energy use in the VRF system with IEC is comparable to the VAV systems. The electrical energy consumption due to fans was lowest in the VRF system with dedicated ventilation. The results illustrate that the electrical consumption due to fans is significantly higher in the VRF system with an IEC than the VRF system with dedicated ventilation; conversely, the electrical energy consumption due to cooling is significantly lower in the VRF system with an IEC than the VRF system with dedicated ventilation. Between the two VRF systems, the electrical energy consumption due to heating is essentially unaffected by the IEC. Overall, the IEC reduces the total electricity consumption compared to the other system types. The results of a water use analysis show that 6,100 gallons of water were evaporated by the IEC. Actual real-world water use would be higher due to bleed and other water use inefficiencies.

Figure 2 illustrates the summer HVAC demand in watts for each of the systems.

**Figure 2: Modeled Summer Peak Demand of Systems at Western Cooling Efficiency Center Site**



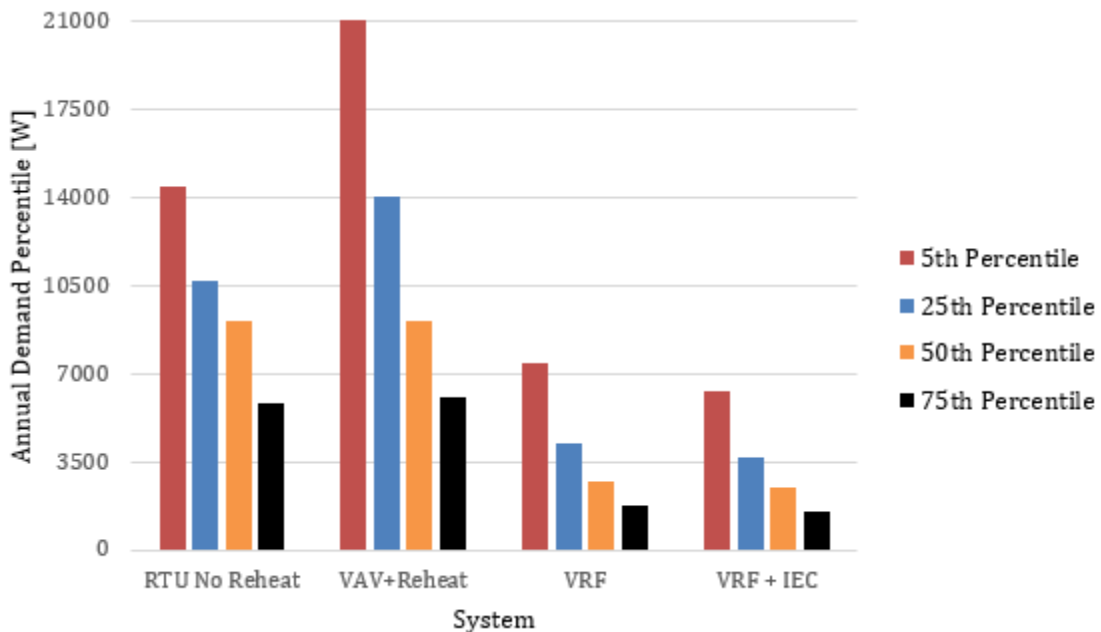
Source: Electric Power Research Institute

The data are shown in terms of percentiles showing the amount of time the HVAC system operated at or above a given power draw. The figure allows for a comparison of the demand profiles of each technology. Consider for instance the 5<sup>th</sup> percentile bar. The figure shows that 5 percent of the time, the RTU and VAV systems demand 14 kilowatts electric (kWe) or more. This is higher than the 5<sup>th</sup> percentile of demand for the VRF system (11.8 kWe). The 5<sup>th</sup> percentile of demand for the VRF with IEC is the lowest, at 10.3 kWe. The data show that both VRF systems consistently have a lower electric demand than the baseline systems. Between the baseline systems, the VAV with reheat has a higher peak demand than the RTU without reheat. However, from the 25<sup>th</sup> percentile down, the RTU without reheat system has a higher demand. The reason for the switch is that the VAV with reheat is more efficient at cooling than

the RTU system, but also meets the highest peak cooling loads better, which requires more energy. Comparing the two VRF systems, it is clear that the IEC consistently reduces demand in the summer. The demand reduction is 12 percent in the high range of demand, as high as 24 percent in the mid-range of demand, and 11 percent at the low end of demand.

Figure 3 is similar to Figure 2, but illustrates the demand profile over the whole year. The figure shows that the VRF systems both consistently reduce demand throughout the year compared to the baseline systems. The data show that, for the VAV with reheat, the annual demand in the 5<sup>th</sup> percentile range is much higher than demand in summer. The difference is caused by significant heating demand in the winter. Figure 3 also shows that, in the 5<sup>th</sup> and 25<sup>th</sup> percentile range, the VAV with reheat has significantly higher demand than the RTU without reheat. The result means that for periods of the year, when there is significantly high heating demand, the VAV with reheat results in more electric demand than the RTU. The extra demand is due to the VAV with reheat system meeting the setpoint in all zones more frequently than the RTU without reheat. This increases energy use, but also significantly increases occupant comfort in winter. The VRF system reduces annual demand by more than 50 percent compared to the baseline systems. The savings are better than the summer demand results, due to the difference in efficiency between heat pump heating and electric heating.

**Figure 3: Modeled Annual Demand Profile of Systems at Western Cooling Efficiency Center Site (Watts)**



Source: Electric Power Research Institute

A set of generic models was created from a United States Department of Energy (USDOE) commercial reference building to study the four HVAC systems in each of the 16 California climate zones. The USDOE building is representative of a small office with post-1980 construction. The building has five conditioned zones and an unconditioned attic. The HVAC systems in the generic models are almost all the same as the HVAC systems in the site models. The notable exceptions are that the VRF systems in the generic models only have non-ducted fan-coil units, and for the VAV system, the minimum damper position is selected by the auto-sizing routine.

Table 2 presents the important parameter values that were used in the final generic building simulations. Notable differences between the site models and the generic models include the construction R-Value and the electric and light gains.

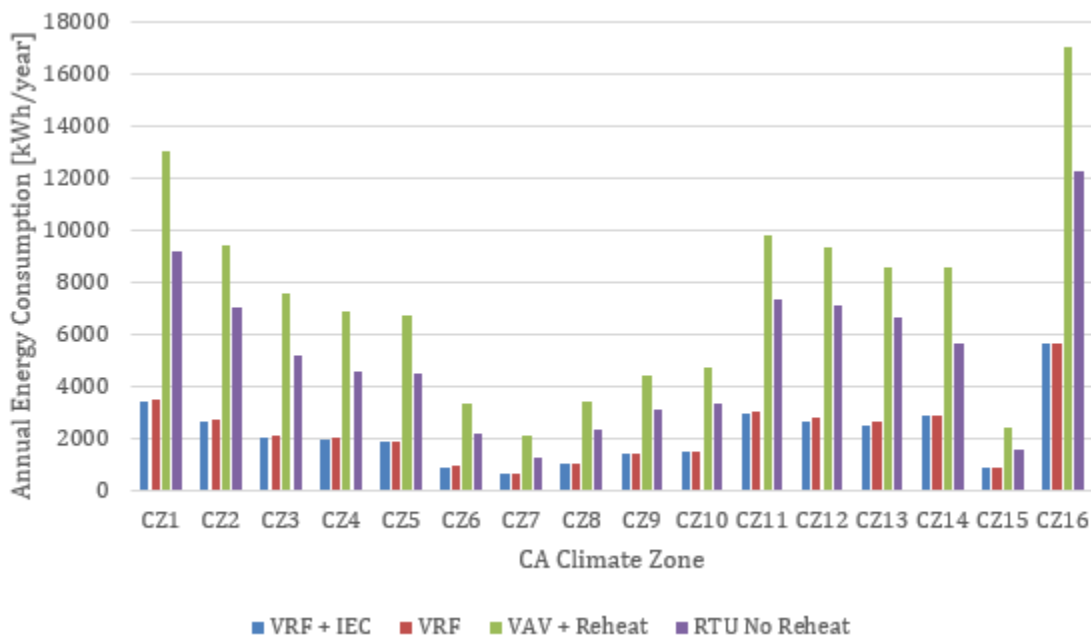
**Table 2: Parameter Values for Final Generic Building Simulations**

Parameter	Value
Schedule	7 a.m. to 7 p.m.
Electric Gains / Lighting Gains	10.76 W/m <sup>2</sup> / 19.48 W/m <sup>2</sup>
People	18.58 people/m <sup>2</sup>
Winter Set Point	75°F (24°C)
Summer Set Point	72°F (22°C)
Exterior Wall Construction R-Value	1.54 hr-ft <sup>2</sup> -°F/BTU

Source: Electric Power Research Institute

Figure 4 shows the electrical energy use due to heating in 16 California climate zones.

**Figure 4: Modeled Electric Heating Consumption per California Climate Zone**



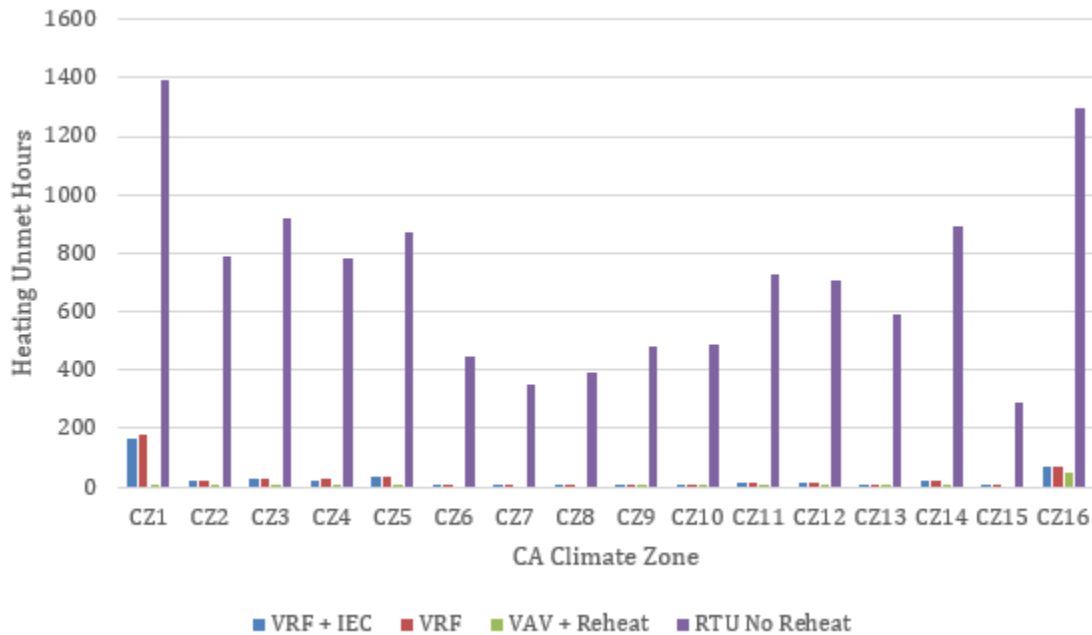
Source: Electric Power Research Institute

Figure 5 shows the number of hours the heating set point was unmet for each system in each climate zone. It is clear from Figure 5 that the RTU system has many more unmet hours than the other systems. This is due to the fact that the RTU system is controlled based on one zone, meaning that it can meet the set point in that zone and yet not meet the set point in other zones. Although the VAV is more efficient than the RTU, since the RTU performs less heating it also uses less energy. The results show that the VRF systems perform better in heating than the baseline systems in every climate zone. The VRF with IEC performs slightly better in heating than the VRF system. Although evaporative cooling is off during the winter,



the IEC fan is still able to provide additional “free heating” in favorable weather, reducing the load on the VRF.

**Figure 5: Modeled Unmet Set Point Heating Hours per California Climate Zone**



Source: Electric Power Research Institute

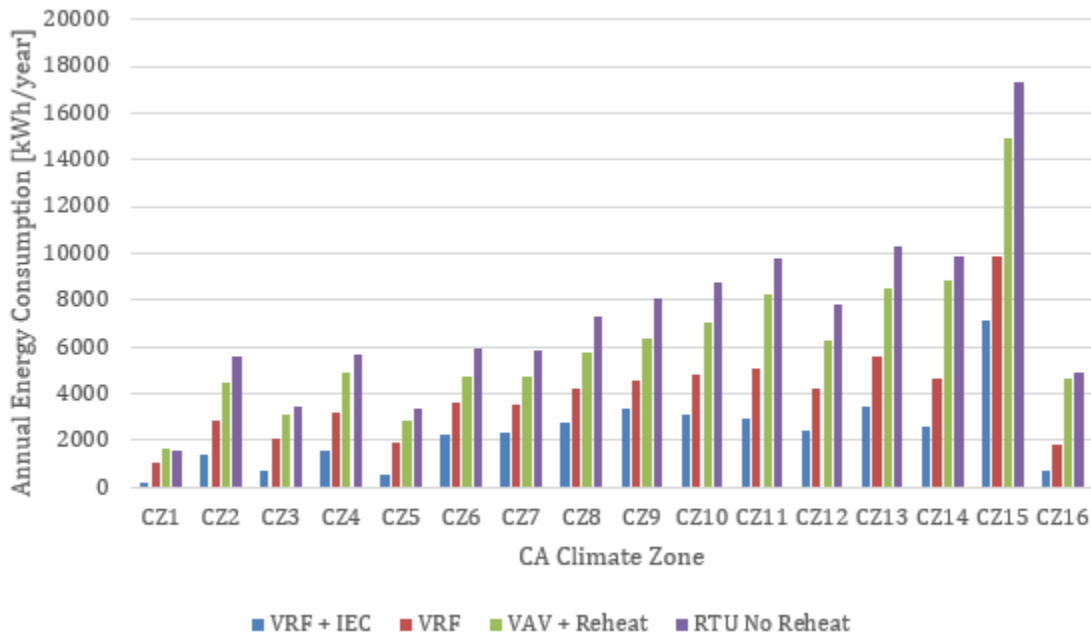
In terms of unmet heating hours, the VAV with reheat system performed consistently better than the other systems. VRF systems were more capable of meeting the target set points than the RTU with no reheat system, due to the ability to cool and heat different zones simultaneously. For 15 of the 16 climate zones, the VRF systems had at most 38 more unmet hours than the VAV system. The difference in unmet hours between the VRF system and the VAV system is primarily due to differences in the sizing of the VRF coils and the reheat coils in the VAV system. The unmet hours would not have caused a significant change in the energy use for the VRF system for these 15 climate zones. The only exception is climate zone 1, where there were 170 more unmet hours attributed to the VRF systems than the VAV with reheat. In this case, the VRF system energy use would be higher to meet the unmet loads, but still not as high as the VAV with reheat system.

Figure 6 shows the cooling electrical energy use in 16 California climate zones. The results show the same trend in climate zones 2 through 16. In these climate zones, the cooling energy use of the four systems is ranked from low to high as follows:

1. VRF+IEC
2. VRF
3. VAV with reheat
4. RTU with no reheat

In Climate Zone 1, the RTU with no reheat uses slightly less energy than the VAV system, although the VAV is actually more efficient.

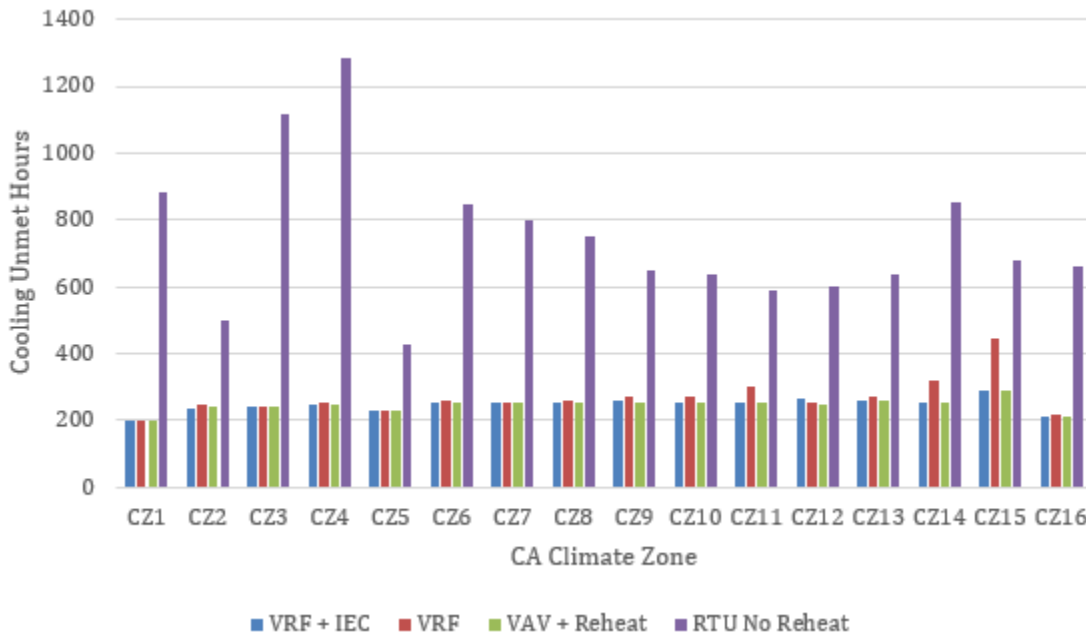
**Figure 6: Modeled Cooling Electricity Use in 16 California Climate Zones**



Source: Electric Power Research Institute

Figure 7 shows the number of hours that the cooling set point is not met for each system in each climate zone. Generally, the VRF systems and the VAV with reheat system have roughly the same number of unmet hours in each climate zone. The exceptions are climate zones 11, 14, and 15. The effect on the energy use was not significant enough to change the energy trends in these climate zones.

**Figure 7: Modeled Unmet Set Point Cooling Hours per California Climate Zone**



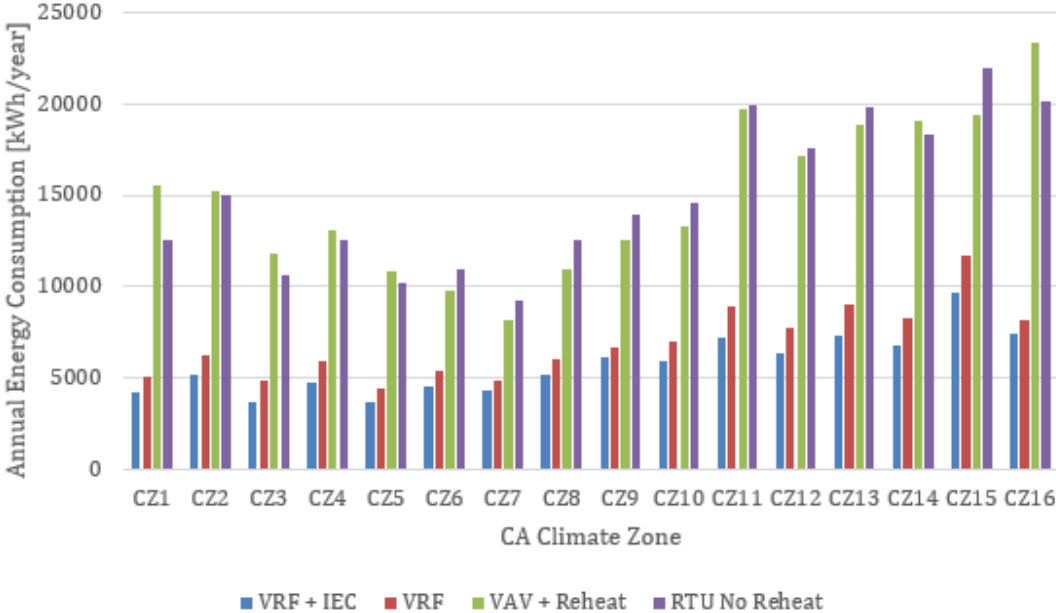
Source: Electric Power Research Institute

An interesting trend was observed when comparing unmet hours and cooling coil sizing between the VRF system and the VRF+IEC system. In climate zones where the VRF system has more unmet cooling hours than the VAV with reheat system, adding the IEC reduces the

number of unmet cooling hours to be on par with the VAV with reheat system, while also reducing cooling energy use. The result means that, in terms of design, installation of the IEC offsets size increases in the VRF system. Therefore, some fraction of the capital costs of installing the IEC could be offset by reducing the VRF sizing. This could also result in lower refrigerant charge in the VRF system.

Figure 8 shows the cumulative electrical energy use per year of each HVAC system. The results show that the VRF systems use significantly less energy than the baseline systems in every climate zone. The VRF+IEC also has lower electrical energy use than the VRF system in every climate zone.

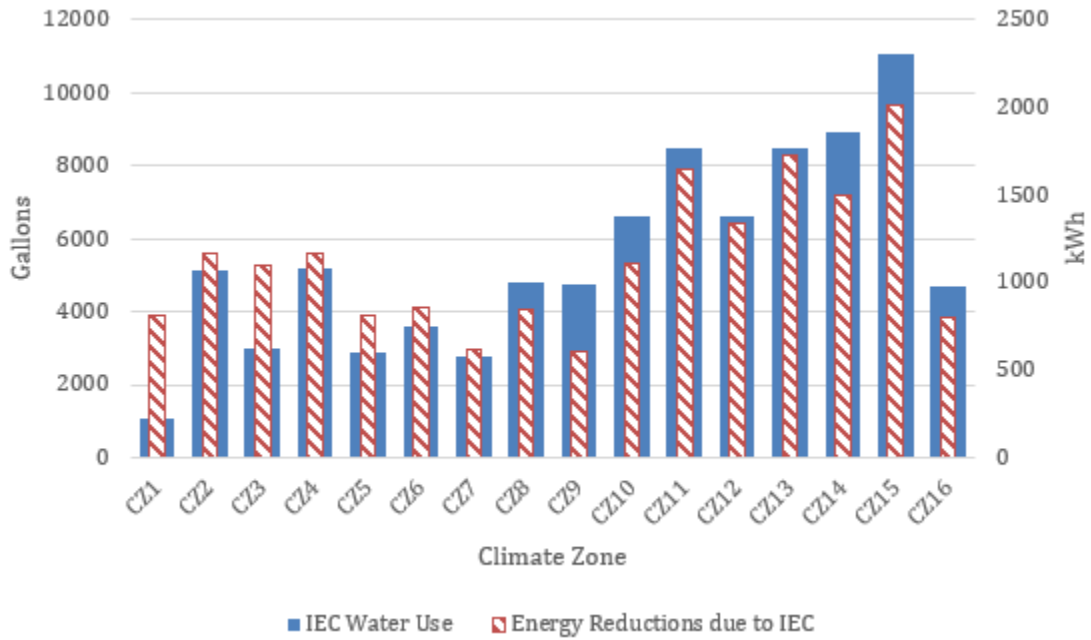
**Figure 8: Modeled Annual Electricity Use per Heating, Ventilation, and Air Conditioning System per Climate Zone**



Source: Electric Power Research Institute

Figure 9 shows the cumulative annual savings and water savings from installing and using a VRF+IEC system. The results show that water use is correlated with how hot the climate is. On the contrary, the energy savings associated with installation of the IEC is not well correlated with how hot the climate is. The best example is Climate Zone 1, which has a low water use and high energy savings. According to the Pacific Energy Center, the highest number of cooling degree days in Climate Zone 1 is 47. Compare this to Climate Zones 5 through 9, which have similar energy savings as Climate Zone 1, but much higher water use. The average number of cooling degree days in these climate zones ranges from 464 to 1,456.

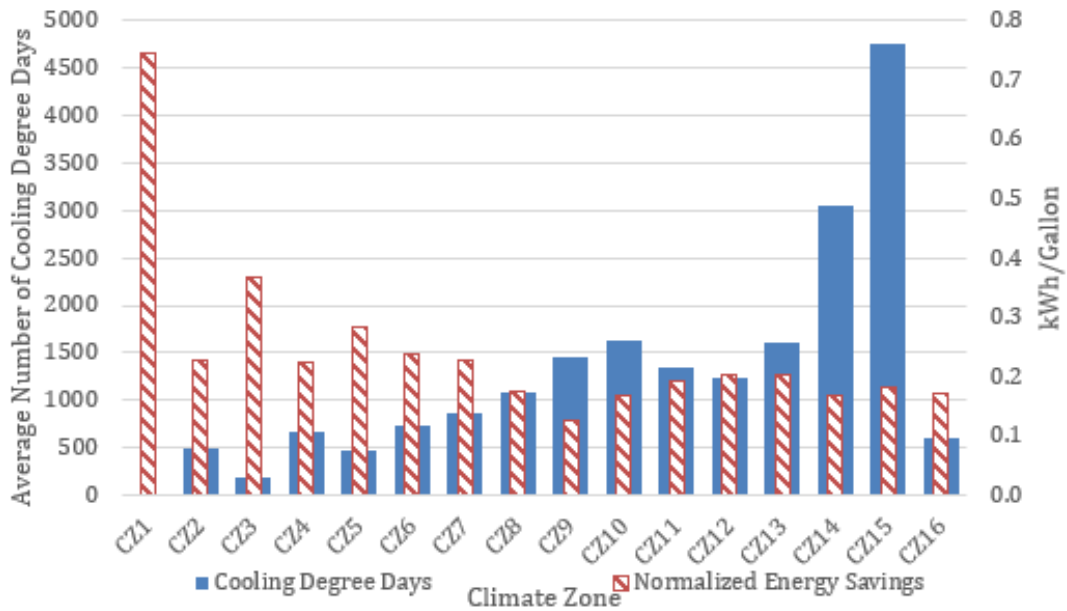
**Figure 9: Modeled Variable Refrigerant Flow + Indirect Evaporative Cooling Annual Energy and Water Savings per Climate Zone**



Source: Electric Power Research Institute

The results mean that the savings from the IEC are not only due to evaporative cooling. This is further illustrated in Figure 10, which shows the modeled energy savings of a VRF+IEC system by California climate zone, normalized by water use. The average cooling degree days is based on a characterization of California climate zones by the Pacific Energy Center. The results show that some climate zones, such as Climate Zone 1, with a low number of cooling degree days have a high ratio of energy savings to water use.

**Figure 10: Variable Refrigerant Flow + Indirect Evaporative Cooling Energy Savings by Climate Zone, Normalized by Water Use**

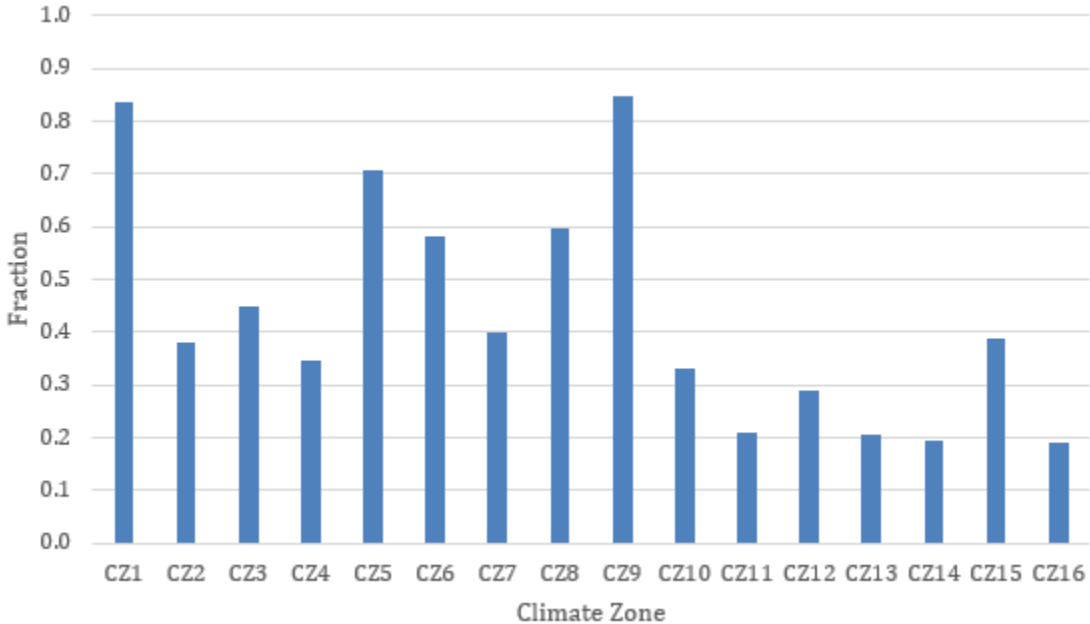


Source: Electric Power Research Institute

In cooler climate zones, such as Climate Zone 1, the high savings associated with the IEC are mostly due to “free cooling” due to increased outdoor airflow of the IEC over a standard ventilation system. Less than 20 percent of the savings in Climate Zone 1 can be attributed to evaporative cooling. In climate zones where the outdoor air temperature during operating hours is both lower and higher than the indoor set point temperatures, the energy savings are due to a mix of outdoor air “free cooling”, and evaporative cooling. In the hottest climate zones, such as Climate Zones 14 and 15, the savings are primarily due to evaporative cooling. The results show that in cooler climates, simply installing a DOAS with appropriate economizer controls would be sufficient.

Figure 11 shows the results of an additional simulation study to determine the percentage of IEC savings due to economizing. The economizing model represents a retrofit to the VRF with dedicated ventilation where the ventilation system size is increased and capable of increasing ventilation rates during economizing hours. The figure shows that the energy savings Climate Zones 1, 5, 6, 8, and 9 are mostly due to the economizer. The savings in the other climate zones are mostly due to evaporative cooling.

**Figure 11: Modeled Share of Energy Savings from Indirect Evaporative Cooling Economizing**



Source: Electric Power Research Institute

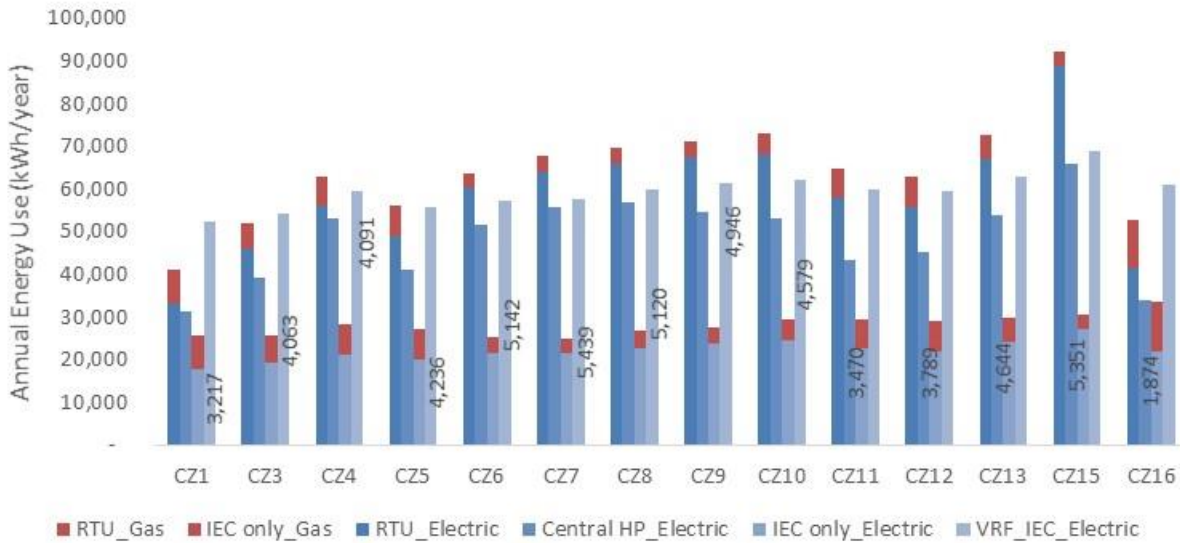
**Modeling Results for Del Taco Site**

The researchers updated the site model prior to simulation using actual, historical weather and available site data as model inputs and utility-meter and other observed data available prior to the retrofit modeling study.

A Del Taco fast food restaurant located in Aliso Viejo, California (Climate Zone 8) was an identified field site at which to deploy VRF and IEC technologies, characterize their performance in real buildings, and use calibrated whole-building energy simulations to assess statewide effects. Site-metered energy use for HVAC was recorded for each scenario simulated. Annual HVAC energy use (detailed by fuel and climate zone) is shown for each scenario in Figure 12. Natural gas use values have been converted from BTU to kilowatt-hours

(kWh) for convenient visualization, and zone cooling setpoint has been set at 74°F. Unmet cooling hours are shown as text, where applicable.

**Figure 12: Del Taco Simulated Annual Energy Use by Climate Zone**

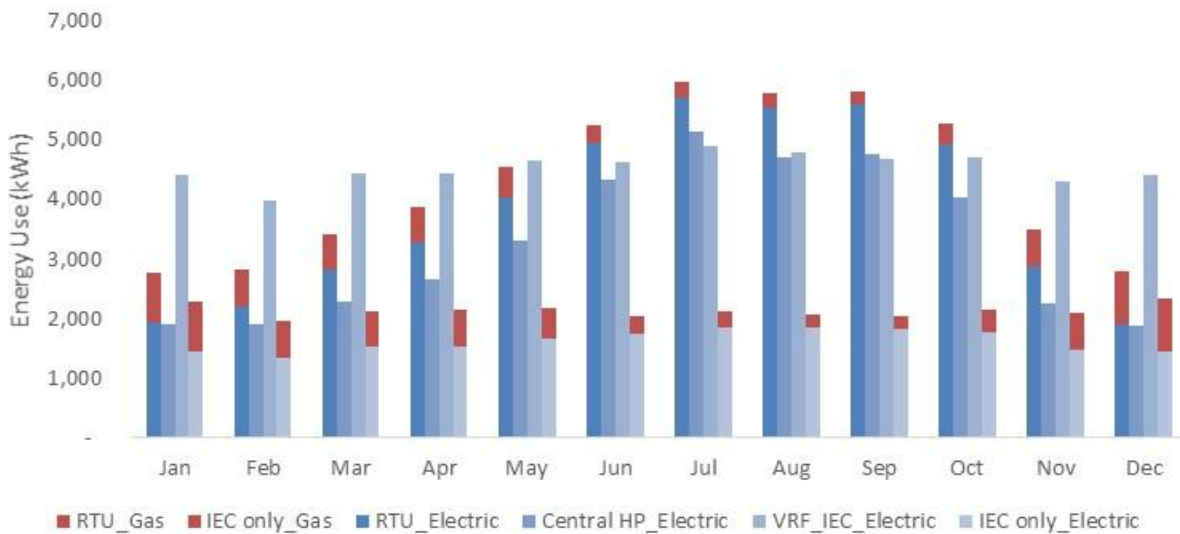


Source: Electric Power Research Institute

Note that while the RTU scenario shows significant variation in energy use across climates, as expected, the IEC-only scenario demonstrates relatively consistent energy use, since the primary IEC function simulated was satisfaction of ventilation loads, with space cooling only arising as a supplementary benefit. Similarly, the RTU with IEC and VRF+IEC scenarios exhibit higher than expected energy use in several climates, due to the dominance of fan energy use (to satisfy dedicated ventilation loads). Moreover, expected performance benefits from diversity of thermal loads across zones do not appear to be exploited in these results due to the low number of zones and coincident scheduling of thermal loads across zones in the fast-food restaurant building type.

In addition to observing annual effects for typical weather years in each climate, seasonal energy effects are also of interest. To illustrate, monthly HVAC energy use values are shown in Figure 13 for one climate zone (Climate Zone 3 Oakland/San Francisco) with a zone cooling setpoint of 74°F.

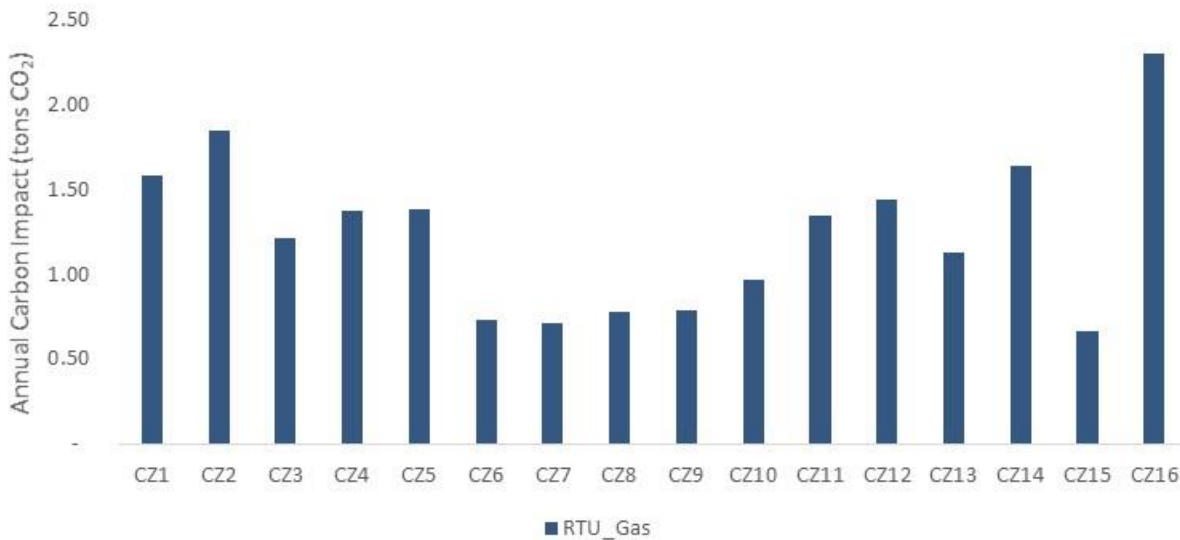
**Figure 13: Del Taco Monthly Energy Use for Climate Zone 3**



Source: Electric Power Research Institute

Given that several scenarios simulated involve fuel switching from natural gas to electricity, to assess potential for carbon emission savings, the researchers assumed 100 percent carbon-free electricity supply. Potential carbon effects are therefore presented based on the annual HVAC energy use values above for each climate zone and HVAC scenario as follows in Figure 14. A zone cooling setpoint of 74°F, and per USDOE’s Energy Information Administration, an emissions factor of 117 pounds of carbon dioxide (CO<sub>2</sub>) per million BTU was assumed for gas used.<sup>3</sup>

**Figure 14: Del Taco Carbon Impact of Avoided Gas Use by Climate Zone**



Source: Electric Power Research Institute

Gas use values from the RTU scenario are shown above to demonstrate carbon savings potential. Annual carbon savings potential (due to avoided gas use) appears to be lowest for

<sup>3</sup> URL: [https://www.eia.gov/environment/emissions/co2\\_vol\\_mass.php](https://www.eia.gov/environment/emissions/co2_vol_mass.php) (Last accessed: 9/27/19)

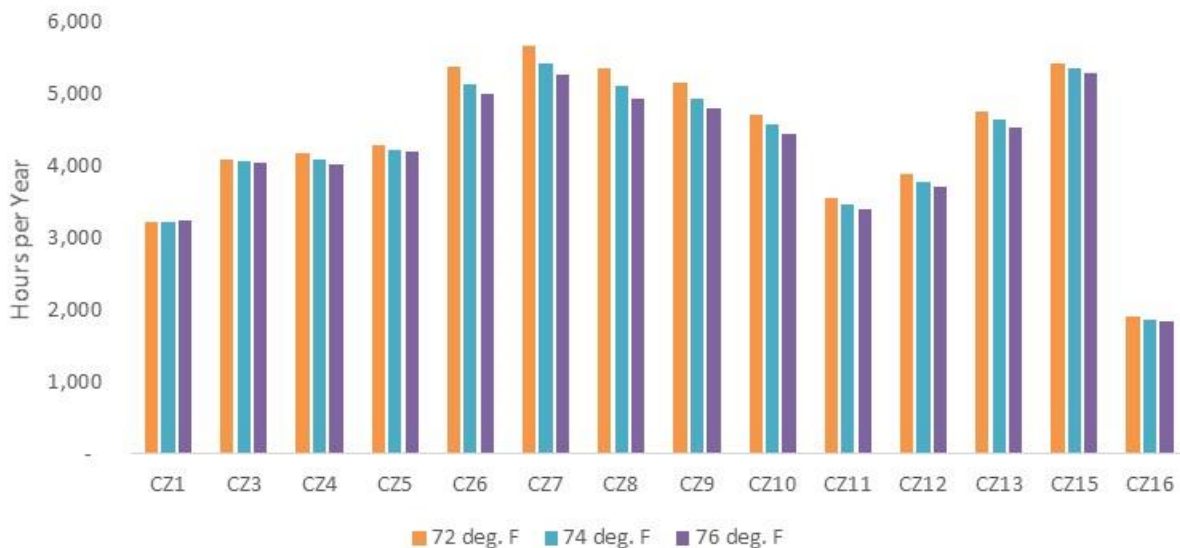
warmer climates (for example, Climate Zone 15) and highest for colder climates (for example, Climate Zone 16).

In addition to assessing energy use and carbon emissions effects, HVAC technology selection can also have notable effects on thermal comfort of building occupants. There is also a growing body of research into the role of HVAC technologies in supporting both energy efficiency and thermal comfort objectives, while minimizing their tradeoffs. For instance, the use of personalized cooling systems (including fans) has been discussed as an approach to improve thermal comfort while achieving energy savings.<sup>4</sup> Combining these advanced HVAC strategies with established HVAC control measures, such as zone temperature setbacks, additional energy/carbon savings potential may be assessed while maintaining or improving thermal comfort.

The HVAC technology scenarios simulated for this report highlight the relative opportunities for minimizing negative thermal comfort effects while maximizing energy/carbon savings. To illustrate, simulation results of annual unmet cooling hours for three different zone cooling setpoints, 72°F, 74°F, and 76°F, across all California climate zones for the IEC-only scenarios are shown in Figure 15.

As expected, thermal comfort (as quantified by facility unmet cooling hours) effects for the IEC-only scenarios are shown to vary by climate and to be partially offset by changes in zone temperature settings. The use of advanced HVAC (such as VRF), traditional technologies (such as ventilation fans), or thoughtful combinations of both may support thermal comfort goals while achieving energy-efficient performance. However, additional research and analysis would be needed to demonstrate these potential effects for real buildings.

**Figure 15: Del Taco Unmet Cooling Hours by Setpoint, Indirect Evaporative Cooling Only**



Source: Electric Power Research Institute

<sup>4</sup> He, Yingdong, et al. "Comfort, energy efficiency and adoption of personal cooling systems in warm environments: A field experimental study." *International journal of environmental research and public health* 14.11 (2017): 1408.



## **Modeling Results for Energy Innovation Center Site**

Due to problems associated with accessing baseline data for the EIC site, energy modeling was not possible. The site underwent a change in building automation vendor during the term of our study. As a result, custody of historical energy performance data of the pre-existing IEC units was uncertain, and the data that was retained was incomplete and unsuitable for analysis.

### **Model Calibration**

Extensive literature exists regarding the construction and calibration of whole building energy models. It is generally accepted in the literature that the current methods of calibrating whole building energy models rely on an insufficient amount of data to perform the calibration.

In one study, Coakley et. al. reviewed methods of matching building energy simulations to measured data (Coakley et. al. 2014). The study reviewed the existing literature and highlighted the problems and merits of several calibration techniques. According to the study, a detailed model calibration using a “fully descriptive law-driven model of a building system” provides “the most detailed prediction of building performance.” EnergyPlus is recognized as one of the most robust modeling tools for simulating building energy use and relies on first principles for much of the modeling techniques; however, some of the energy management system modeling strategies are not fully descriptive of the technology.

Despite the strengths of the law-driven calibration method, Coakley et. al. indicate that the calibration method falls short because it requires “significant time, effort, and expertise,” and because the building system is always “over-parameterized and under-determined.” The authors further point out that the under-determined system is typically treated by tuning parameters to match the performance data. Although parameter tuning allows the energy modeler to match the model performance to the measured data, the energy modeler cannot be certain that the chosen parameter is the parameter driving the change in the real system.

### **Calibration Process**

The simulations reported are based on building models that use actual, historical weather and available site data as model inputs and utility-metered and other observable data to achieve realistic results. The calibration described in this report was conducted by defining several known parameters and then tuning unknown parameters to match the performance of the monitored building. Measured data was used for the demand of the lighting and internal loads. A modeling study was conducted to determine a reasonable ground boundary condition. Manufacturer data was used for the system performance curves. Measurements and visual inspections of the building envelope performance informed the calibration.

After tuning unknown parameters to match the calibration periods, the researchers tested the model against other periods of field data, for periods when (1) the performance data was verified to be captured accurately, and (2) the HVAC systems were not being worked on or changed. Due to the complexity of the field study, the early monitoring periods did not always meet the criteria for high quality data.

## Calibration Results

Calibrating a model by applying measured results in the field is a key component of improving its soundness and accuracy. This section summarizes the model calibration process and results.

### Western Cooling Efficiency Center Site

The final results of the parametric variation are tabulated in Table 3. Source: Electric Power Research Institute

Table 4 contains a comparison of the final calibrated model results to the experimental results. The data illustrate that the model consistently under predicts the building loads in both heating and cooling. The cumulative error in the load predicted by the model compared to the measured data was -minus 7 percent.

The modeled power use was calibrated to match the observed power use by changing the heat pump’s cooling and heating coefficient of performance (COP). The modeled electrical energy consumption during heating matched the field data to within 1 percent during the winter calibration period. Matching the cooling data was more challenging than matching the heating data. The main difficulty was due to low overnight cooling loads in the measured data that are not present in the model. These loads have an outsized effect on the modeled electrical energy use. Importantly, the calibrated model does not account for these loads. Since the final model includes a thermostat setback, the researchers focused on matching electrical energy consumption during occupied periods. The researchers matched the electrical energy consumption to within 13 percent for occupied periods in the summer calibration period.

**Table 3: Calibrated Modeling Parameters**

Parameter	Value
Schedule	Always Available
Electric Gains / Lighting Gains	12 W/m <sup>2</sup> / 2.54 W/m <sup>2</sup>
People	18.58 people/m <sup>2</sup>
Winter Set Point	75°F (24°C)
Summer Set Point	72°F (22°C)
Exterior Wall Construction R-Value	1.4 hr-ft <sup>2</sup> -°F/BTU

Source: Electric Power Research Institute

**Table 4: Comparison of Calibrated Model Results to Experimental Results**

Period	Field Data Cumulative Load	Overall Model % Error
Summer Calibration Period (2 weeks)	12,796 kBTU* cooling	-20%
Winter Calibration Period (2 weeks)	13,893 kBTU heating	-10%
Summer Test Data (1 month)	28,234 kBTU cooling	-17%
Winter Test Data (2 weeks)	3,782 kBTU heating	-38%

\*kBTU = thousand British thermal units

Source: Electric Power Research Institute

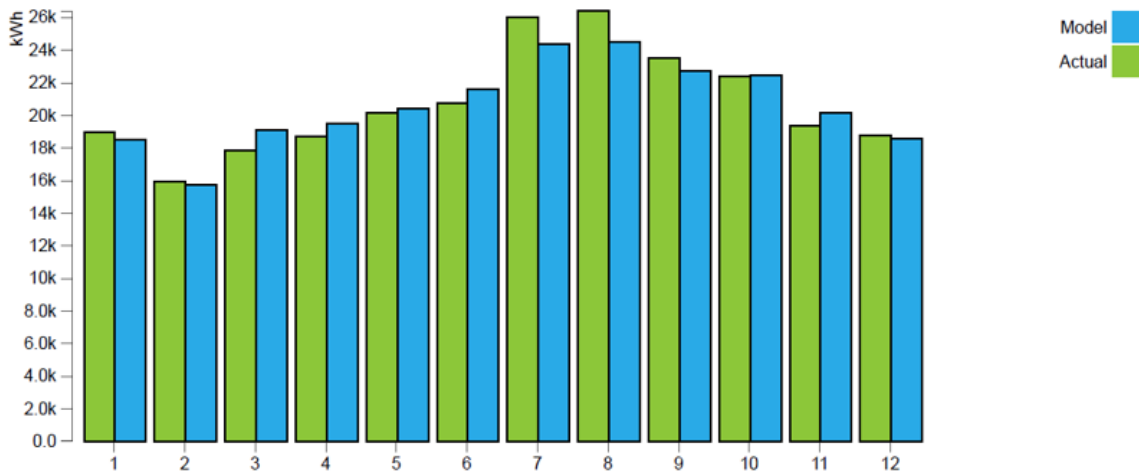
## Del Taco Site

Industry-standard guidelines for calibrated simulations (ASHRAE Guideline 14-2014 and U.S. Department of Energy Federal Energy Management Program) were used to establish criteria for satisfactory agreement with ground truth. Detailed calibration results are depicted in **Error! Reference source not found.**, based on monthly data comparisons over a full calendar year (May 2018 – April 2019). Actual weather year data were obtained for the closest available weather stations from White Box Technologies and converted to EnergyPlus weather format using the Elements freeware tool. Historical utility interval meter data were obtained via the Customer Information Standardized Request process from Southern California Edison for the fast-food restaurant site.

**Figure 16: Model Calibration Results, Electricity Consumption – Del Taco Site**  
**Electricity Consumption (kWh)**

CV(RMSE) = 4.77

NMBE = 0.51



	1	2	3	4	5	6	7	8	9	10	11	12
Start	1/1	2/1	3/1	4/1	5/1	6/1	7/1	8/1	9/1	10/1	11/1	12/1
End	1/31	2/28	3/31	4/30	5/31	6/30	7/31	8/31	9/30	10/31	11/30	12/31
Actual	18,941	15,931	17,828	18,724	20,172	20,723	26,017	26,386	23,490	22,382	19,380	18,804
Model	18,525.35	15,744.33	19,073.08	19,518.23	20,391.1	21,603.24	24,400.92	24,474.52	22,718.42	22,445.82	20,163.69	18,545.22
NMBE	-2.19%	-1.17%	6.98%	4.24%	1.09%	4.25%	-6.21%	-7.24%	-3.28%	0.29%	4.04%	-1.38%

Source: Electric Power Research Institute

The base case model was deemed well-calibrated when the estimated mean bias error and coefficient of variation of the root mean square error were within specified ASHRAE and Federal Energy Management Program guidelines for the calibration period. Once the base case model was sufficiently well-calibrated, inputs to the calibrated model were modified to reflect all additional scenarios of interest and typical weather for each climate.

## Energy Innovation Center

Initial analysis of site-monitored HVAC power data revealed significant data quality issues that prevented the completion of calibration activities and additional parametric simulations. Data were found to be missing or incomplete for both the time period of interest and the number of

HVAC systems of interest. As such, modeled HVAC use significantly exceeded the monitored HVAC use.

## **Improving Future Modeling of Integrated Variable Refrigerant Flow+Indirect Evaporative Cooling Systems**

EnergyPlus is a robust whole-building energy modeling program; however, throughout the course of this project several gaps in its capabilities were identified that affected the building modeling efforts. Gaps in the objects available in EnergyPlus were identified in several categories including ducting, ventilation, evaporative cooling, VRF systems, calibration tools, and runtime errors.

### **Ducting**

The objects for modeling air distribution ducting are flexible and allow for simulation of duct leakage and thermal losses. One aspect of the air distribution objects that often fails to be representative of reality is that any zone that has a supply air inlet must also have a return air outlet. Many real buildings have air distribution systems with a single centrally located return and several branches of ducts that distribute the supply air throughout the building. In these buildings, air must flow from the zones with supply inlets to the zone(s) with return outlets. Requiring a supply inlet and return outlet in each zone simplifies calculations but fails to capture the effects that the flow of transfer air between zones has on building performance.

### **Ventilation**

- Supply ventilation: EnergyPlus has no built-in objects that support positive pressure ventilation systems.
- Exhaust ventilation: Although it is possible to simulate negative pressure ventilation systems in EnergyPlus using the "AirflowNetwork" objects, these objects cannot be simultaneously simulated with an air-loop or any other objects that incorporate a fan.
- Balanced ventilation: The majority of objects in EnergyPlus are compatible with a widely implemented pseudo-balanced ventilation system. It is "pseudo" because only a single fan is used to exhaust return air and supply outdoor in equal quantities. Modeling a ventilation system as pseudo-balanced may introduce acceptable error.

### **Evaporative Cooling**

The version of EnergyPlus that was used to complete the modeling efforts in this project included objects for modeling direct, indirect, and indirect-direct evaporative coolers. These objects could only serve one zone and could not be incorporated into an air loop or air distribution system. As a workaround, "EnergyManagementSystem" objects, which allow insertion of user-defined programs into EnergyPlus, were used to simulate the evaporative cooling equipment in multizone air loops. Recent updates to EnergyPlus have addressed this shortcoming, and evaporative cooling equipment can now be modeled in multizone air loops without any custom programs.

### **Variable Refrigerant Flow**

Significant discrepancies between manufacturer-*rated* and actual VRF performance, attributable to differences in manufacturer-specific system controls, have been observed and reported. Such discrepancies may manifest as calibration errors or prediction errors between

simulated outputs and observed performance, undermining the validity of underlying building models.

When actual VRF performance is unknown or uncertain, the modeler has a limited set of actual performance data from similar or related systems on which to rely. Platforms such as the National Renewable Energy Laboratory's (NREL's) Building Component Library (<https://bcl.nrel.gov/>) and modeling forums such as Unmet Hours (<https://unmethours.com/questions/>) could be used to alert modelers to best-practice guidance, EnergyPlus components, and additional measures that better reflect real-world performance of rapidly evolving HVAC technologies such as VRF. As of the time of writing, only one example of a real-world VRF system (Daikin's REQY series) is available on NREL's Building Component Library site. NREL has conceded that "VRF systems have improved rapidly in the last few years, and researchers need to update the curves, especially for low-temperature operation."

Moreover, objects for modeling VRF systems are included in EnergyPlus; however, only ductless cassettes are supported and objects for modeling ducted indoor fan coils are not included. The control strategy implemented in these objects is rigid and cannot be reconfigured to match the behavior of many commercially available VRF systems.

### **Calibration Tools**

Existing calibration tools/techniques for EnergyPlus currently require use of OpenStudio reporting measures or the OpenStudio Parametric Analysis Tool. However, for certain HVAC application scenarios that still cannot be accurately modeled in OpenStudio (for example, certain energy management system controls measures) such tools cannot be used, limiting the scope for model improvements. Enabling a modeling workflow that allows for seamless importation of EnergyPlus input (.idf) files for use in OpenStudio would expand the possibilities and ease of model calibration to ground truth and real building performance.

### **Runtime Errors**

There are simulation runtime errors that occur when VRF measures such as the "ZEDG VRF with DOAS" and "NZEHVAC" from NREL's Building Component Library are applied to EnergyPlus models with energy management system controls (such as those present in the VRF+IEC model described above). This issue limits the ease of modifying existing models with site-specific HVAC controls to simulate more advanced HVAC systems such as VRF. This is a known issue and is reportedly to be resolved by NREL.

# CHAPTER 4:

## Field Demonstration of Variable Refrigerant Flow Indirect Evaporative Cooling Systems

---

This chapter describes the field demonstrations of the VRF+IEC systems, covering:

- Site selection
- Controller development
- Baseline determination
- Process description (instrumentation, installation, commissioning)
- Results analysis

### Site Selection

The project team ultimately demonstrated the VRF+IEC system at three sites (Table 5), each located in the service territory of a different California IOU, and each featuring a different equipment retrofit action.

**Table 5: Summary of Variable Refrigerant Flow + Indirect Evaporative Cooling Demonstration Sites**

Site Location	Utility	Building Type	Installation
Western Cooling Efficiency Center (WCEC) UC Davis West Village Bldg. MU-5 215 Sage St Davis, CA 95616	PG&E	Multi-purpose office and laboratory research	Retrofit IEC unit to pair with incumbent VRF unit
Del Taco 26951 Aliso Creek Rd. Aliso Viejo, CA 92656	SCE	Quick-serve restaurant	Replace existing RTU with a VRF unit and IEC unit
SDG&E Energy Innovation Center (EIC) 4760 Clairemont Mesa Blvd. San Diego, CA 92117	SDG&E	Multi-purpose offices, conference, and kitchen demonstration	Retrofit VRF unit to pair with incumbent IEC units

Source: Electric Power Research Institute

It was important to have a site in each of the three IOU service territories, representing a cross-section of California climate zones. It was equally important to encompass a diversity of building types, including facilities with multi-purpose zones, to understand system performance under a variety of load and occupancy conditions and comfort requirements. Finally, it was instructive to have a diversity of retrofit scenarios to gain insight into different installation processes. The three sites collectively encompassed every possible circumstance of installation:

1. Retrofit an IEC into a building to combine with an incumbent VRF system (WCEC site)
2. Retrofit both a VRF and an IEC unit to replace an incumbent RTU system (Del Taco site)
3. Retrofit a VRF to condition building zones with incumbent IEC units (EIC site)

### **Western Cooling Efficiency Center Site**

This field demonstration evaluated the baseline performance of the HVAC system installed in a light commercial office building in Davis, California. To establish the baseline performance of the HVAC system, the sensible cooling, latent cooling, heating, ventilation rate, and energy used for HVAC in the building were monitored. The building was monitored for one year so that system performance under a complete set of seasonal conditions could be observed.

The building is located in Davis, California, which is located in a hot dry climate zone (CEC Climate Zone 12 or ASHRAE Climate Zone 3). The office is located on the bottom story of a four-story mixed residential/commercial building seen in Figure 17. Heating and cooling for the occupied spaces is provided by a VRF system. The office space is continuously ventilated by a roof-mounted supply fan that delivers air from outside through a chase where it is ducted to the indoor VRF fan coils. The three-pipe VRF system is capable of simultaneous heating and cooling and is controlled by 13 individual thermostats.

**Figure 17: Rendering of Western Cooling Efficiency Center Exterior**



Source: Electric Power Research Institute

The HVAC system consists of 13 indoor fan coils and two outdoor heat pumps, which are plumbed and controlled to function as a single unit. Each fan coil has a dedicated thermostat and the fan coil capacities range from 7.5 thousand BTUs per hour (MBH) to 48 MBH of cooling and 8.7 MBH to 54 MBH of heating. Each outdoor heat pump is rated at 92 MBH of cooling and 103 MBH of heating for a combined rated capacity of 184 MBH for cooling and 206 MBH for heating. The fan coils represent a total connected capacity of 234 MBH of cooling and 274 MBH of heating. The ratio of connected capacity to available capacity is 127 percent for cooling and 133 percent for heating. A ratio higher than 100 percent is common practice because in most cases the fan coils should not need to operate simultaneously under normal operating conditions.

The objective of the field evaluation was to establish baseline data regarding performance of the HVAC system, including the effects of occupant behavior. The baseline data was used to

validate an EnergyPlus™ model of the bottom story of the building, which assisted in the development of improved control algorithms for VRF systems with integrated ventilation.

Upon the conclusion of the baseline monitoring, the demonstration site was retrofitted with a DOAS with an indirect evaporative cooler. A new control system based on the modeling results was implemented to integrate the DOAS, IEC, and VRF systems in a way that optimized performance. Monitoring continued for an additional year to evaluate the performance of the DOAS, IEC, and new control scheme.

## **Del Taco Site**

One of the commercial building segments identified as a viable candidate for a hybrid VRF+IEC system was fast food, or quick-serve, restaurants, based on the following attributes:

- Two major conditioning zones — the kitchen area and the customer dining area — each with its unique loading conditions and setpoint requirements for comfort
- High ventilation requirements
- Peak times of operation on a daily and weekly basis

The hybrid VRF+IEC system lent itself well to these building attributes, since it offered individual zonal control, high ventilation with IEC as a DOAS system, and the ability to switch to VRF operation during periods of high cooling demand.

Del Taco is a nationwide operator and franchisor of quick-serve restaurants across 15 states concentrated in the Pacific-Southwest region, with 372 of its 596 locations in California. Through a relationship with the HVAC contractor that services Del Taco's locations in Orange County, the project team identified a Del Taco restaurant in Aliso Viejo, California, whose HVAC equipment was due for a retrofit or upgrade and was therefore a prime candidate for demonstrating the VRF+IEC system.

This Del Taco location is a single-story building with an indoor space measuring 1,894 square feet (Figure 18). The majority of space (and cooling needs) are taken up by the dining room and kitchen. Each of these areas had an independent, 7½-ton York HVAC unit previously installed in 2014. There is also a small, back-office area next to the kitchen, which was originally served by a 3½-ton HVAC unit. Del Taco desired to have these units replaced.

Original (incumbent) Del Taco HVAC unit models were:

- York model ZXG12D2B1AA1A111A1 nominal 7½-ton gas electric unit
- York model ZXG08D2B3AA1A111A2 nominal 7½-ton gas electric unit
- York model ZXG12D2B1AA1A111A2 nominal 3½-ton gas electric unit



**Figure 18: Aliso Viejo Del Taco**



Source: Electric Power Research Institute

A nearly identical Del Taco location was identified four miles away in Irvine, California, that could serve as a control site, or basis of comparison. The description of baseline determination is explained in later in this section.

Rooftop views of both the Del Taco Aliso Viejo treatment site and Del Taco Irvine control site are shown in Figure 19.

**Figure 19: Rooftop Views Del Taco Treatment (left) and Control (right) Sites**



Source: Electric Power Research Institute

### **Energy Innovation Center Site**

The SDG&E EIC is a multi-purpose education, training, and meeting facility that showcases innovative energy efficiency technologies and green building practices to the public (

Figure 20). As a double LEED® platinum facility, the EIC serves as a living laboratory that provides visitors with hands-on interactions with emerging energy-efficient technologies, building materials, and design practices. The EIC features versatile classrooms and meeting rooms that can be partitioned in a variety of ways to host groups throughout the year. One of the distinguishing features of the EIC is its commercial demonstration kitchen, which provides the food service industry with a hands-on opportunity to test innovative energy-efficient commercial cooking equipment.

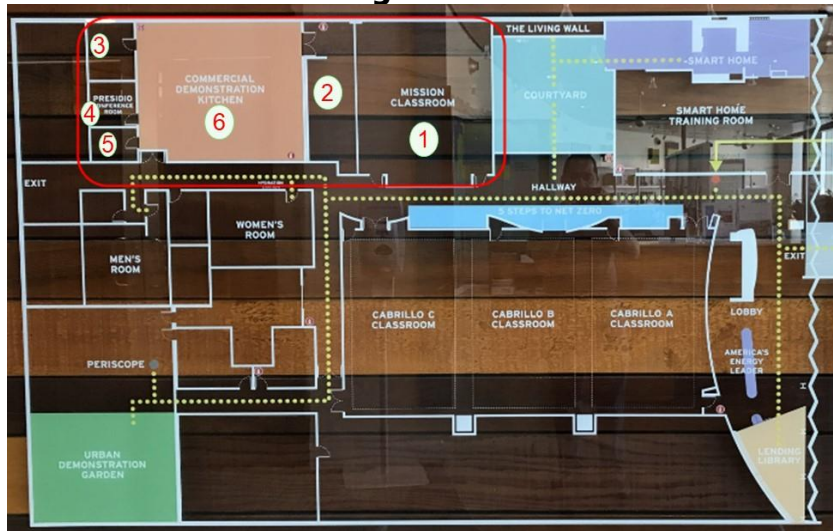
**Figure 20: Energy Innovation Center Street Facing View**



Source: Electric Power Research Institute

Six conditioning zones along one side of the building, as shown in the bird's eye view of Figure 21, had been served by three incumbent IEC units. SDG&E and EIC staff had indicated that the IEC units were unable to provide sufficient cooling during peak loading periods (that is, during the summer months), particularly to sustain comfort levels for high occupancy. As a result, the project team deemed this an appropriate opportunity to retrofit a VRF to provide cooling for peak demand and high occupancy periods.

**Figure 21: Energy Innovation Center Conditioned Zones for Variable Refrigerant Flow Retrofit**



Source: Electric Power Research Institute

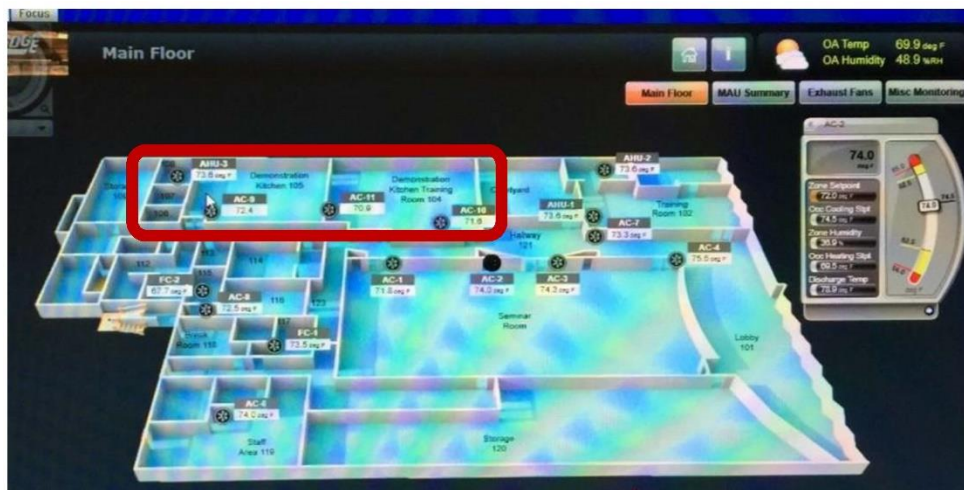
These six zones, collectively an area of 5,000 square feet, were served by three IEC units as shown in Table 6 and in Figure 22.

**Table 6: Mapping of Indirect Evaporative Cooling Units to Conditioning Zones**

Zone	IEC Unit
1) Mission Classroom	#1 ("AC-10")
2) Kitchen staging area	#2 ("AC-11")
3) Storage room	#3 ("AC-9")
4) Conference room	#3 ("AC-9")
5) Conference room	#3 ("AC-9")
6) Commercial Demonstration Kitchen	#3 ("AC-9")

Source: Electric Power Research Institute

**Figure 22: Incumbent Heating, Ventilation, and Air Conditioning Equipment at Energy Innovation Center, Building Automation View**



Source: Electric Power Research Institute

For this site, the operative goal was not energy savings but rather increased comfort and use of space through as energy-efficient a method as possible. Although the existing building automation system had baseline data on the energy consumption of these IEC units, which could be compared to the post-retrofit VRF+IEC system, the operative metrics were qualitative, based on feedback from the EIC staff on the performance of the hybrid system and tangible effects on occupant comfort and increased use of space to host events during hot days and with higher occupancies.

## Controller Development

One of the most technically challenging elements, and key advancements, of the project was developing an integrated controller to regulate and optimize the operation of the VRF+IEC hybrid system. The primary function of the controller was to regulate the operation of the VRF+IEC system to optimize energy savings while maintaining occupant comfort requirements. The secondary function was to manage operation of the VRF+IEC system during simulated demand response events.

Developing the controller involved the following steps:

1. Develop governing logic for system operation.
2. Source a solutions provider to implement the controller.
3. Convert governing logic into control sequence algorithms.
4. Design control architecture, combining site hardware with cloud computing.
5. Establish data input and output requirements.
6. Install and commission controller.
7. Integrate controller with data monitoring devices.
8. Test performance on-site.

Traditionally, VRF and IEC systems operate as stand-alone systems, with an optional additional interface that connects them to the building management system using standards such as BACnet, Modbus, or other proprietary communication protocols. The integrated control schema developed for the VRF+IEC hybrid system was based on governing logic informed by adaptive capabilities (learned building behaviors) and response to monitored inputs such as ambient temperature, indoor temperature set points, humidity control, occupancy sensing, and occupant comfort preferences. These inputs served as triggers to shift between the following four modes of operation:

1. Economizer-only mode
2. IEC mode
3. VRF (partial or full loading) mode
4. Simultaneous VRF and IEC mode

### **Economizer-Only Mode to Provide “Free-Cooling”**

When outside air dry-bulb temperature (OAT DB) is lower than supply air dry-bulb temperature (SAT DB) the optimal operational mode is economizer-only ( $OAT\ DB < SAT\ DB = Economizer\ mode$ ).

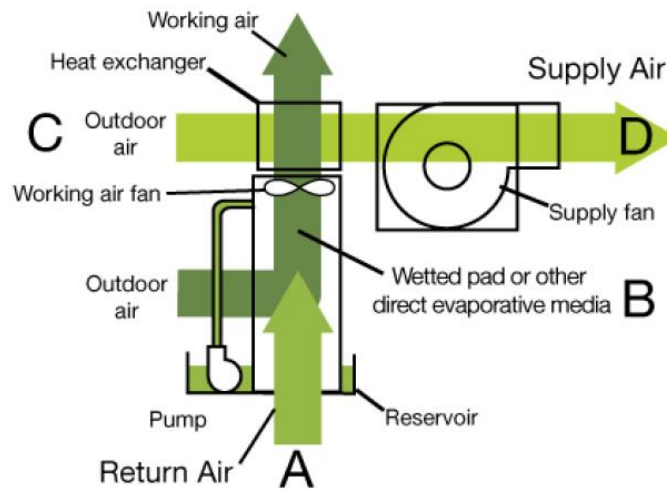
SAT DB is typically set at the building balance point temperature when neither heating nor cooling is needed, typically 65°F. In this mode, either the outside air damper or a variable speed fan regulates the amount of air intake and reaches 100 percent of damper position, or fan speed, when OAT DB is equal to 65°F.

### **Indirect Evaporative Cooling Mode**

When OAT DB is higher than the building balance point temperature (65°F) but less than the outside air wet-bulb temperature (OAT WB), the optimal operational mode is IEC mode only ( $building\ balance\ point\ (65^\circ F) < OAT\ DB < OAT\ WB = IEC\ mode$ ).

The rationale for this control logic is illustrated in the IEC schematic diagram of Figure 23. Return air passes from the conditioned space over a wetted medium to remove sensible heat, and the outside air enters and is indirectly cooled evaporatively before being delivered to the space.

**Figure 23: Indirect Evaporative Cooler Schematic Diagram**



Source: Electric Power Research Institute

### **Variable Refrigerant Flow Only Mode**

This mode can be an option to toggle the control mode from operation of IEC to the VRF only mode. When OAT DB is greater than 65°F and OAT WB is greater than 58°F, the operational mode can be the following two conditions: VRF only or VRF+IEC.

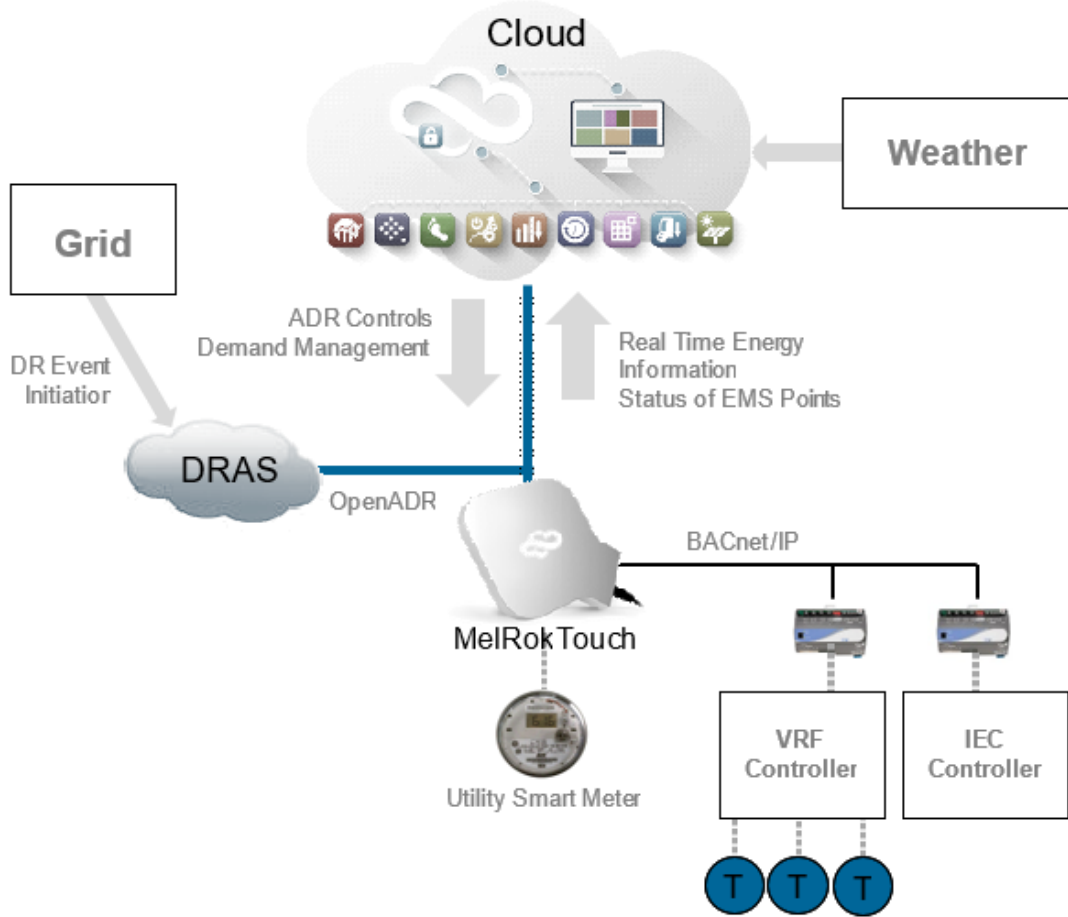
### **Variable Refrigerant Flow + Indirect Evaporative Cooling Mode**

In this mode, the IEC ramps up as the first stage and then activates the VRF system as a second stage of cooling to meet any individual zone's cooling loads.

Return air passes from the conditioned space over a wetted medium in the IEC system to remove sensible heat, and the outside air enters and is redirected to second stage cooling for the VRF system.

The next step was converting governing logic into corresponding control sequence algorithms and developing a cloud-based architecture and communications platform to provide overlaying controls for both a VRF and an IEC system. The research team addressed this challenge by identifying and securing a controls vendor, MeIRok, with the requisite expertise to build a controller using generic hardware and applying BACnet to extract data and send control signals to the VRF system. This challenge was compounded by the fact that all commercial VRF systems employ proprietary control systems. The control system architecture is illustrated in Figure 24.

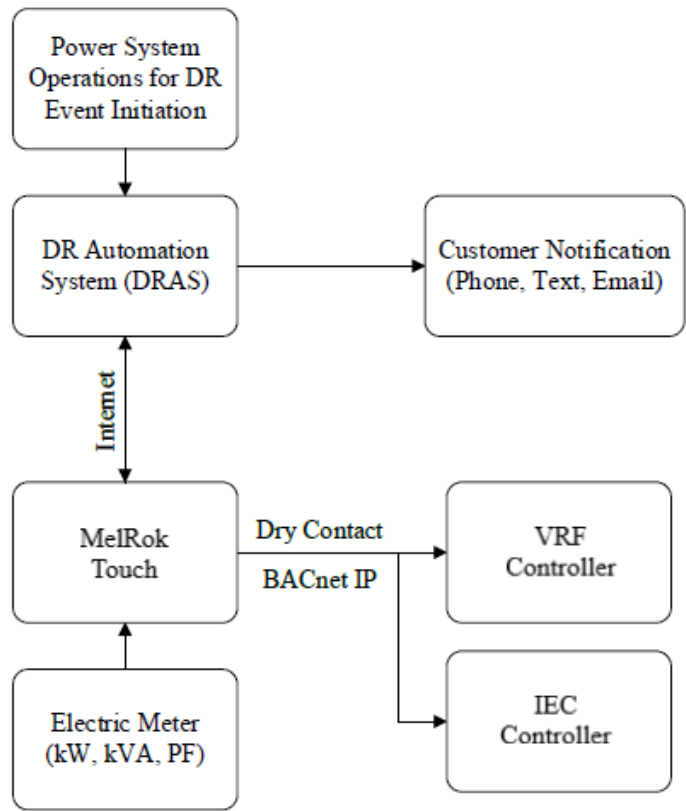
**Figure 24: Control System Architecture**



Source: Electric Power Research Institute

While the controller’s primary objective was to optimize for energy savings, a secondary objective was to enable demand response (DR). DR signals are initiated by the utility’s system operations, requesting load shedding to rebalance energy demand with supply. Referring to the DR control architecture depicted in Figure 25, this signal is processed by the DR automation server, which sends the control mode in a discrete signal to the building and also sends a notification in advance of the event. This control mode is typically sent over the internet, typically as an extensible markup language (XML) instruction. Thus, the setup typically requires a Java Application Control Engine controller to integrate loads for unified real-time control. Then the control modes are implemented as a set of load control strategies, codified as algorithms, to provide load controls to respond to DR events.

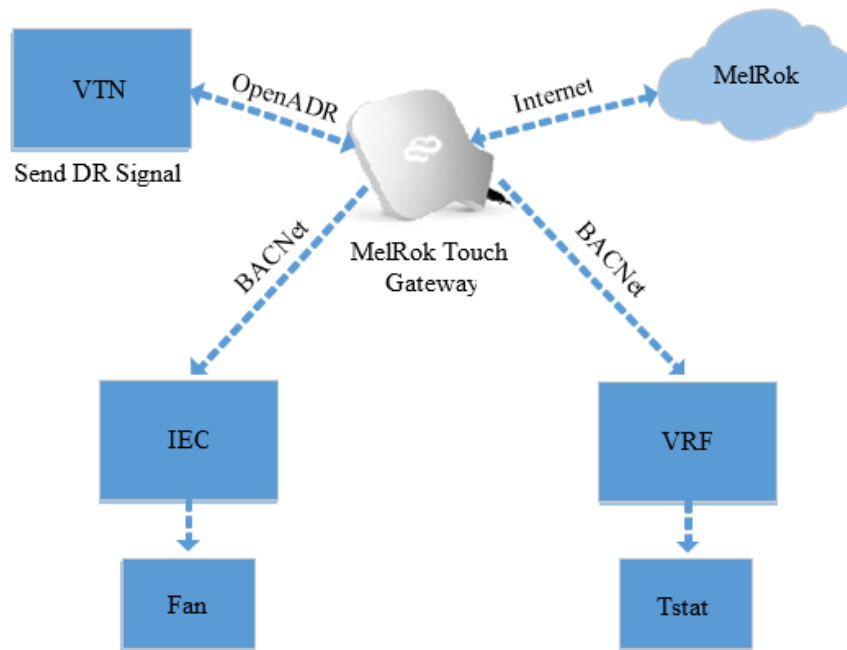
**Figure 25: Automatic Demand Response Control Architecture**



Source: Electric Power Research Institute

The communications among components is achieved via open standards — OpenADR 2.0b and BACnet. As shown in Figure 26, the MelRok cloud on the upper right sends control commands that determine which of the four operational modes of the VRF+IEC system are actuated, and the sequence of components that are activated for a DR event. The control sequence is sent out via MelRok Touch to the VRF units. The controlled object of the IEC was the fan speed, and the controlled object of the VRF was the thermostat setpoint. During a DR event, the virtual top node (VTN) – the system operations, sends the signal to the MelRok Touch as the virtual end node (VEN) via OpenADR 2.0b, and acknowledges the VTN – DR Automation Server, upon receiving the signal. Then, the MelRok Touch translates the DR event information (for example, critical peak pricing info, kW reduction requirement, and other details) into signals that interoperate with the components for end-use controls.

**Figure 26: Open Standards Communications for Control of Components**



Source: Electric Power Research Institute

## Western Cooling Efficiency Center Site

### Instrumentation and Baseline Measurement

The researchers conducted field tests to demonstrate the performance of adding a DOAS with an IEC to a building with a VRF space conditioning system. The demonstration site was monitored for one year prior to the installation of the IEC to establish the performance of the baseline system as installed. The performance of the system was characterized based on the power consumption and the cooling and heating delivered. After the installation of the IEC, the system performance was monitored for an additional one-year period to determine the performance of the retrofitted system.

HVAC system monitoring included continuous measurements as well as a series of one-time measurements to develop pressure-flow and power-flow correlations for each fan. The following is a list of measurements that were collected at one-minute intervals for the entire year of baseline monitoring:

#### Ventilation

- Ventilation supply differential fan pressure
- Indoor ventilation duct differential pressures
- Ventilation inlet temperature and relative humidity
- Indoor ventilation duct air stream temperatures

#### Indoor Fan Coils

- Supply and return temperature
- Supply and return relative humidity



- Static pressure across each indoor fan coil
- Voltage
- Current
- Power factor

### **Outdoor Heat Pumps**

- Temperature of refrigerant at outdoor coil outlet, compressor suction, compressor discharge
- Static pressure across the outdoor coil fan
- Ambient pressure
- Voltage
- Current
- Power factor

### **Thermal Zones**

- Temperature and relative humidity
- CO<sub>2</sub> concentration
- Occupancy

### **Fan Coil Sensors**

Indoor fan coil monitoring included measurement of voltage, current, power factor, return air temperature, return air relative humidity, supply air temperature, and supply air relative humidity. Additionally, the duct pressure of the ducted indoor fan coils was measured.

Voltage taps were installed on the screw terminals for the fuses for each of the fan coils. Current transducers were installed before the fuse on each leg of power supplying each indoor fan coil. The power meter measuring the voltage and current also captured the phase angle between the voltage and current of each leg. The phase angle was used to calculate the power factor of each fan coil.

Return air temperature and relative humidity sensors were installed before the return air filter on each fan coil. For ducted fan coils, the supply air temperature and relative humidity sensors were installed downstream of the fan coil before the first splitter. For ductless fan coils, the supply air temperature and relative humidity sensors were installed on one of the supply air louvers.

The duct pressures across the ducted fan coils were measured with differential pressure transducers. One pressure port of each differential pressure transducer was open to ambient and the other was connected to an averaging array of four pressure taps equally spaced along the circumference of the duct. The array of pressure taps was installed as far from the fan coil as possible and before the first splitter.

### **Ventilation Sensors**

Monitoring of the ventilation system included ventilation air temperature, ventilation air relative humidity, and pressure drop across each register. The ventilation air temperature and relative humidity sensors were installed in the ventilation duct downstream of the ventilation

fan. The pressure drop across each register was measured with a differential pressure transducer. One pressure port of the differential pressure transducer was open to ambient and the other was connected to an averaging array of four pressure taps equally spaced along the circumference of the ventilation duct. An array of pressure taps was installed just before each register.

### **Outdoor Heat Pump Sensors**

Monitoring of the heat pump included voltage, current, power factor, fan static pressure, and ambient air temperature and relative humidity. Voltage taps were installed on the screw terminals for the heat pump fuses. Current transducers were installed before the fuse on each leg of power supplying the heat pump. The power meter measuring the voltage and current also captured the phase angle between the voltage and current of each leg. The phase angle was used to calculate the power factor of the heat pump. The ambient air temperature and relative humidity sensors were installed inside a radiation shield mounted in an open area on the same roof as the heat pump.

### **Room Sensors**

The monitoring of each room included air temperature, relative humidity, CO<sub>2</sub> concentration, and occupancy. The sensors for each measurement were packaged into a single device and mounted in each room 0.6 meters from the ground, which is the standard location for assessing occupant thermal comfort.

### **One-Time Measurements**

One-time measurements were taken for flow measurements throughout the system. A mapping method was used whereby flow was measured by a non-installed instrument, and either supply pressure or fan power was measured simultaneously by an installed instrument. Tracer gas measurements were used for all ducted flows, whereas flow hoods were used for all non-ducted flows. The tracer gas measurements were mapped to the corresponding duct pressure within the operating range, while the flow hood readings were mapped to the corresponding power of the fan within the operating range. The flow was mapped against power for the non-ducted units because there was no way to reliably measure the pressure rise across the fan within these units. Likewise, tracer gas tests could not be conducted on the non-ducted units because the supply and return paths are not separated and cannot be easily isolated for tracer gas injection and sampling.

The tracer gas system is composed of an injection system and a measurement system. The CO<sub>2</sub> injection rate is measured and controlled by a mass flow controller. The CO<sub>2</sub> enters the duct at several injection sites, where it mixes with the airstream. The researchers placed the measurement system far downstream of the injection site where the CO<sub>2</sub> would be sufficiently well mixed. The CO<sub>2</sub> concentration before and after injection was measured to calculate a baseline value of the CO<sub>2</sub> concentration, and a python analyzer calculated the air flow in the duct. The procedure was repeated for three speeds of the fan-coil, and the pressure-flow map was developed using concurrent pressure readings.

The pressure-flow correlations were developed using the relationship that the volumetric flow rate (Q) is proportional to the square root of the pressure:

$$Q = C * \sqrt{P}$$

Because the flow from the tracer gas system was reported in standard cubic feet per minute, the units of  $Q$  are also standard cubic feet per minute. The constant,  $C$ , was determined for each fan coil from the one-time flow measurements and applies over the full range of flows. Once  $C$  was calculated, the error of the correlation was checked and was typically between 1 percent and 5 percent. One fan coil had an error of 6.5 percent at the bottom end of the correlation.

The powered flow hood system was composed of a calibrated duct blaster fan and controller and a ducted flow hood. The measurements were taken at the return grille of the non-ducted units. A DG-700 digital pressure sensor was used to monitor the differential pressure across the duct blaster fan and the differential pressure between the flow hood and ambient. The resistance imposed by the ducted flow hood on the fan-coil, which is not present during normal operation, is overcome by powering the duct blaster fan. The researchers increased the fan power until the differential pressure between ambient and the inside of the flow hood was reduced to zero, simulating the typical pressure at the return grille. The flow was recorded concurrently with power measurements to develop the power-flow correlations.

The power mapping revealed that five of the six non-ducted fan coils had only marginal change in power with fan speed setting change, had a very poor power-flow correlation, or had both problems. Because it was difficult to distinguish between the fan speeds based on the power alone, the flows were averaged over the expected range of operation, and the flow was calculated based on whether the unit is on or off.

The sixth non-ducted fan coil, which was larger than the others, had a distinguishable trend between power and flow. Four fan speeds were mapped; however, two of the fan speeds produced identical results. Because there were effectively only three fan flow rates, the data was modeled with a linear correlation to allow for calculation of the trend uncertainty. The correlation  $R^2$  was 0.979, which means the linear model worked well over the observed range.

One-time measurements were also recorded for the ventilation fan power consumption and the volumetric flow rate. The ventilation system had a single speed fan, so the volumetric flow rate was also constant. Pressure sensors in the ventilation system were used to determine when the ventilation fan was on.

## **Installation and Commissioning Process**

The ideal location to install the IEC would have been on the roof, adjacent to the ventilation chase for convenient connection of IEC ventilation air into the building's existing ventilation ducting. However, since project time constraints precluded this option, the IEC was instead installed inside the lab space on the first floor of the building.

Since the IEC is designed for outside placement — to directly draw air from, and exhaust air to, the ambient environment — indoor placement required the installation of new ducting to connect outside air into the unit and supply air from the unit into the ventilation air ducts. To replicate an outdoor environment, booster fans were installed in each duct, with a proportional-integral-derivative controller to compensate for the pressure drop imposed by adding ducting to the IEC's intake and exhaust. The installation of the IEC is shown in Figure 27, Figure 28, and Figure 29.

**Figure 27: Indirect Evaporative Cooling Insulated Supply Flex Duct During Construction**



Source: Electric Power Research Institute

Figure 28 shows the supply air ducted from the IEC to the indoor ducted air distribution system and exhaust air ducted to an exhaust loop.

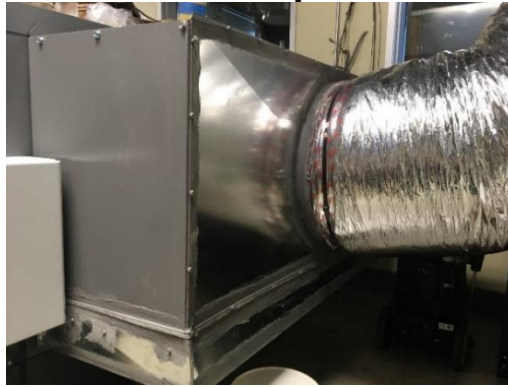
**Figure 28: Completed Indirect Evaporative Cooling Supply and Exhaust Connections**



Source: Electric Power Research Institute

The completed IEC inlet was ducted to allow the use of a booster fan to overcome extra friction due to the flex ducts, as shown in Figure 29.

**Figure 29: Completed Indirect Evaporative Cooling Inlet Ducting**



Source: Electric Power Research Institute

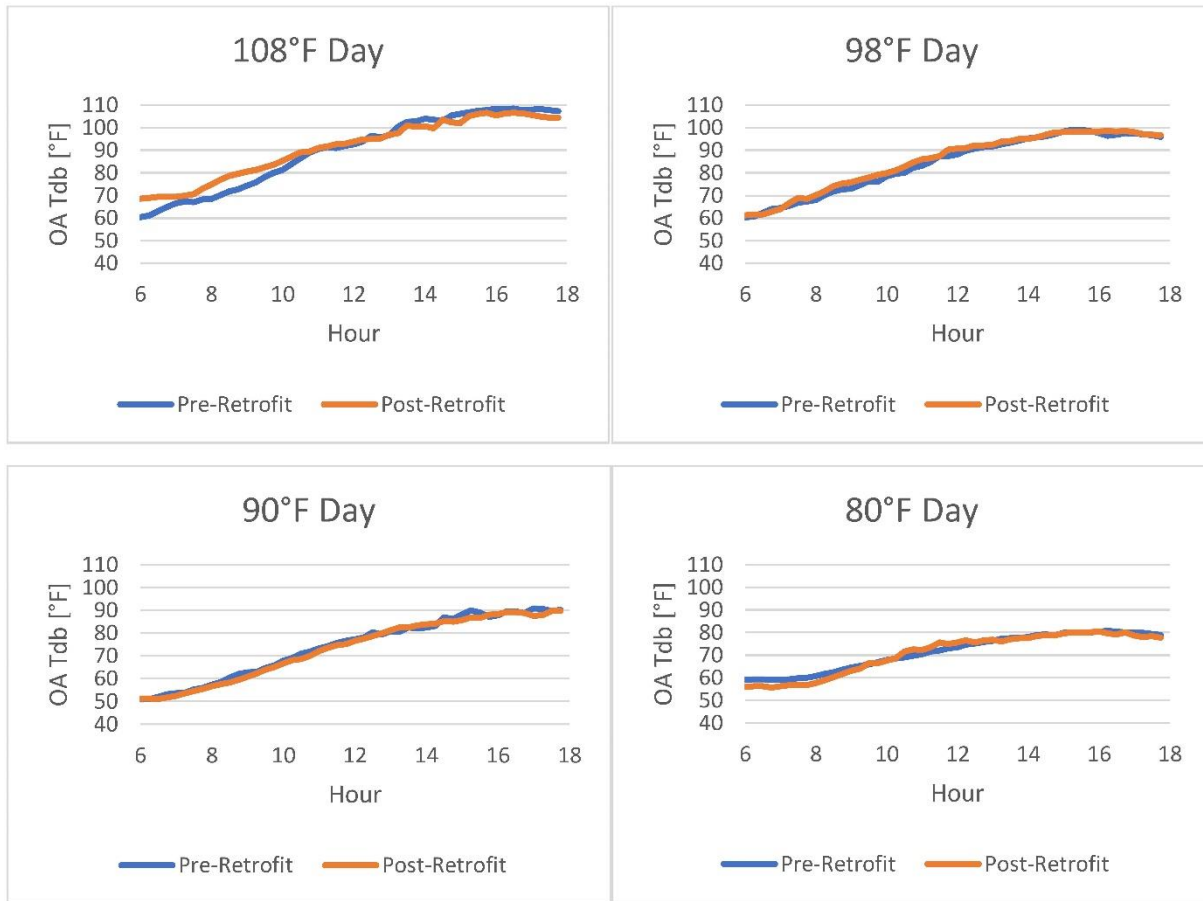
The VRF and IEC systems were configured for the IEC to serve as the primary cooling source with the VRF system activated when the building's load exceeded the IEC's cooling capacity. Accordingly, the thermostat controlling the IEC was set at 70°F while the minimum setpoint for the VRF controllers was set to 72°F, assuring that the VRF system would not turn on unless cooling from the IEC was insufficient to maintain an indoor temperature below 72°F.

### **Field Results**

Energy savings at this site were based on the measured difference in energy consumption between the pre-existing VRF system and the retrofit configuration with the IEC. One of the challenges of this approach was accounting for pre- versus post-retrofit variability in such factors as outdoor air conditions and daily occupancy behavior, which affected indoor loads, efficiency, and cooling capacities of both the VRF and IEC systems. This variability made it difficult to discern trends in comparative plots of VRF (pre-retrofit) versus VRF+IEC (post-retrofit) performance, such as daily energy use as a function of maximum daily outdoor air dry-bulb temperature.

The approach was to compare pre-retrofit and post-retrofit energy use on *similar days*, as defined by closely matched outdoor air dry-bulb temperature profiles that vary no more than 3.5°F for every hour between 6:00 a.m. and 6:00 p.m. The temperature profiles for four sets of pre-retrofit and post-retrofit *similar days* are shown in Figure 30, representing maximum daily temperatures of 80°F, 90°F, 98°F, and 108°F, respectively.

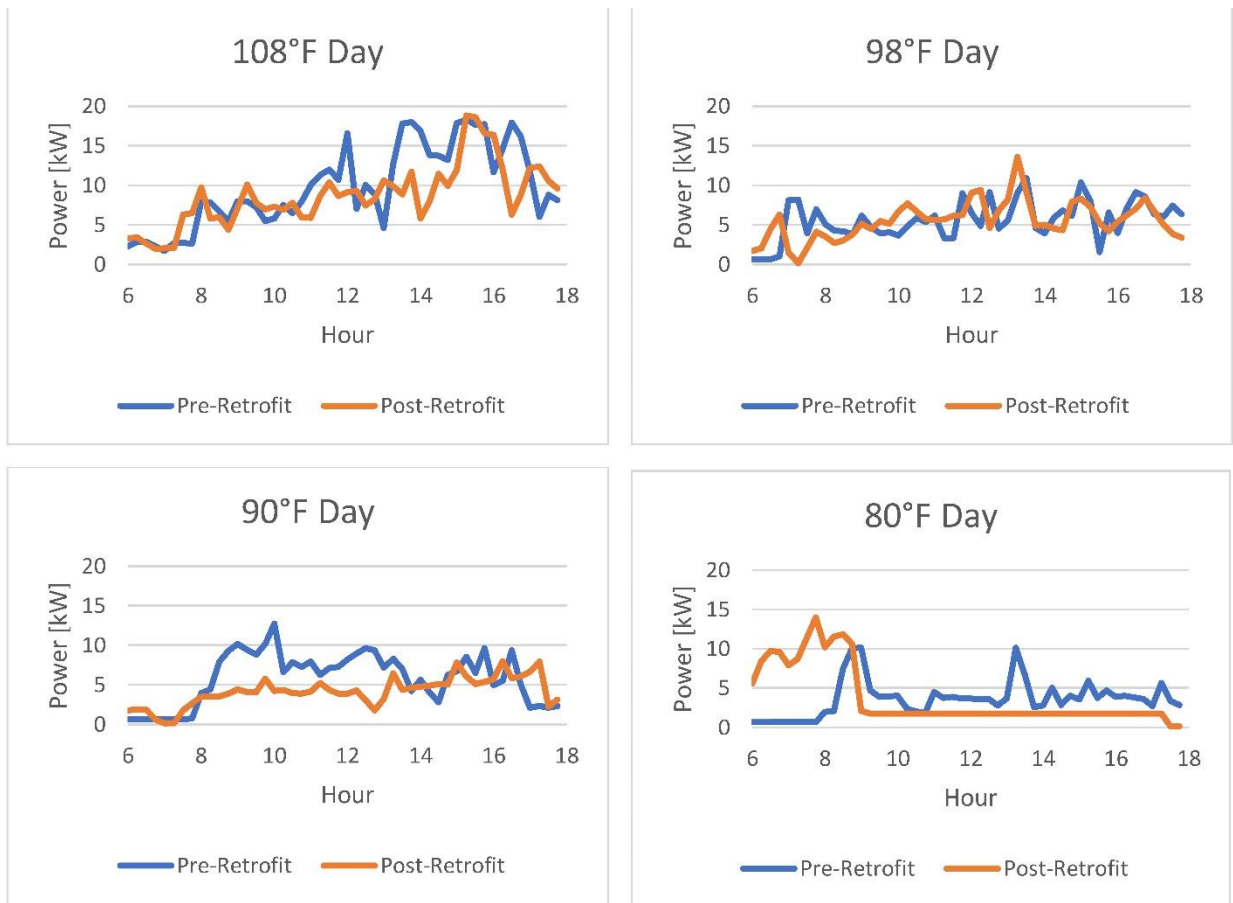
**Figure 30: Outdoor Dry-Bulb Temperature on Similar Days**



Source: Electric Power Research Institute

The hourly power draw of the pre-retrofit and post-retrofit HVAC systems on these four sets of similar days is shown in Figure 31.

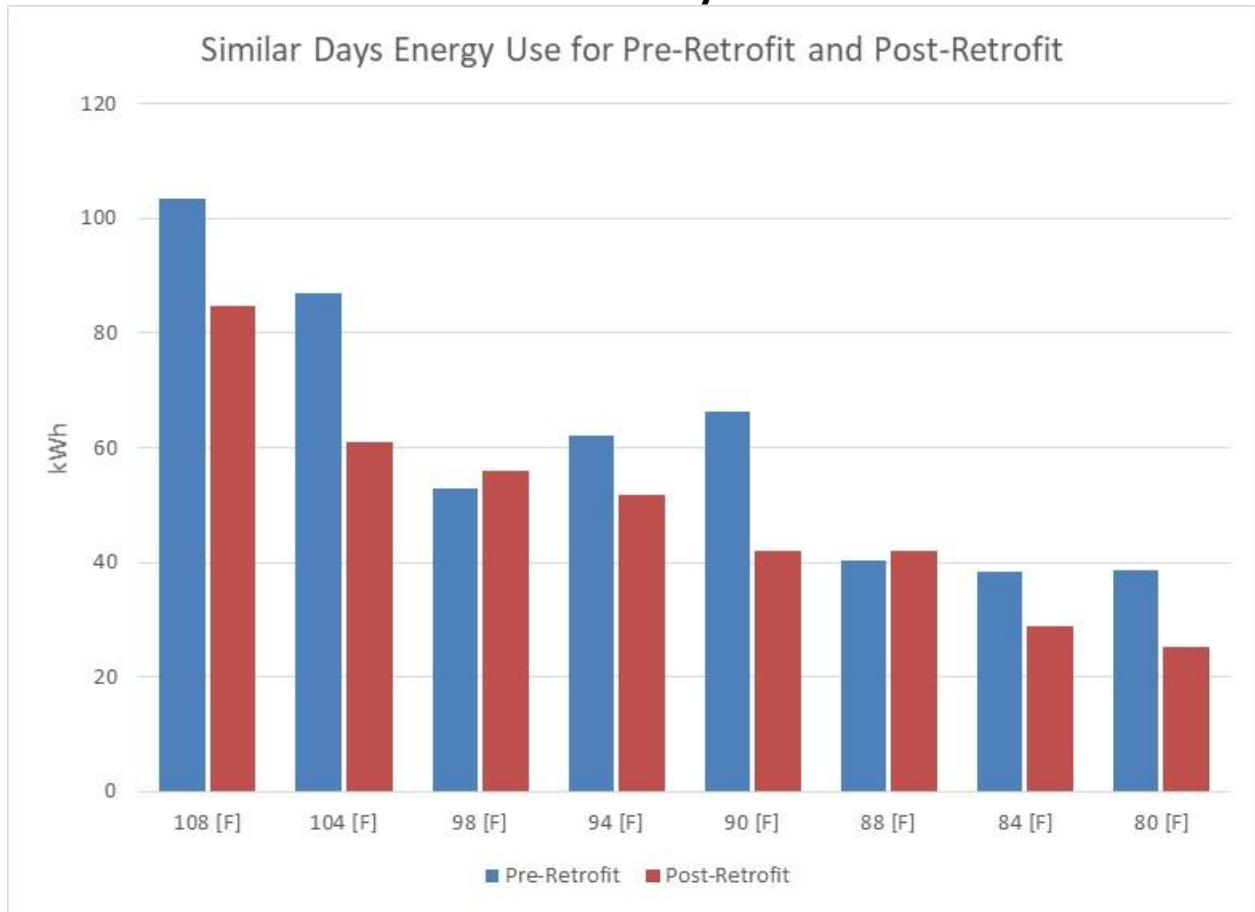
**Figure 31: Power Draw on Similar Days, Pre-Retrofit and Post-Retrofit**



Source: Electric Power Research Institute

Although the outdoor air conditions are very similar during these days, the power use profiles are very dynamic, and it is not obvious whether and by how much the daily energy consumption differs between the pre- and post-retrofit cases. The daily pre-retrofit and post-retrofit daily energy consumption of the VRF and ventilation systems is shown in Figure 32 and Table 7.

**Figure 32: Total Heating, Ventilation, and Air Conditioning Energy Consumption on Similar Days**



Source: Electric Power Research Institute

The results of Figure 33 are tabulated in Table 7.

**Table 7: Total Heating, Ventilation, and Air Conditioning Energy Consumption on Similar Days**

Maximum Outdoor Air-Dry Bulb Temperature [°F]	Savings [kWh]	Percent Savings [%]
108	18.66	18.0
104	26.06	29.9
98	-3.22	-6.1
94	10.47	16.8
90	24.20	36.6
88	-1.77	-4.4
84	9.39	24.5
80	13.31	34.4
Average	12.1	18.7

Source: Electric Power Research Institute

The daily post-retrofit energy consumption is less than or almost the same as the pre-retrofit energy use. The days with almost equal energy use are likely due to the IEC being on the cusp



of changing from ventilation to cooling mode and adjusting the discrete fan speed. Not having a continuous change between ventilation and indirect evaporative cooling mode meant the VRF system would provide additional heating or cooling to offset the output of the IEC to equal building load. Based on the information in Table 7, it is estimated that the annual cost savings would be about \$300 per year, assuming an average savings of 12 kWh/day, 120 days and \$0.20/kWh.

## **Del Taco Site**

### **Baseline Determination**

A control-treatment experimental design was employed for the Del Taco site. Performance of the VRF+IEC system at the Del Taco restaurant in Aliso Viejo (treatment site) was compared to a simultaneous performance of an RTU at an identical Del Taco restaurant (control site) located four miles away in Irvine.

- Del Taco treatment site: 26951 Aliso Creek Road, Aliso Viejo, CA 92656
- Del Taco control site, 6211 Lake Forest Dr., Irvine, CA 92618

The control site was selected because of its physical similarity to the treatment site and close proximity. Since Del Taco is a restaurant chain, its locations have the same square footage and identical physical layout. Both sites also had similar historical occupancy patterns and sales volumes, which minimized the risk of variances in load from differences in customer occupancy and kitchen activity. Finally, since the two sites were located only four miles apart, they were subject to the same weather conditions. Accordingly, this baseline approach controlled for variances in weather, occupancy, and other exogenous factors that can affect thermal load so as to isolate the energy effect of the HVAC systems in the respective sites.

Both sites were instrumented with identical sets of monitoring devices to measure the energy consumption of their respective HVAC systems, as well as indoor temperature and humidity and ambient temperature. Both sites were operated with the same indoor setpoint schedules.

### **Process Description**

After identifying the Del Taco locations for the treatment (Aliso Viejo) and control (Irvine), the project team reached an agreement with Del Taco on April 24, 2019, to install the VRF and IEC units and associated instrumentation for monitoring. Drawings were submitted to the city of Aliso Viejo for permitting in mid-May and were approved by June 6, 2019. Construction began on June 10, 2019, and was completed at the end of July 2019 with the installation of a new 16-ton Mitsubishi VRF unit and two Seely IEC units.

HVAC equipment installed at Del Taco treatment site included:

- Mitsubishi 16-ton PURY-P192TSLMU-A VRF, with 3½-ton concealed air handler
- Two Seely Climate Wizard CW-H-15 IEC units

Construction was arranged and scheduled to minimize disruption to the operation of the Del Taco restaurant. The existing RTU system was decommissioned and removed, and cranes were used to install the equipment on the roof. A number of HVAC contractors, including electrical and mechanical subcontractors, worked as a team to install and commission the VRF and IEC equipment.

Two new Seely IEC units and one new VRF rooftop unit were installed at the Del Taco treatment site (Figure 33). The VRF unit featured two ducted fan coils serving two separate occupancy zones: the kitchen and the dining area.

**Figure 33: Variable Refrigerant Flow and Indirect Evaporative Cooling Units Installed on Roof of Del Taco**



Source: Electric Power Research Institute

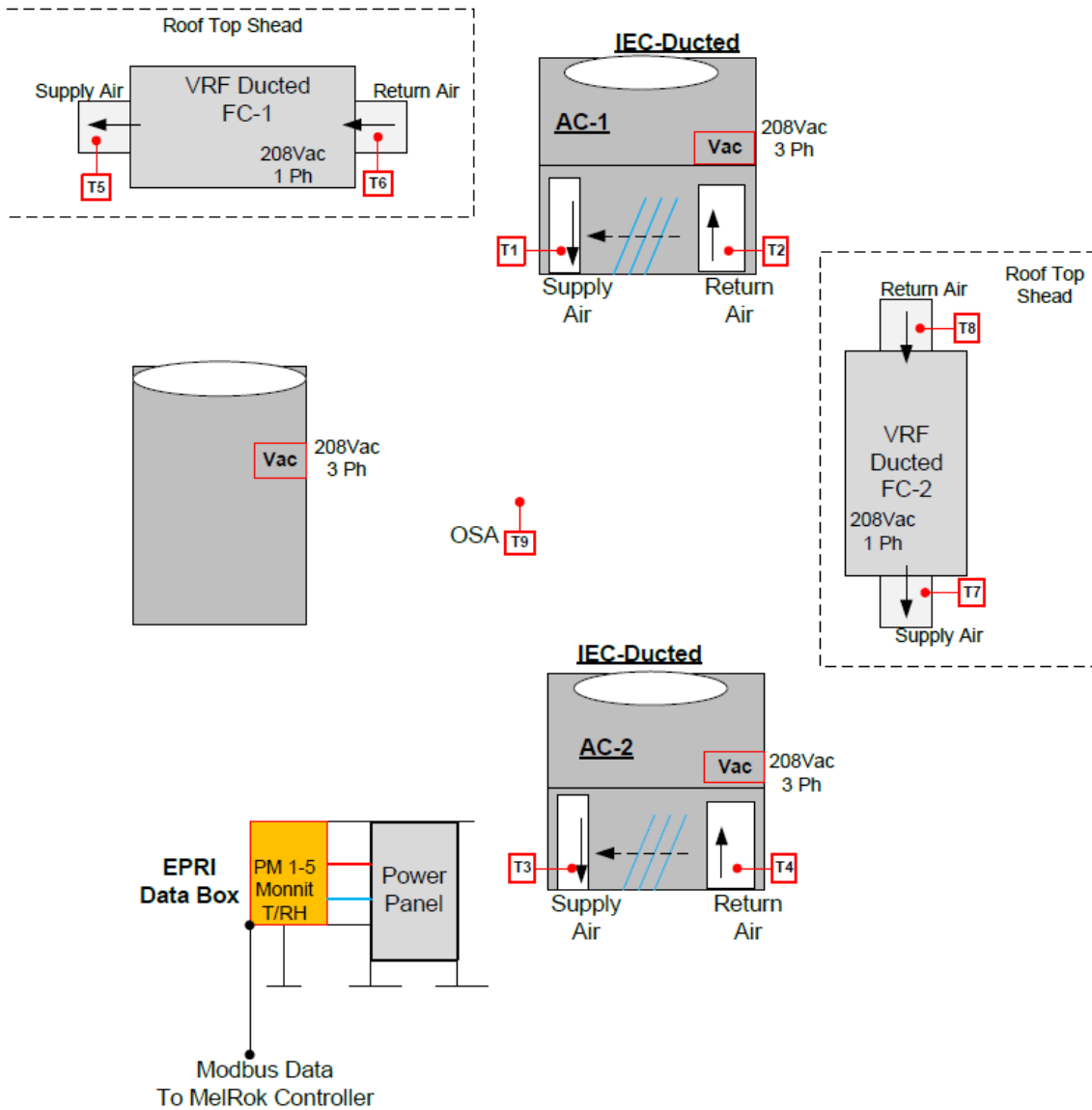
The next step was to install instrumentation to measure and monitor the VRF and IEC systems at the Aliso Viejo treatment location as well as the Irvine control location. Sensors were installed to measure and monitor the following data points for each outdoor unit and fan coil system:

- Voltage
- Current
- Power
- Energy
- Power factor
- Temperature (supply duct, return duct, outside air)
- Humidity (supply duct, return duct, outside air)
- Air Flow (one-time measurement, from an outside source)

The project team developed data boxes to integrate inputs from these sensors with the MelRok controller described in Section 4.2.

Figure 34 illustrates the data monitoring layout at the Del Taco treatment site from the rooftop perspective.

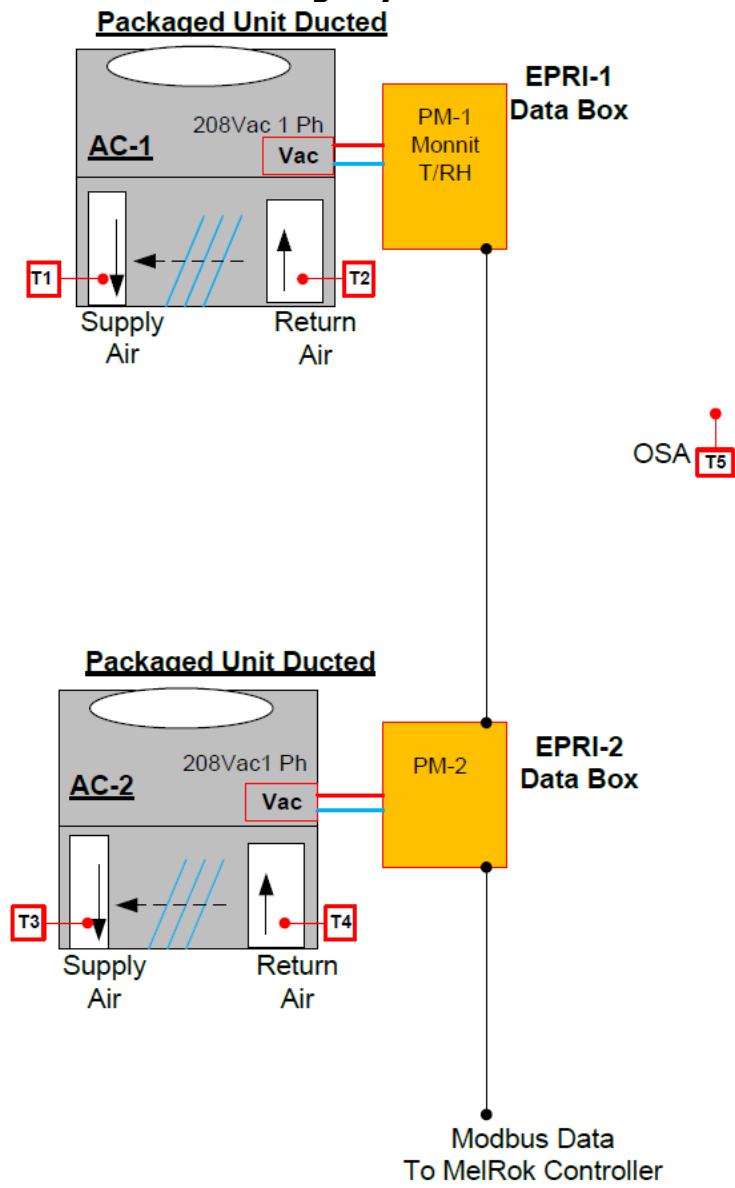
**Figure 34: Data Monitoring Layout at Del Taco Treatment Site**



Source: Electric Power Research Institute

Similarly, Figure 35 illustrates the data monitoring layout at the Del Taco control site from the rooftop perspective.

**Figure 35: Data Monitoring Layout at Del Taco Control Site**



Source: Electric Power Research Institute

### Field Results

A portion of the month of August 2019 was spent commissioning the equipment and installing the instrumentation. As such, September represented the first month of meaningful data, capturing the tail of the summer cooling season into the fall and winter through February 2020. Cumulative measured savings per month are show in Table 8.

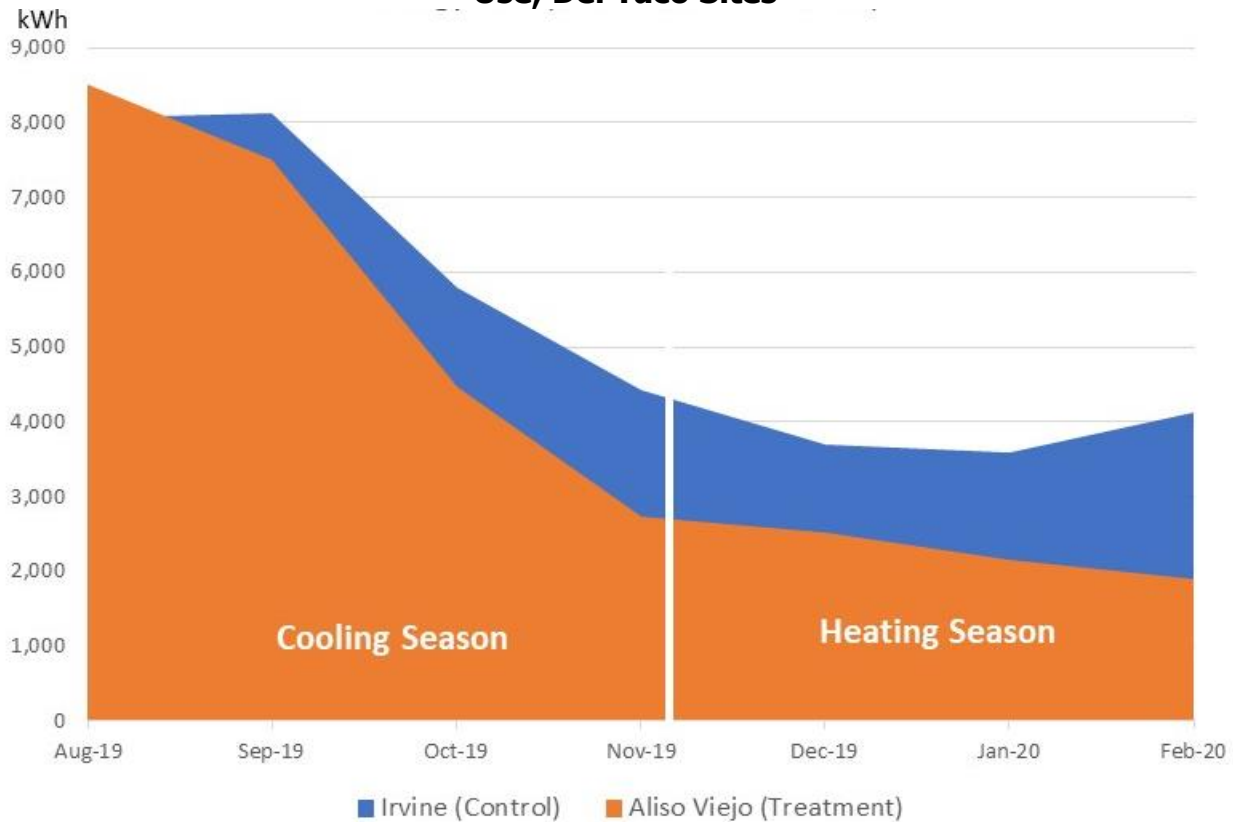
**Table 8: Monthly Cumulative Energy Savings for Del Taco Site**

Month	Cumulative Energy Use Control Site (Irvine, RTU)	Cumulative Energy Use Treatment Site (Aliso Viejo)	Energy Savings
September 2019	8,131	7,499	7.8%
October 2019	5,801	4,470	22.9%
November 2019	4,427	2,736	38.2%
December 2019	3,689	2,510	32.0%
January 2020	3,584	2,163	39.6%
February 2020	4,130	1,908	53.8%
AVERAGE MONTHLY ENERGY SAVINGS			32.4%

Source: Electric Power Research Institute

These results are illustrated in Figure 36.

**Figure 36: Monthly Cumulative Heating, Ventilation, and Air Conditioning Energy Use, Del Taco Sites**



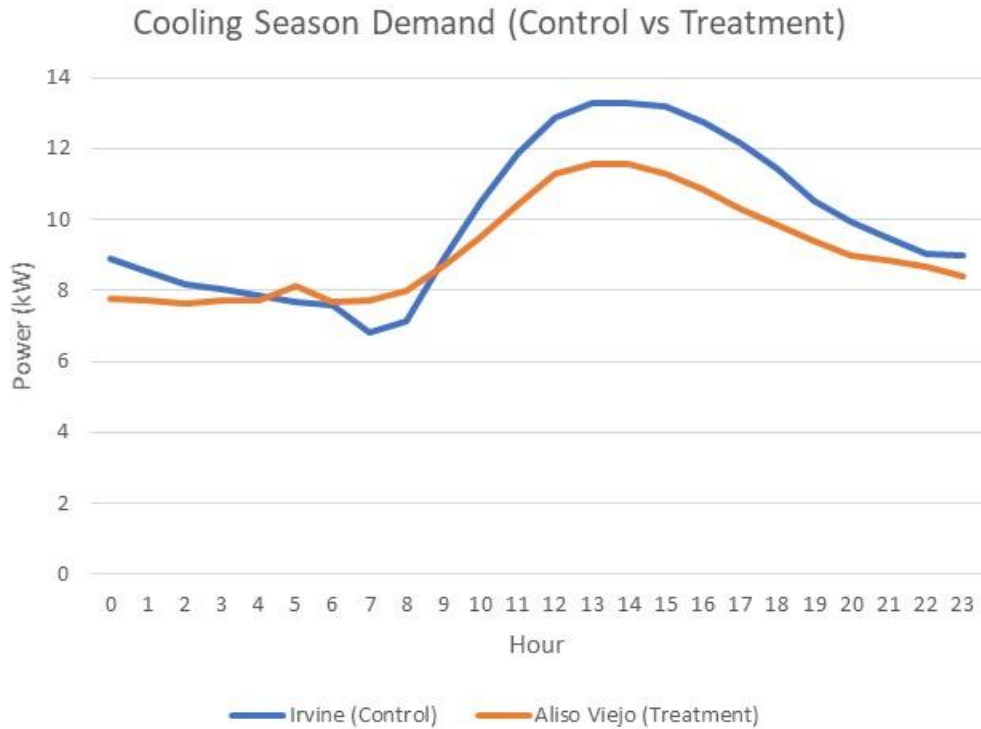
Source: Electric Power Research Institute

The average composite daily demand profile of the two sites for the August – October cooling period is shown in Figure 37, showing that the VRF+IEC treatment site yields a modest demand reduction beginning at around 10:00 a.m. that expands to a more significant

reduction through the afternoon peak. Both restaurants are open 24 hours, hence the persistence of air-conditioning load throughout the 24-hour cycle.

Based on the information from Table 8, the Del Taco site that received the new technology saved about \$3,400 per year.

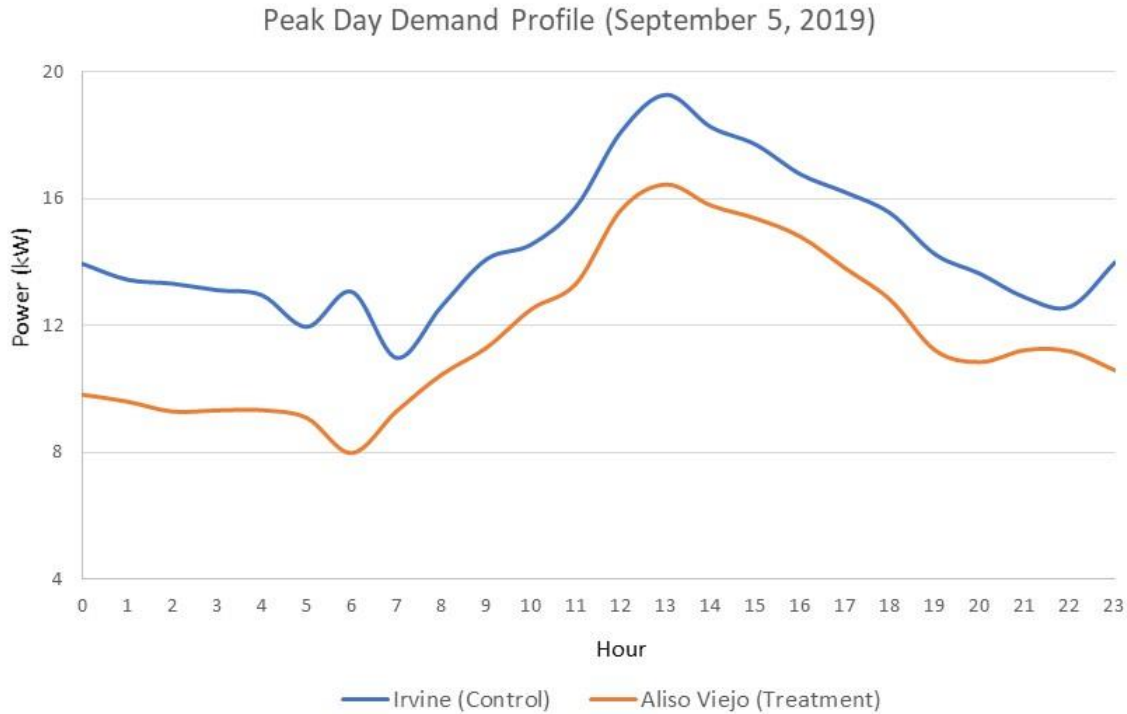
**Figure 37: Del Taco Cooling Season Average Daily Heating, Ventilation, and Air Conditioning Demand Profile**



Source: Electric Power Research Institute

For comparison, the demand profile of the peak day of this period on September 5, 2019, is shown in Figure 38.

**Figure 38: Del Taco Summer Peak Day Heating, Ventilation, and Air Conditioning Demand Profile**



Source: Electric Power Research Institute

The figure illustrates the significant savings of the VRF+IEC unit operating during the late night and early morning hours, compared to the RTU of the control site. Data measurements indicate that the control system dispatched simultaneous use of the VRF and IEC systems that day, with the IEC units providing most of the cooling for the kitchen area while the VRF units provided cooling for the larger dining room.

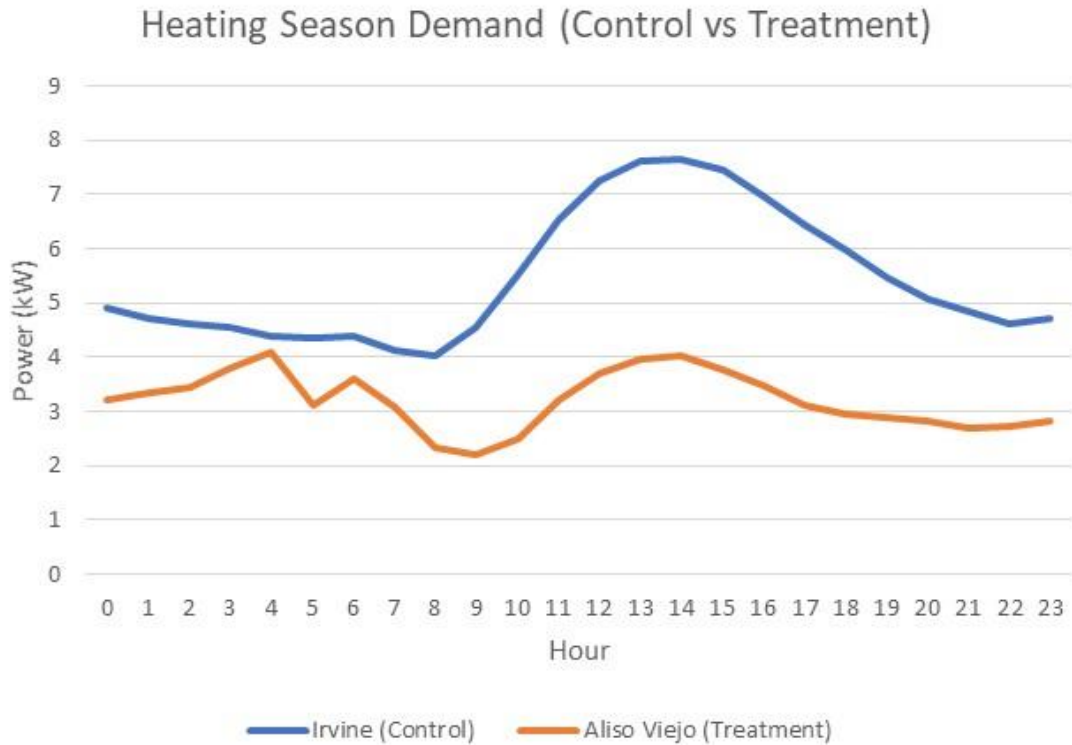
VRF systems are noted for their higher efficiency and energy savings at partial loading conditions compared to RTU units operating at a fixed compressor speed, so the margin of lower demand during these periods aligned with modeled expectations. As the morning progressed through the breakfast period, with the higher occupancy and increasing ambient temperatures, the demand at both locations escalated with the VRF particularly ramping in demand to sustain indoor temperature settings in the dining room.

It is important to note that even as the VRF unit was ramping to near-peak loading conditions through the peak demand periods of the early- to mid-afternoon, the treatment site retained a consistent demand savings margin compared to the control site. Throughout this period, the IEC continued to condition the kitchen area, which helped to alleviate some burden from the VRF. As a result, during the peak hour of 1:00 p.m., the cooling load of the control site was 19.30 kW while the cooling load of the treatment site was 16.47 kW for a demand savings of 14.7 percent. Throughout the 24-hour cycle on this peak day, the average demand savings of the VF+ IEC at the treatment site compared to the RTU at the control site was 20 percent.

The average composite daily demand profile of the two sites for the November – February heating period is shown in Figure 39, showing that the VRF+IEC treatment site yields a modest demand reduction compared to the RTU control site in the early morning hours. As the morning progressed from the breakfast period through lunch, the demand margin between the

two sites increased significantly. Again, since both restaurants are open 24 hours, air conditioning load persisted throughout the 24-hour cycle.

**Figure 39: Del Taco Heating Season Average Daily Demand Profile**

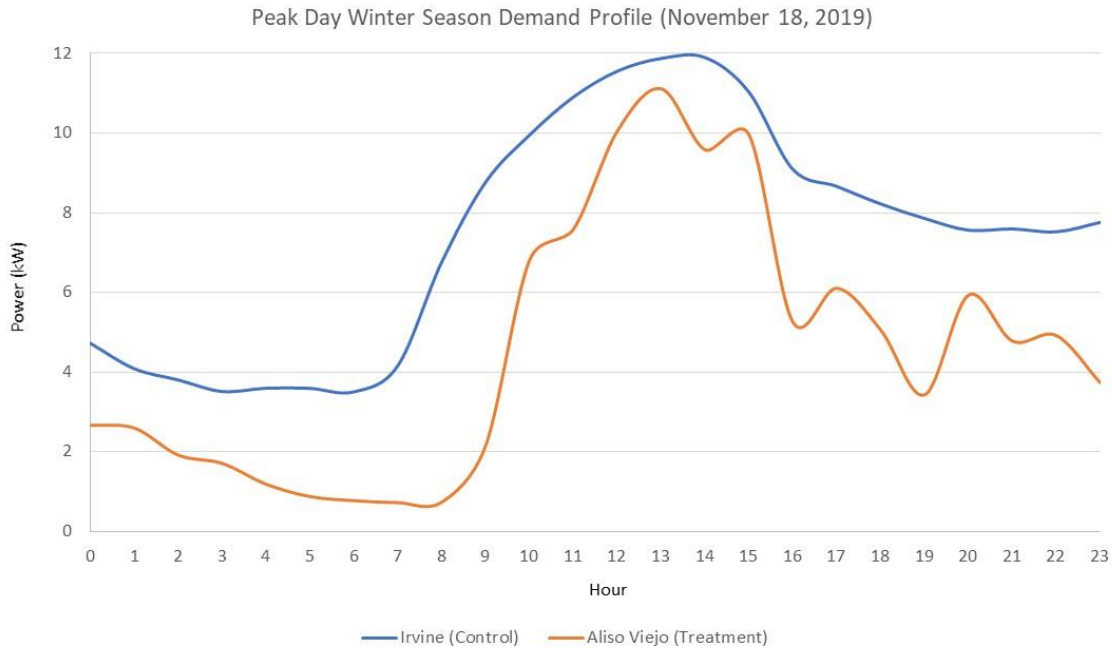


Source: Electric Power Research Institute

For comparison, the demand profile of the peak day of this period on September 5, 2019, is shown in Figure 40. The figure illustrates the significant savings of the VRF+IEC unit operating during the late night and early morning hours, compared to the RTU of the control site. Data measurements indicate that the control system dispatched simultaneous use of the VRF and IEC systems that day, with the IEC units providing most of the cooling for the kitchen area while the VRF units provided cooling for the larger dining room.



**Figure 40: Del Taco Winter Peak Day Heating, Ventilation, and Air Conditioning Demand Profile**



Source: Electric Power Research Institute

As the morning progressed through the breakfast period, with the higher occupancy and increasing ambient temperatures, the demand at both locations escalates with the VRF particularly ramping in demand to sustain indoor temperature settings in the dining room. The figure shows that HVAC demand at the treatment site (VRF+IEC) approaches but does not meet the RTU demand of the control site. While the control site's peak demand for the day at 2:00 pm was 11.89 kW, the simultaneous demand at the treatment site was 9.58 kW, for a savings of 19.4 percent. Throughout the 24-hour cycle on this winter peak day, the average demand savings of the VRF + IEC at the treatment site compared to the RTU at the control site was 45 percent.

## Energy Innovation Center Site

### Baseline Determination

The pre-existing IEC units that had been serving the targeted zones within the EIC building had each been previously instrumented with power meters, with the results being logged into the building automation system, Johnson Controls Metasys. However, retrieving this data proved to be problematic. For one, the Metasys data dashboard for the building did not include information on the power consumption of these IEC units. Secondly, during this project the EIC changed its building control system provider, which required transfer of historical energy consumption data for those IEC units. For a significant period, the baseline data were not available or otherwise accessible to the project team. The data that was eventually obtained were incomplete.

As a result of the problems with obtaining baseline data, a more qualitative approach was taken at the EIC site. The premise of investigation was that the existing IEC units were not adequately cooling the EIC's zones during periods of high ambient temperatures and/or high occupancy. It was explained to the project team that, for example, events planned for the

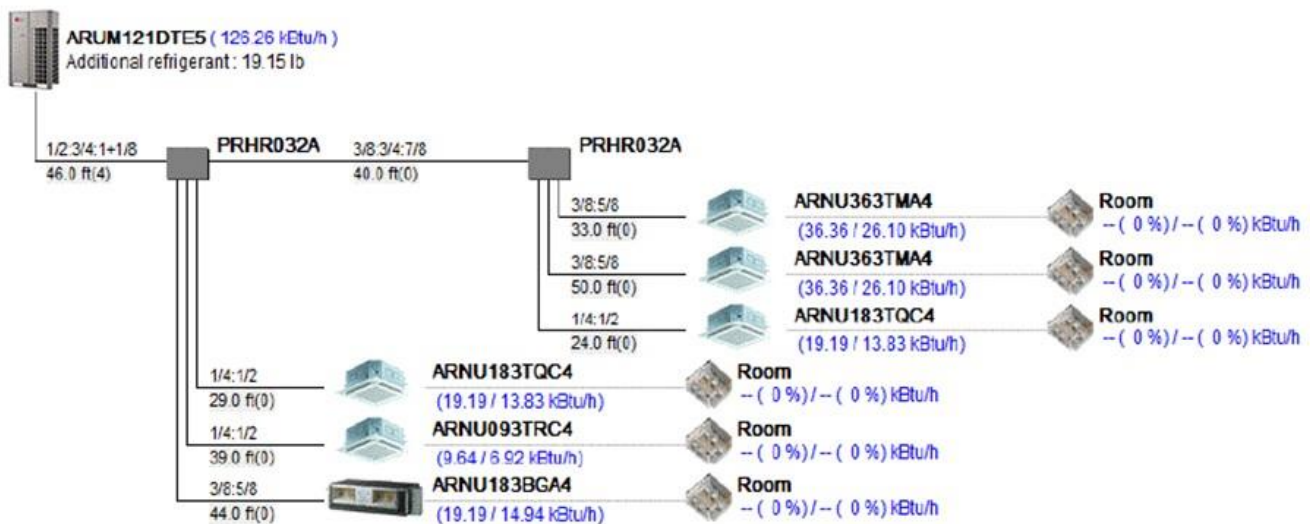
Mission Classroom in the past would sometimes have to be moved or rescheduled due to uncomfortable conditions, particularly during the summer, and to support higher occupancies. The solution, therefore, was to install a VRF system to augment the cooling load for these peak periods while allowing the existing IECs to continue operation during most periods of the year, as regulated by the newly developed master controller.

It was understood that VRF solution was not intended in this case to provide energy savings, since the IEC units themselves are highly energy efficient, but rather to enhance use of the designated spaces and increase occupant comfort. Therefore, the metrics of a successful installation were qualitative measures of improved comfort and usability of the spaces during times of peak cooling loads and high occupancy, as determined by EIC facility staff.

### Process Description

The project team specified and sized a 10-ton VRF system capable of providing sufficient cooling for the six conditioned zones without the operation of the pre-existing IEC units. To provide vendor diversity in VRF units across the three demonstration sites, the VRF model selected for the EIC site was the LG ARUM121DTE5, a 10-ton (cooling) outdoor unit. Six ceiling cassettes were also installed as indoor units for the conditioned zones. The retrofit also required the installation of 305 feet of piping along with thermostats for each zone. A diagram of the VRF installation is shown in Figure 41.

**Figure 41: Energy Innovation Center Variable Refrigerant Flow Installation Diagram**



Source: Electric Power Research Institute

The major activities of the installation process undertaken by the HVAC contractor were:

1. Develop drawings for city permit approvals
2. Provide and install one new LG 10-ton VRF condensing unit
3. Set new condensing unit on lay down polymer roof pad
4. Provide hoisting and rigging to set new condenser on roof
5. Core holes through roof to allow for new refrigerant lines
6. Provide roofer to patch cores and seal tight

7. Provide unistrut and hangers to mount fan coils
8. Install soft copper refrigerant lines to connect cassettes to condensing unit
9. Install hard copper and fittings to connect condensing unit to branch
10. Install pipe hangers to properly support new piping
11. Insulate new copper refrigerant piping
12. Install pipes and fittings to drain condensate from all fan coils
13. Tie condensate drain into nearest acceptable receptacle
14. Install new thermostats for fan coil units
15. Run new thermostat wire from fan coils to new thermostats
16. Run new thermostat wire from fan coils to condensing unit
17. Provide electrician to run new power to ceiling cassettes and condensing unit
18. Provide startup technician to start and test and commission new units for proper operation

### **Field Results**

After the VRF retrofit plans were finalized, but prior to VRF installation, the EIC staff and IEC vendor (Seeley) determined that the insufficient cooling from the incumbent Coolerado IEC units was due to a sensor malfunction. Those sensors were recalibrated by Seeley and as a result the cooling capacity improved noticeably to the point that it was deemed sufficient for most occupancy conditions. Nevertheless, with the installation plans in place, the VRF installation commenced.

The VRF unit was commissioned and deemed to work satisfactorily, providing sufficient cooling for all the zones during the test periods. EIC staff indicated that the blast of cool air from the VRF indoor cassettes was a big difference from what the Coolerado IEC units had been able to provide previously. The controller was also installed and tested for control of the VRF and pre-existing Coolerado IEC units. For a brief period, the hybrid VRF+IEC system operated between alternating modes of exclusive IEC operation and exclusive VRF operation.

However, during a round of LEED re-certification testing, the EIC staff determined that the operation of the VRF system would invalidate the building's distinguished LEED Double Platinum status — a recognition shared by fewer than two dozen facilities around the world — based on not meeting a minimum ASHRAE fresh air ventilation standard for each zone. To retain its LEED Double Platinum status, the EIC facilities staff decided to limit the annual operating hours of the VRF unit. As a result, during the summer season of 2019 there was insufficient data of operation beyond attestation of the EIC staff that the VRF unit worked well. During the winter heating season, the VRF is available as a secondary backup heating source but has rarely been operated in this capacity.

# CHAPTER 5:

## Laboratory Testing of Alternative Refrigerants

---

### Background

Another significant California climate policy goal is to reduce the use of refrigerants with high global warming potential (GWP). Leakage of synthetic refrigerants into the atmosphere, including chlorofluorocarbons and hydrochlorofluorocarbons widely used in HVAC and refrigeration systems, are known to have high GWP potential. California Assembly Bill 3232 requires the CEC, in consultation with the California Public Utilities Commission, California Air Resources Board, and the California Independent System Operator, to assess by January 1, 2021, the potential to reduce GHG emissions in buildings by 40 percent below 1990 levels by 2030. In addition, California Senate Bill 1477 allocates funding for building decarbonization programs. The USEPA mandates a phase-out of hydrochlorofluorocarbons, including the common refrigerants R-22 and R-142b, due to their ozone depleting attributes. Although their production and import are banned starting in 2020, continued use of existing stockpiles can continue through 2030.<sup>5</sup>

Conversion to HVAC systems using alternative low-GWP refrigerants is therefore an important component to achieving these California policy objectives. An added consideration is the use of natural refrigerants, which do not have to be synthetically manufactured because they exist in nature. Although some natural refrigerants have been used in niche market applications for decades, their use is virtually absent in packaged air-conditioning systems, and there is limited understanding of their potential market and energy effect.

Therefore, conversion requires extensive testing to identify suitable refrigerants based on GWP, thermodynamic properties that drive energy efficiency performance, compatibility with existing equipment, and safety issues such as corrosion, toxicity, and flammability. Laboratory testing of low GWP, natural refrigerant HVAC systems warrants California ratepayer funding to inform policy makers and HVAC equipment manufacturers and contractors, and thereby accelerate market adoption and use.

This project provided laboratory testing and system design considerations needed to understand what refrigerants might provide improved performance for VRF operation in California climates. It currently appears likely that the most efficient non-HFC non-GWP refrigerants could be slightly flammable, in which case a pumped secondary heat transfer fluid loop can isolate potentially hazardous refrigerants from the indoor environment. This research developed options for technology opportunities to better clarify future needs and challenges.

Collectively, propane, carbon dioxide, and ammonia are the leading natural refrigerant options based on their low GWP, availability, and favorable thermal properties. Under this project task, heat pump and chiller systems featuring each of these refrigerants were evaluated and tested in three different laboratories in California, Illinois, and Tennessee.

---


<sup>5</sup> U.S. Environmental Protection Agency. <https://www.epa.gov/ods-phaseout>.

# Bundgaard Propane (R290) Chiller

## Equipment Information

EPRI acquired a hydronic heat pump from Bundgaard Refrigeration (model WWC1XS2), a leading manufacturer specializing in propane chillers and heat pumps for more than 15 years located in Copenhagen, Denmark. Table 9 provides the exact specification for Bundgaard’s WWC1XS2.

**Table 9: Bundgaard R290 Chiller Specifications**

Item	Specification	
Manufacturer	Bundgaard Refrigeration	
Model	WWC1XS2	
Unit Load	100%	
Total Cooling Capacity	28.2 kW	
Total Heating Capacity	34.2 kW	
Part Load Minimum	32.7%	
Compressor EER (Cooling COP)	3.58	
Compressor COP (Heating COP)	4.35	
Refrigerant	R290/Propane	

Source: Electric Power Research Institute

Distribution of cooling and heating to indoor units by hydronic means eliminates the need for refrigerant piping to indoor units and the associated risk of leaking a refrigerant, especially one that is flammable such as propane. Using hydronic distribution with multiple indoor units was considered as an alternative to replace a VRF system. This section analyzes energy effects and other issues related to using hydronic heating and cooling in place of a VRF system.

An R-290 refrigerant-based hydronic heat pump was procured and was tested in the PG&E testing facility in San Ramon, California, under Air Conditioning, Heating, and Refrigeration Institute (AHRI) test conditions so the results can be compared with a VRF system.

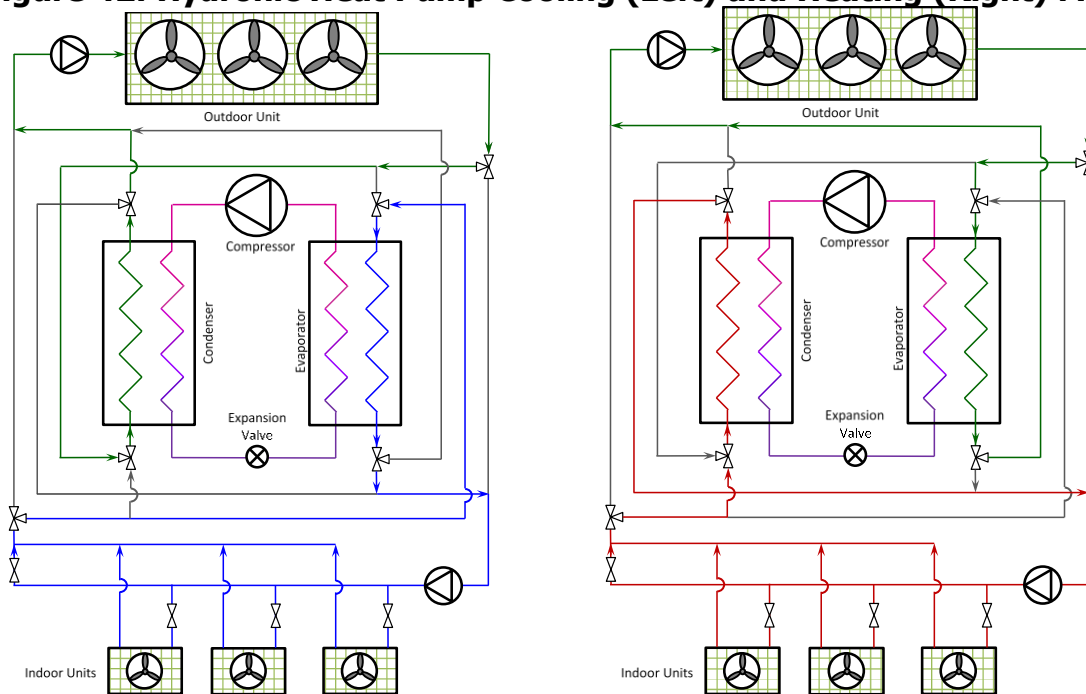
The R-290 heat pump is thermodynamically more efficient than a traditional R-410A refrigerant-based heat pump. But the use of a secondary fluid (antifreeze) to deliver heating or cooling requires its compressors to operate at lower temperatures to account for heat transfer from the refrigerant to the secondary fluid. It also must account for temperature rise in the single-phase working fluid versus two-phase heat transfer in indoor units. Therefore, use of a secondary fluid for cooling and heating distribution will reduce the overall efficiency and heating and cooling capacity of a heat pump. However, it will also reduce the carbon emissions from refrigerant leakage. Though the refrigerant circulates in a sealed environment in a VRF system, experience has shown that it does leak during and at the end of its service life and affects the global warming potential (R-410A GWP is 2,088 versus just 3 for R-290). It is quite common to have a refrigerant charge of about 3 pounds for each ton capacity of the

VRF system. This means that just one pound of an R410A leak is more potent than a ton of CO<sub>2</sub> emitted to the environment. For comparison, an automobile emits about 4.6 tons of CO<sub>2</sub> per year. Therefore, from the global warming perspective, use of R-290 with a secondary fluid may produce less GWP if renewable energy is used for driving the heat pump.

For the test unit, there were two limitations: First, the unit could not be built with a reversible refrigerant circuit for lack of fire-rated four-way valves needed for building a heat pump. Therefore, the researchers had to reverse water flows to obtain heating and cooling as discussed below. Second, since the team had to use a water-to-water heat pump for the reasons previously stated, a water-to-air heat exchanger was used to reject heat from the condenser in summer and pick up heat in winter. These modifications would severely affect energy performance. Therefore, the results aren't reflective of available efficiency from such systems but should be used as a proof-of-concept for distributed heating and cooling with secondary fluids. Using the data from the tests, a computer model was calibrated to predict performance of the secondary fluid type of systems.

The use case for the Bundgaard hydronic heat pump is to serve a hydronic space conditioning system. Typical examples are included on the left side of Figure 42.

**Figure 42: Hydronic Heat Pump Cooling (Left) and Heating (Right) Mode**

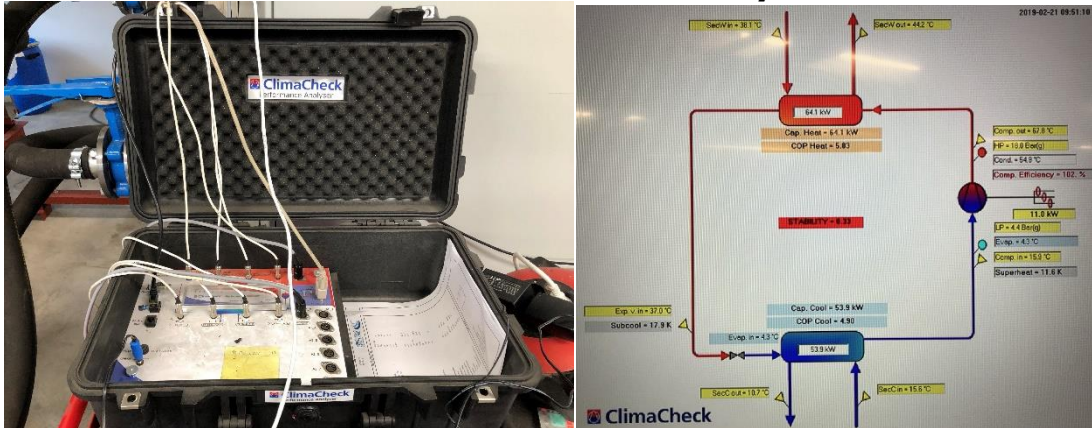


Source: Electric Power Research Institute

Three-way diverting control valves in the system are arranged so the secondary fluid passes through the Bundgaard evaporator section and is sent to the indoor fan coils for heat transfer. Secondary fluid passing through the Bundgaard condenser section is sent to the outdoor unit. In a heating application, as shown on the right side of Figure 42, three-way diverting valves send secondary fluid from the condenser to the indoor fan coil units. The Bundgaard WWC1XS2 does not have a reversing valve and thus must make use of these three-way diverting valves to switch between cooling and heating processes. A four-way refrigerant reversing valve would be required to replace the need of the three-way diverting valves, but no such valve that is ATEX certified was available.

The Bundgaard hydronic heat pump is compatible with the ClimaCheck onsite PA Pro III Portable Performance Analyzer, a turn-key portable analyzer supplied with all standard refrigeration sensors, that gathers all sensor data during each test run. The ClimaCheck onsite software connects to online cloud servers either through insertion of the SIM card or through a LAN/WiFi connection and allows for integration with third-party sensors/controllers if additional data collection points are desired. This performance analyzer could be used for the commissioning process but is not intended to provide the level of accuracy found in a laboratory test. Figure 43 shows the ClimaCheck onsite PA Pro III Performance Analyzer connected to the Bundgaard system and a snapshot of the information displayed on the online platform.

**Figure 43: ClimaCheck Portable Performance Analyzer and Online Platform**



Source: Electric Power Research Institute

The following data points were collected using the pre-installed instrumentation provided by the manufacturer and used for calculating the actual performance:

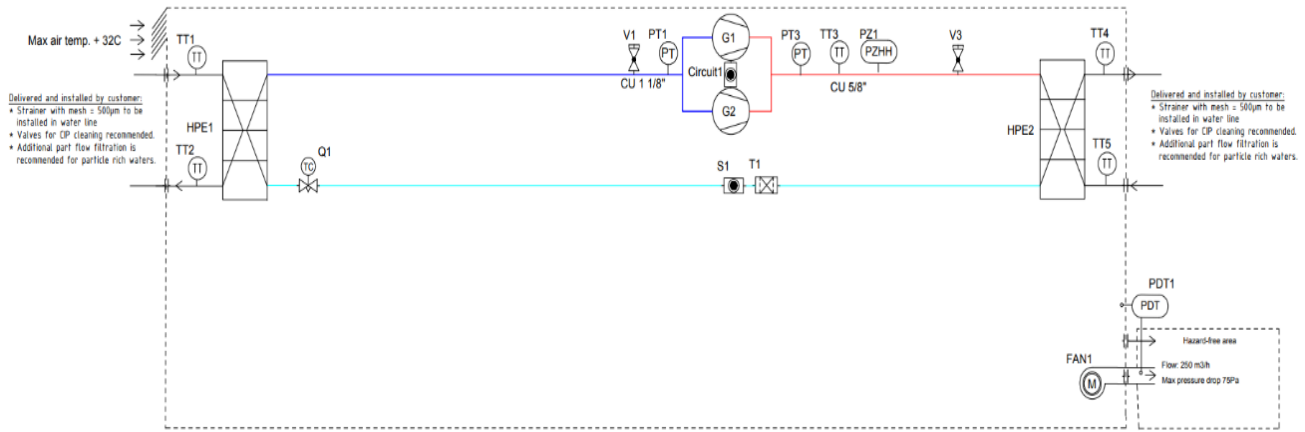
- Evaporator inlet temperature
- Evaporator outlet temperature
- Condenser inlet temperature
- Condenser outlet temperature
- Compressor inlet pressure
- Compressor outlet pressure

Additional simple sensors were set up to collect the remaining data points:

- Indoor fan energy consumption
- Outdoor fan energy consumption
- Circulation pump energy consumption
- Refrigerant flow rates
- True input power

The layout of all instrumentation contained within the Bundgaard WWC1XS2 responsible for collecting the required information can be found in Figure 44 and associated list of materials detailed in Table 10.

**Figure 44: Bundgaard R290 Chiller Piping and Instrumentation Diagram**



Source: Electric Power Research Institute

**Table 10: Bill of Material in Bundgaard R290 Chiller Piping and Instrumentation Diagram**

Diagram Code	Description	Product
HPE 2	Condenser	SWEP B86HX80/IP
HPE 1	Evaporator	SWEP F80ASHX40/IP-SC-M
G1	Compressor	Emerson, Copeland Scroll, ZHI6KCU-TFMN-424
G2	Compressor	Emerson, Copeland Scroll, ZHI6KCU-TFMN-424
Q1	Expansion valve	Danfoss Colibri C12
V1	Schrader Valve	HECAPO
V3	Schrader Valve	HECAPO
PT3	Pressure Transmitter	Danfoss AKS33
PT1	Pressure Transmitter	Danfoss AKS33
TT1	Temperature Sensor	Danfoss AKS 12
TT2	Temperature Sensor	Danfoss AKS 12
TT3	Temperature Sensor	Danfoss EKS 221
TT4	Temperature Sensor	Danfoss AKS 12
TT5	Temperature Sensor	Danfoss AKS 12
FAN1	Fan	Ostberg
S1	Sight Glass	Sanhua SYJ
T1	Filter Dryer	Sanhua DTG
PZ1	Pressure Switch	Emerson PS4-WI
PDT	Air Pressure Switch	HECAPO F32 0.3 to 3 MBA

Source: Electric Power Research Institute

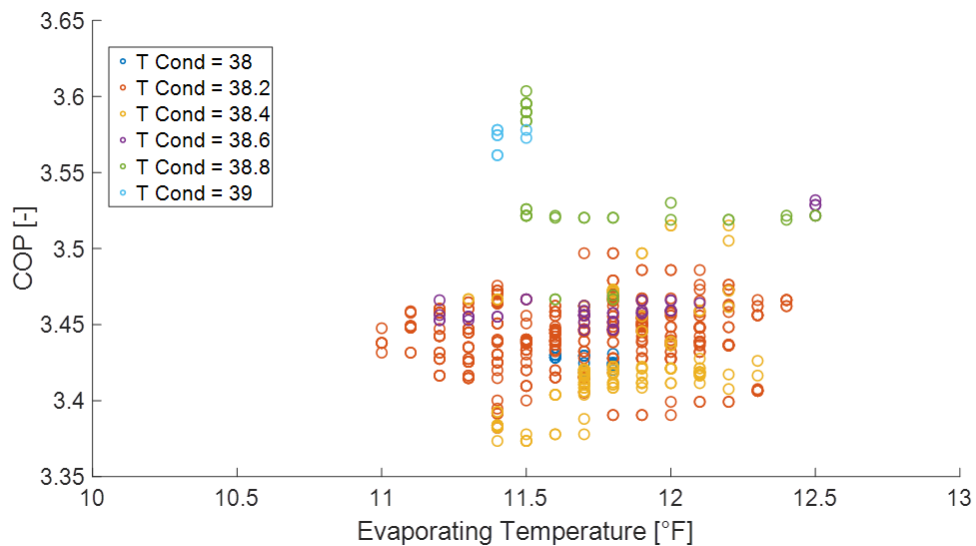
### Testing Plan

Initial factory acceptance testing was performed prior to shipment to the laboratory testing site to verify the equipment was built and operating in accordance with the design specifications. The factory acceptance test took place at Bundgaard’s manufacturing plant in Copenhagen, Denmark by a Bundgaard technician accompanied by an EPRI representative. The tests were carried out to verify safety functions, electrical connections, and thermal



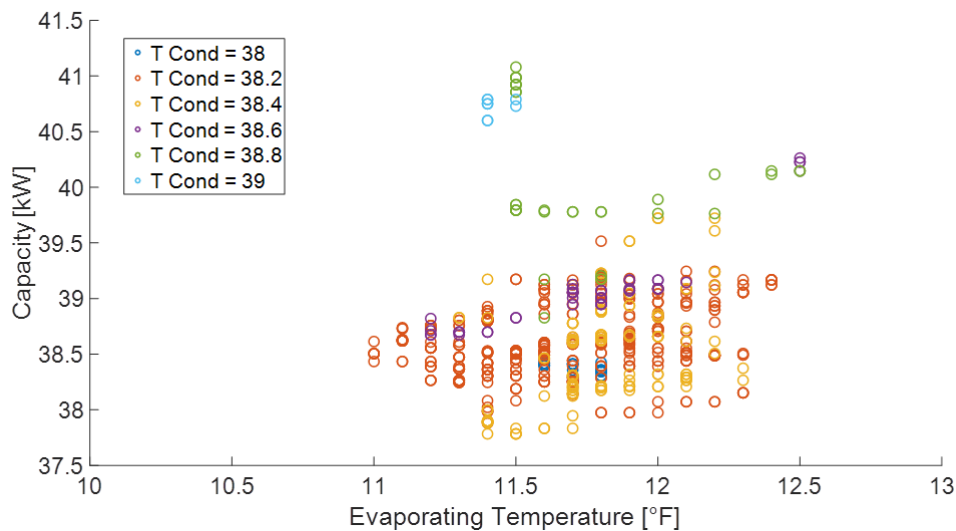
performance. Figure 45 and Figure 46 show the coefficient of performance (COP) and capacities plotted as a result of the factory acceptance test.

**Figure 45: Bundgaard R290 Chiller Cooling Mode Factory Acceptance Test of Coefficient of Performance Values**



Source: Electric Power Research Institute

**Figure 46: Bundgaard R290 Chiller Factory Acceptance Testing Cooling Mode Test Capacity Values**



Source: Electric Power Research Institute

The objective was to demonstrate the performance of the Bundgaard WWC1XS2 in a realistic use case simulated in a laboratory environment, rather than to establish typical performance of such a system. To accomplish this task, a custom-built hydronic tempering apparatus with an option to use indoor fan coils was created in the Advanced Technology Performance Lab (ATPL) at PG&E’s San Ramon Technology Center. The testing apparatus consisted of independent hydronic tempering systems, each capable of providing a simulated hydronic load with very tight control of entering water or glycol temperature. The test system also included an air to glycol indoor unit that was placed inside an environmental chamber within the

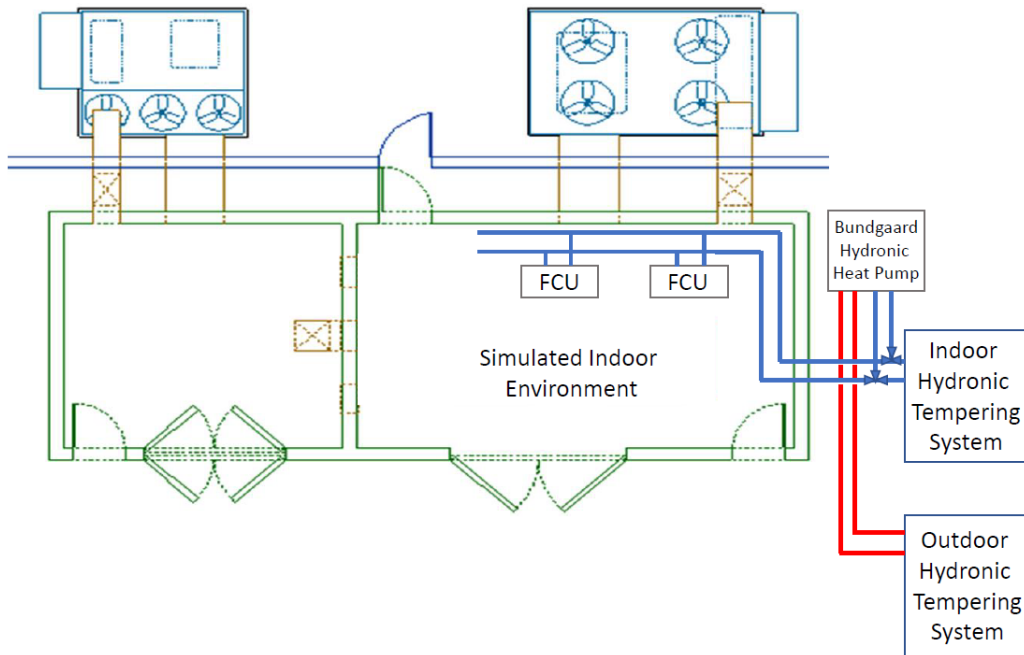
laboratory. The ATPL contained a variety of environmental chambers, some designed in accordance with ASHRAE Standard 37. Each chamber had an independent space conditioning system to control temperature and humidity, consisting of packaged commercial heat pump units with electric resistance heating elements to fine-tune the temperature and separate electric humidifiers. The packaged units were equipped with economizers that allowed the test chambers to be flushed with outside air to provide stability.

Each room had its own airflow measurement apparatus constructed according to ASHRAE standard design. These apparatuses consisted of a sealed box with a partition having several flow nozzles that could be opened or closed in combination to provide the required range of differential pressure for the current airflow. Variable-speed blowers on the outlets of each airflow station were set to maintain the desired outlet static pressures and airflow rates to compensate for the added resistance of the flow measurement system and ductwork. The airflow stations were not needed for testing the Bundgaard WWC1XS2 as all the instrumentation needed to measure capacity was in the hydronic loop.

The Bundgaard WWC1XS2 was placed outside, along with the independent evaporator and condenser hydronic tempering systems. Indoor fan coil units were placed in the large environmental chamber for demonstration. A supply and return line to and from the evaporator was sent inside the laboratory environmental chamber with mounted fan coil units to demonstrate the typical operation of the indoor half of this system. Figure 47 shows the locations of the Bundgaard WWC1XS2 and the indoor and outdoor hydronic tempering systems.

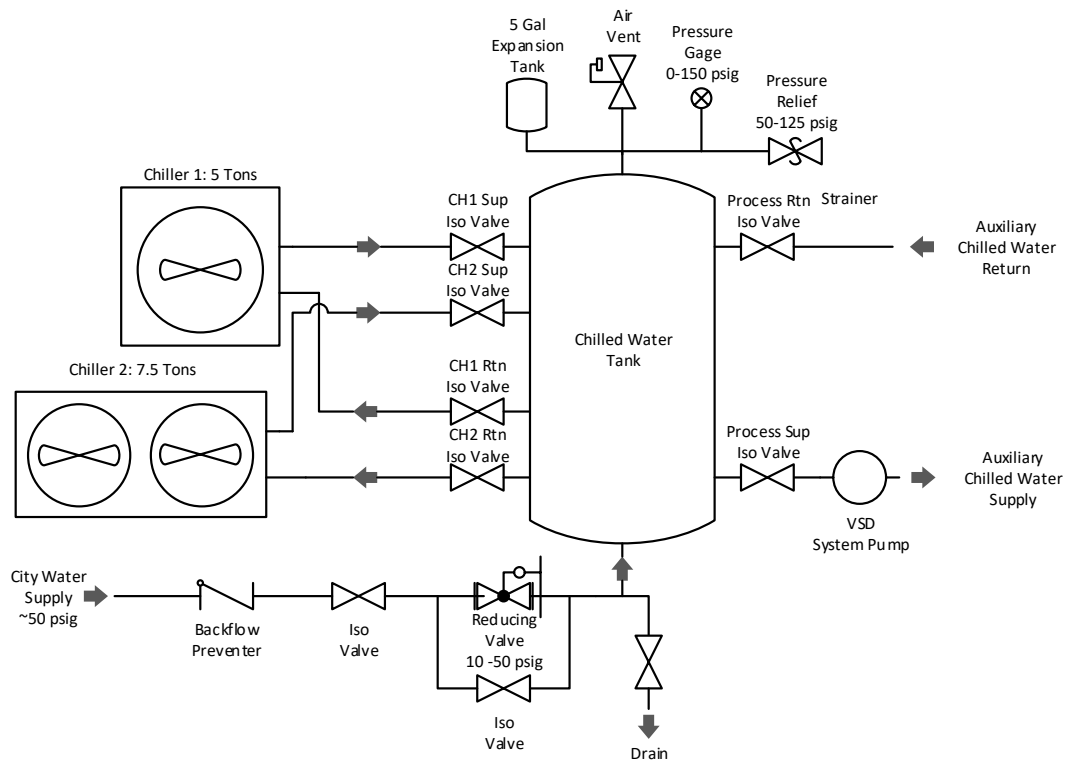
A chilled water plant (Figure 48) was built to support a tempering system used to maintain the inlet condition to the condenser during testing. The system contained two portable chillers paralleled to a chilled water tank. A 2-horsepower (HP) variable speed pump provided circulation from the chilled water tank to the condenser side hydronic tempering system.

**Figure 47: Schematic Layout for Testing Propane Refrigerant System**



Source: Electric Power Research Institute

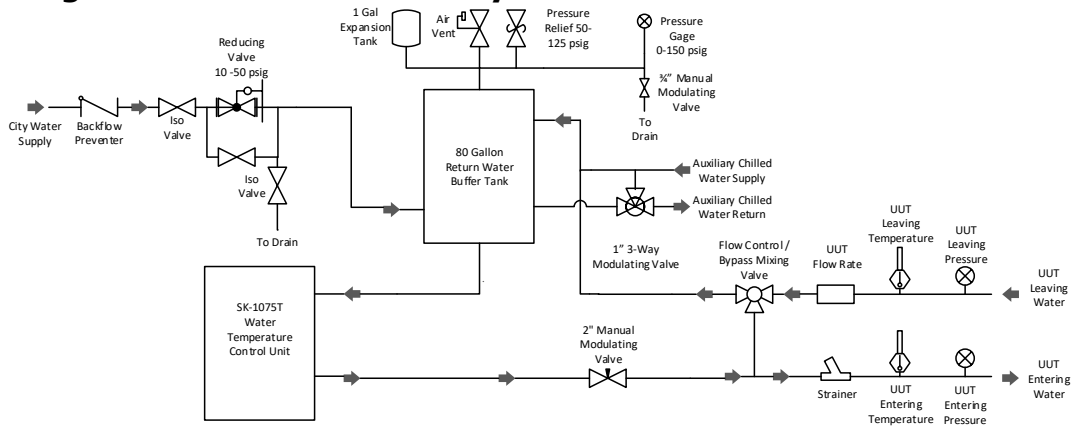
**Figure 48: Chilled Water Feeding Condenser Side Hydronic Tempering System**



Source: Electric Power Research Institute

The condenser side hydronic tempering system (Figure 49) uses a magnetically actuated needle valve to feed chilled water into the condenser leaving water stream from the Bundgaard. A return water buffer tank was employed to damp out momentary fluctuations in temperature, resulting in a steady temperature entering the condenser.

**Figure 49: Condenser Side Hydronic Instrumentation Schematic**



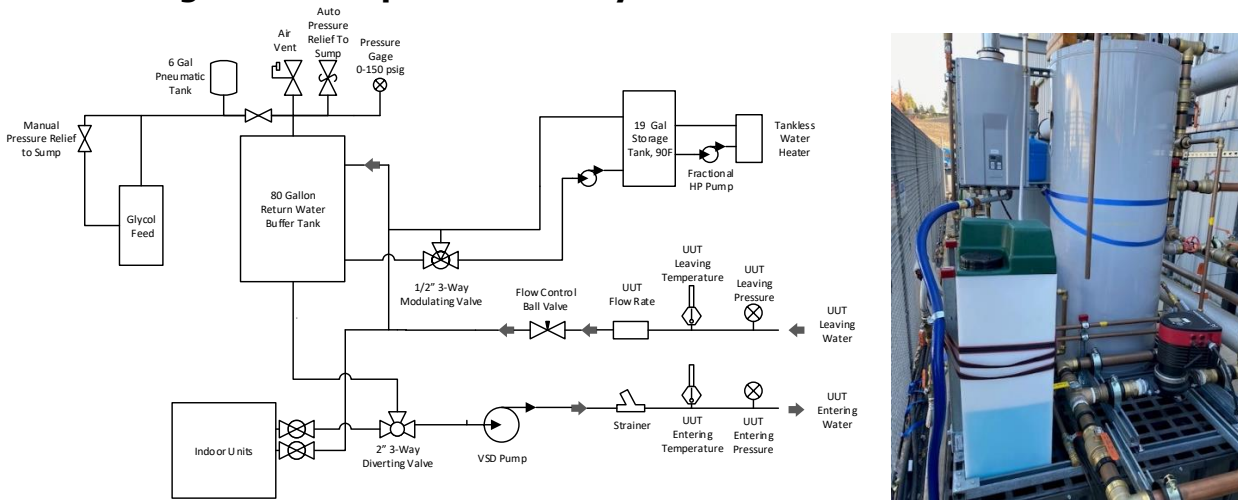
Source: Electric Power Research Institute

A glycol/water charged system with a commercial water heater was constructed to support the second tempering system used to maintain the inlet condition to the evaporator during testing. The system contained a 200 million BTU per hour tankless water heater feeding a 19-gallon hot glycol/water storage tank. A fractional HP pump provided circulation from the hot glycol/water tank to the condenser side hydronic tempering system.

The hydronic tempering system used a magnetically actuated needle valve to feed heated glycol/water into the evaporator leaving water stream from the Bundgaard. A return water buffer tank was employed to damp out momentary fluctuations in temperature, resulting in a steady temperature entering the evaporator.

Figure 50 shows a schematic and photo of the evaporator side hydronic tempering system.

**Figure 50: Evaporator Side Hydronic Instrumentation Schematic**



Source: Electric Power Research Institute

Testing, under the controlled environment conditions specified, commenced in August of 2019. All laboratory testing results are included in Table 11. The table lists the selected test conditions that represent a range of operating conditions that would likely be experienced operating in the field. The range of outdoor conditions covered while the unit would be operating in cooling mode are 67°F – 95°F, while the range of outdoor conditions for heating mode are 17°F – 47°F.

**Table 11: Hydronic Heat Pump Cooling and Heating Testing Conditions**

	Evap Entering Temp (°F)	Evap Leaving Temp (°F)	Evap Volume Flow (gpm)	Condense Entering Temp (°F)	Condense Leaving Temp (°F)	Condense Volume Flow (gpm)	Rep Indoor Condition (°F)	Rep Outdoor Condition (°F)
INDOOR COOLING								
#1 Standard Cooling Rating	51.6	42.9	30.5	100.4	111.3	28.9	80/67	95
#2 Cooling	51.8	42.9	30.6	87.4	98.7	28.8	80/67	82
#3 Cooling	52.6	42.9	30.7	72.4	84.6	28.5	80/67	67
INDOOR HEATING								
#4 Standard Heating Rating	42	33.8	30.2	80	90	30	70	47
#5 Heating	30	23.1	29.4	80	88	29	70	35
#6 Heating	22.5	16.2	28.1	80	87	28	70	N/A

Source: Electric Power Research Institute

Table 12 lists the instrumentation used to perform testing at PG&E’s ATPL laboratory. The temperature and pressure instrumentation in the secondary fluid were installed using guidance from the AHRI 550/590 testing method.

**Table 12: Advanced Technology Performance Laboratory Testing Instrument List**

Measurement Parameter	Instrument Used
Evaporator Entering Temperature	4-wire RTD
Evaporator Leaving Temperature	
Condenser Entering Temperature	
Condenser Leaving Temperature	
Evaporator Flow Rate	Positive Displacement Nutating Disc Flow Meter
Condenser Flow Rate	
Evaporator Entering Pressure (Glycol/Water)	Spanned Rosemount Pressure Transmitter
Evaporator Leaving Pressure (Glycol/Water)	
Condenser Entering Pressure (Refrigerant)	
Condenser Leaving Pressure (Refrigerant)	
Refrigerant Liquid Pressure (Refrigerant)	Thermocouple
Refrigerant Vapor Pressure (Refrigerant)	Thermocouple
Refrigerant Liquid Temperature (Cond Leaving)	Hioki Power Meter

Source: Electric Power Research Institute

Using the testing setup, methods and conditions listed above, the following performance parameters were calculated:

- Evaporator capacity via secondary fluid measurement

$$\dot{Q}_{Evap} = \dot{V}_{glycol} * \rho_{glycol} * cp_{glycol} (T_{glycol, evap, in} - T_{glycol, evap, out})$$

Where:

$\dot{V}_{glycol}$  – Measured glycol/water volumetric flow rate, (gpm)

$\rho_{glycol}$  – Calculated glycol/water density, (lb/gal)

$cp_{glycol}$  – Calculated glycol/water mixture specific heat, (BTU/°F\*lbm)

$T_{glycol, evap, in}$  – Measured glycol temperature entering evaporator, (°F)

$T_{glycol, evap, out}$  – Measured glycol temperature leaving evaporator, (°F)

- Condenser capacity via secondary fluid measurement:

$$\dot{Q}_{Cond} = \dot{V}_{water} * \rho_{water} * cp_{water} (T_{water, cond, in} - T_{water, cond, out})$$

Where:

$\dot{V}_{water}$  – Measured glycol/water volumetric flow rate, (gpm)

$\rho_{water}$  – Calculated glycol/water density, (lb/gal)

$cp_{water}$  – Calculated glycol/water mixture specific heat, (BTU/°F\*lbm)

$T_{water,cond,out}$  – Measured glycol temperature leaving condenser, (°F)

$T_{water,cond,in}$  – Measured glycol temperature entering condenser, (°F)

- Condenser capacity via secondary fluid measurement without compressor heat:

$$\dot{Q}_{Cond\ noCH} = \dot{Q}_{Cond} - (kW_{comp} * 3412)$$

Where:

$\dot{Q}_{Cond}$  – Measured condenser capacity, including compressor heat, (BTU/h)

$kW_{comp}$  – Measured Total Package Power of Bundgaard Unit, (kW)

- Heat balance error between secondary fluid capacity measurement of evaporator and condenser:

$$H.B.E. = \frac{(\dot{Q}_{Evap} - \dot{Q}_{Cond\ NoCH})}{\frac{(\dot{Q}_{Evap} + \dot{Q}_{Cond\ NoCH})}{2}}$$

Where:

$\dot{Q}_{Evap}$  – Evaporator capacity via secondary fluid measurement, (Btu/h)

$\dot{Q}_{Cond\ NoCH}$  - Condenser capacity via secondary fluid measurement, minus compressor heat input, (Btu/h)

- Cooling Coefficient of Performance

$$COP_c = \frac{(\dot{Q}_{Evap})}{\frac{3412}{Total\ Power}}$$

Where:

$\dot{Q}_{Evap}$  – Evaporator capacity via secondary fluid measurement, (Btu/h)

$Total\ Power$  - Measured Total Package Power of Bundgaard Unit, (kW)

- Heating Coefficient of Performance

$$COP_h = \frac{(\dot{Q}_{Cond})}{\frac{3412}{Total Power}}$$

Where:

$\dot{Q}_{Cond}$  – Measured condenser capacity, including compressor heat, (BTU/h)

*Total Power* - Measured Total Package Power of Bundgaard Unit, (kW)

## Testing Results

Table 13 lists all testing results at the predefined temperature conditions, and Figure 52 and Figure 52 show the plotted COP values of the Bundgaard hydronic heat pump.

**Table 13: Bundgaard Hydronic Heat Pump Laboratory Test Results**

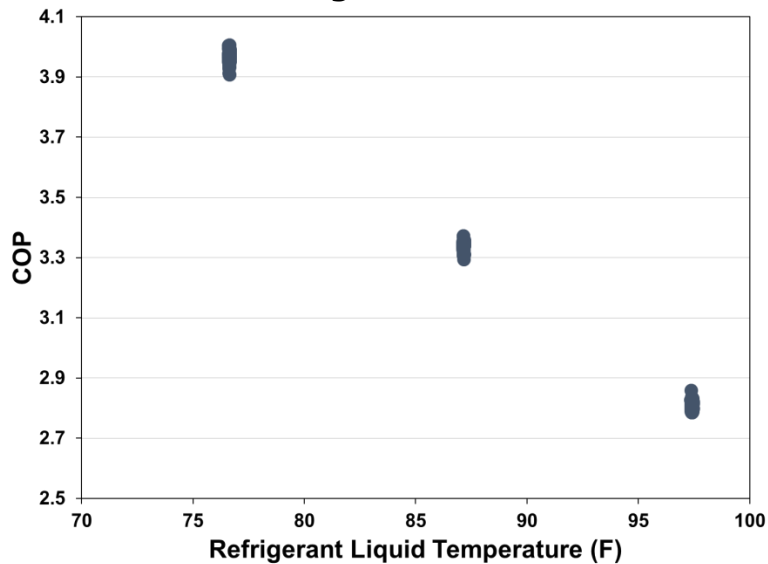
Parameter	#1	#2	#3	#4	#5	#6
	Cooling			Heating		
COP (Cooling)	2.81	3.34	3.97	3.26	2.79	2.47
COP (Heating)	3.74	4.30	4.96	4.20	3.68	3.42
<b>Evaporator</b>						
Entering Glycol Temp (°F)	51.6	51.8	52.6	42.1	30.1	22.5
Leaving Glycol Temp (°F)	42.9	42.6	42.9	33.8	23.1	16.2
Glycol Flowrate (gpm)	30.5	30.6	30.7	30.2	29.3	28.1
Capacity (Btu/h)	117,028	123,830	130,888	108,963	89,524	77,247
Capacity (tons)	9.75	10.32	10.91	9.08	7.46	6.44
Refrigerant Pressure (psig)	54.8	53.2	51.7	42.8	32.6	27.6
Refrigerant Temp. (°F)	47.3	47.4	47.6	39.3	27.9	19.9
Superheat (°F)	15.0	16.4	17.9	17.9	17.2	15.2
<b>Condenser</b>						
Entering Water Temp (°F)	100.2	87.4	72.9	79.8	79.8	80.0
Leaving Water Temp (°F)	111.3	98.7	84.6	89.7	88.1	87.5
Condenser Water Flowrate (gpm)	28.9	28.8	30.7	30.2	29.3	28.1
Capacity w/Comp. Heat (Btu/h)	155,922	123,830	130,888	108,963	89,524	77,247



Parameter	#1	#2	#3	#4	#5	#6
	Cooling			Heating		
Capacity w/Comp. Heat (tons)	12.99	13.30	13.63	11.69	9.85	8.89
Capacity w/o Comp. Heat (Btu/h)	114,248	122,485	130,588	106,908	86,106	75,445
Refrigerant Pressure (psig)	225.7	189.6	153.9	167.6	163.9	162.0
Refrigerant Temp. (°F)	97.4	87.2	76.6	79.7	74.9	75.6
Subcool (°F)	21.8	18.9	14.7	17.5	20.9	19.4
<b>Input Power</b>						
Volt Amps (VA)	13,482	12,202	11,063	11,179	10,825	10,587
Power Factor	0.91	0.89	0.87	0.88	0.87	0.86
True Power Consumption (kW)	12.2	10.9	9.7	9.8	9.4	9.2
<b>Evaporator/Condenser Energy Balance</b>						
Heat Balance Error (%)	2.40%	1.09%	0.23%	1.90%	3.89%	2.36%

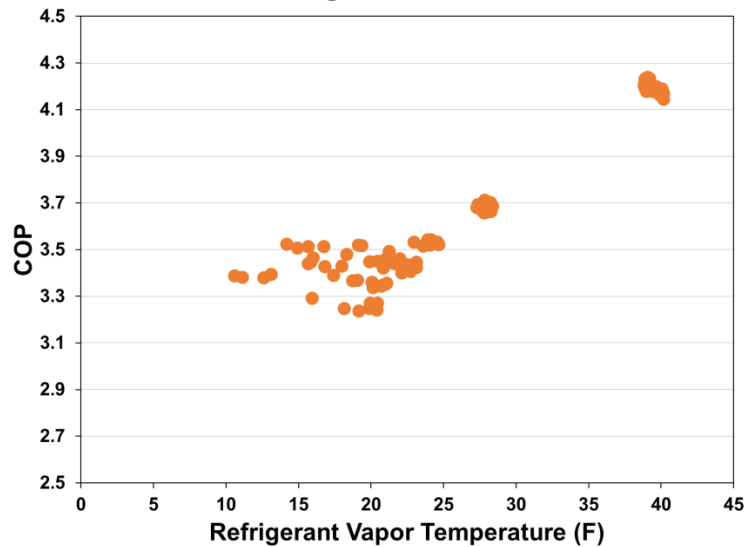
Source: Electric Power Research Institute

**Figure 51: Coefficient of Performance and Liquid Refrigerant Temperature for Cooling Mode Tests**



Source: Electric Power Research Institute

**Figure 52: Coefficient of Performance and Vapor Refrigerant Temperature for Heating Mode Tests**



Source: Electric Power Research Institute

The focus of this effort was to demonstrate the function of a hydronic heat pump using a low GWP refrigerant. Performance results generated in this report do not reflect rating conditions nor should they be used to establish anticipated performance of this unit in its intended application. The results of this study demonstrate that hydronic heat pumps employing low GWP refrigerants are feasible. Further efforts involving performance optimization should be evaluated, such as enhancement of controls that would result in an improvement of cycle efficiency while using R290 as a refrigerant.

An uncertainty analysis was performed to determine the effect of systematic (bias) errors and as random errors in the data. The resulting uncertainty in measured COP is about 6 percent. The highest heat balance error measured during testing was less than 4 percent, indicating good control of measurement and other sources of uncertainty. The results of the uncertainty test are shown in Table 14.

**Table 14: Measurement Uncertainty of Applied Technology Services Laboratory Test Results**

Measurement	Temperature	Flow
Units	(°F)	gpm
Bias limit in calibration std	0.100	0.16
Bias limit in cal bath uniformity	0.050	0
Tolerance of Test Instrumentation to Transfer Standard	0.250	0.96
Worst Case Std. deviation in test data	0.500	0.3
Number of readings during test	60	60
Degrees of freedom	59	59
Precision index in test data fluctuating	0.065	0.039

Bias limit due to spatial variations	0.100	0
Combined bias error	0.287	0.973
Combined precision index	0.065	0.039
Combined degrees of freedom	59	59
Students t (@ combined degrees of freedom)	2.001	2.001
95% conf. combined uncertainty	0.315	0.976

Source: Electric Power Research Institute

## Supplemental Modeling

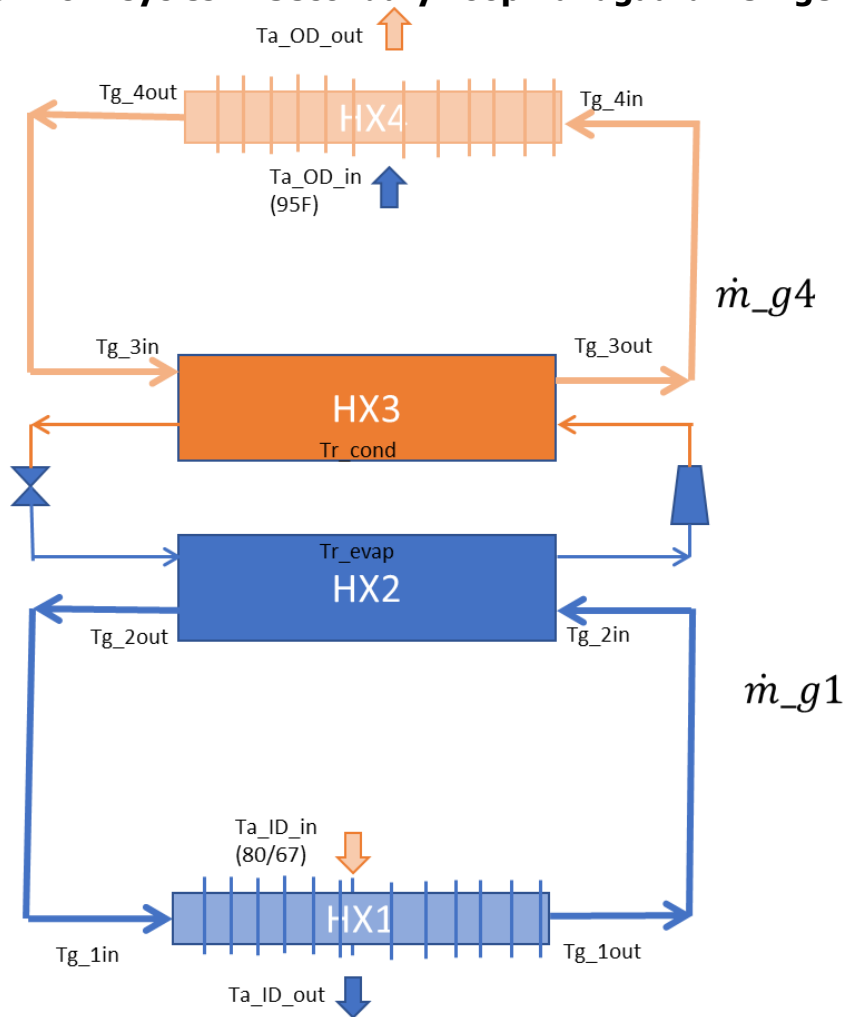
Simulation modeling work was conducted to understand the system operation efficiency when operating in the field with indoor fan coils and outdoor fan coil installed. The model was constructed in three steps:

1. The R290 refrigeration system with glycol heat exchangers was simulated using a commercial software Vapcyc. The model was calibrated with test data, and then the model was used to simulate the refrigerant system capacity and efficiency given any glycol operating conditions.
2. A system model for the Bundgaard R290 refrigeration unit with a second loop was built in Engineering Equation Solution programming (called EES Model in this report). This model includes the refrigerant cycle, the glycol cycles, and the fan coils. The results from the Vapcyc fed the EES model to give the overall system efficiency.
3. A typical R410A VRF system was simulated in Vapcyc. The R410A VRF system simulation results were used to compare with the Bundgaard system's overall simulation results from the EES model.

Figure 54 shows the components and flow cycles in the second loop Bundgaard system. The system has four heat exchanger coils which are marked in the figure as HX1, HX2, HX3 and HX4 respectively, and described as:

- HX1: Indoor glycol-Simulto-air heat exchanger. This is the fan-coil unit installed in the indoor room. It can be multiple indoor units combined.
- HX2: Refrigerant-to-glycol evaporator coil inside the Bundgaard unit
- HX3: Refrigerant-to-glycol condenser coil inside the Bundgaard unit
- HX4: Outdoor glycol-to-air heat exchanger

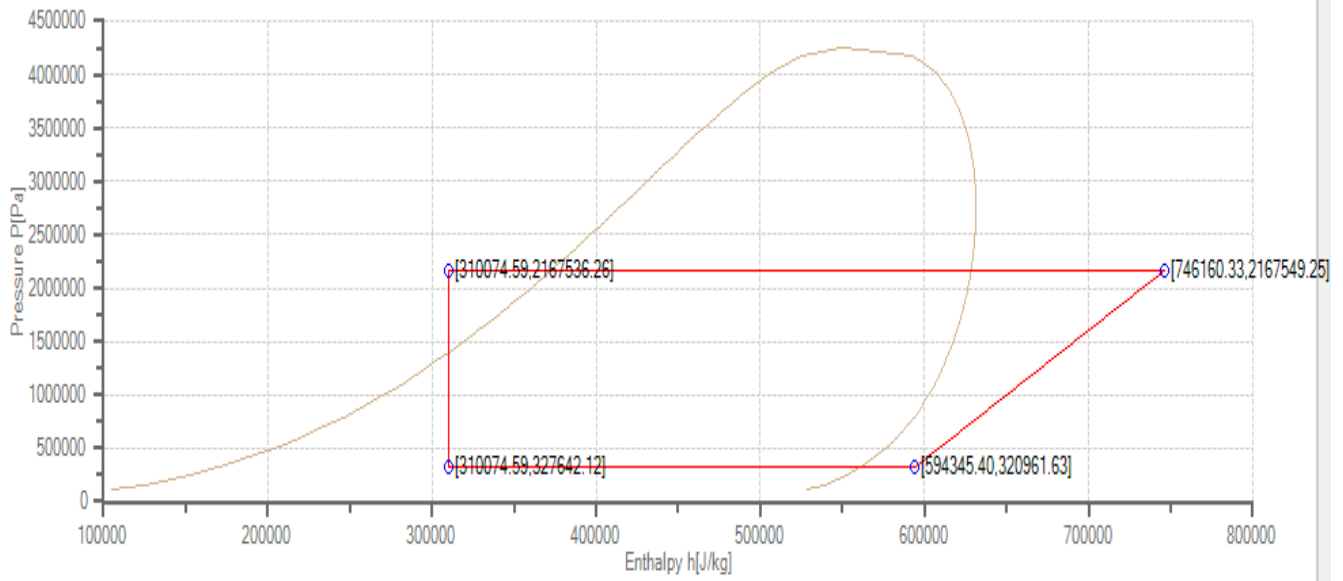
**Figure 53: Flow Cycles in Secondary Loop Bundgaard Refrigeration Unit**



Source: Electric Power Research Institute

The performance (capacity and power) was mainly driven by the compressor performance. The heat exchanger performance moved the compressor operating window on the p-h diagram (Figure 54) and determined the operating performance. There were two glycol pumps, one for high side and one for low side and two air fans, one for outdoor and one for indoor to further affect the system efficiency. Because those power consumptions could be added to the results of the system balance model, those power consumptions were not included in the model.

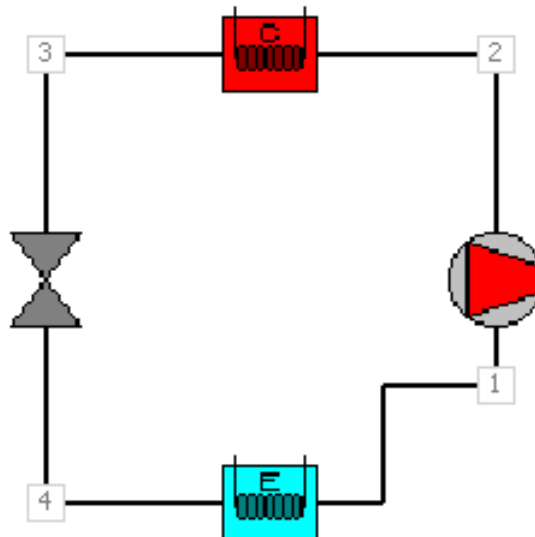
**Figure 54: Example of p-h Diagram in an R290 Refrigeration System**



Source: Electric Power Research Institute

Figure 55 depicts analysis from the Vapcyc component-based refrigerant simulation tool. Four major components were defined in the model, and with specified operating conditions, the software will iterate and find the refrigerant conditions in the system and give the refrigeration system capacity and efficiency. Figure 55 shows the system, in which Point 1 to 2 is the compressor; 2 to 3 is the condenser; 3 to 4 is the expansion valve; and 4 to 1 is the evaporator. The components are defined in an appendix.

**Figure 55: Components in R290 Refrigeration System**



Source: Electric Power Research Institute

## Compressor

The Bundgaard unit has two R290 scroll compressors, made by Emerson, with model number ZH13KCU. The compressor performance of capacity, power, and efficiency are given by the manufacturer, and are shown in **Error! Reference source not found.**, Figure 56, Figure 57, and Figure 58.

The compressor capacity and power can be modeled using Equation (1) at any given evaporating temperature and condensing temperature with 0°K liquid subcooling and 10°K suction superheat.

$$X = C0 + C1*S + C2*D + C3*S^2 + C4*S*D + C5*D^2 + C6*S^3 + C7*D*S^2 + C8*S*D^2 + C9*D^3 \quad \text{Equation 1}$$

Where,

X = Cooling Capacity, kW; Power Input, kW;

S = Evaporating Temperature, °C

D = Cond. Temp., °C

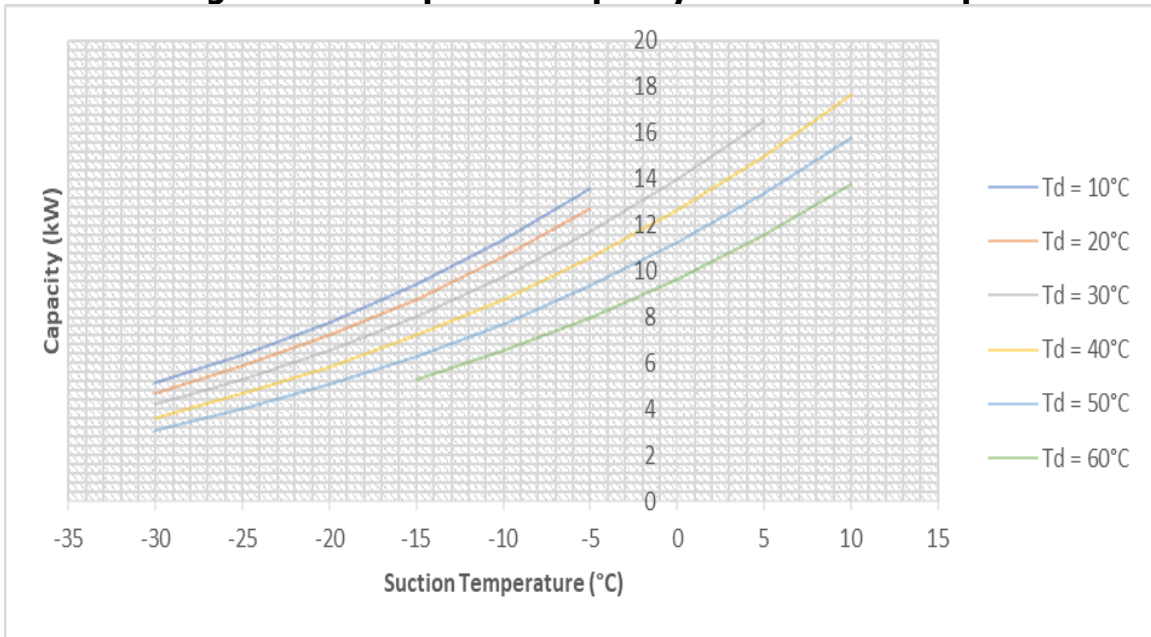
And C0.....C9 are given in Table 15.

**Table 15: 10-Coefficients for Compressor for Capacity & Power Calculation**

Coefficient	Cooling Capacity (kW)	Power (kW)
C0	16.91802305	1.504793488
C1	0.56729912	0
C2	-0.072140655	0.034519777
C3	0.007325951	0
C4	-0.00246032	0.000434366
C5	0.000960136	8.03795E-05
C6	3.42001E-05	0
C7	-4.01523E-05	0
C8	-1.76495E-05	-2.75444E-06
C9	2.4337E-06	3.70823E-06

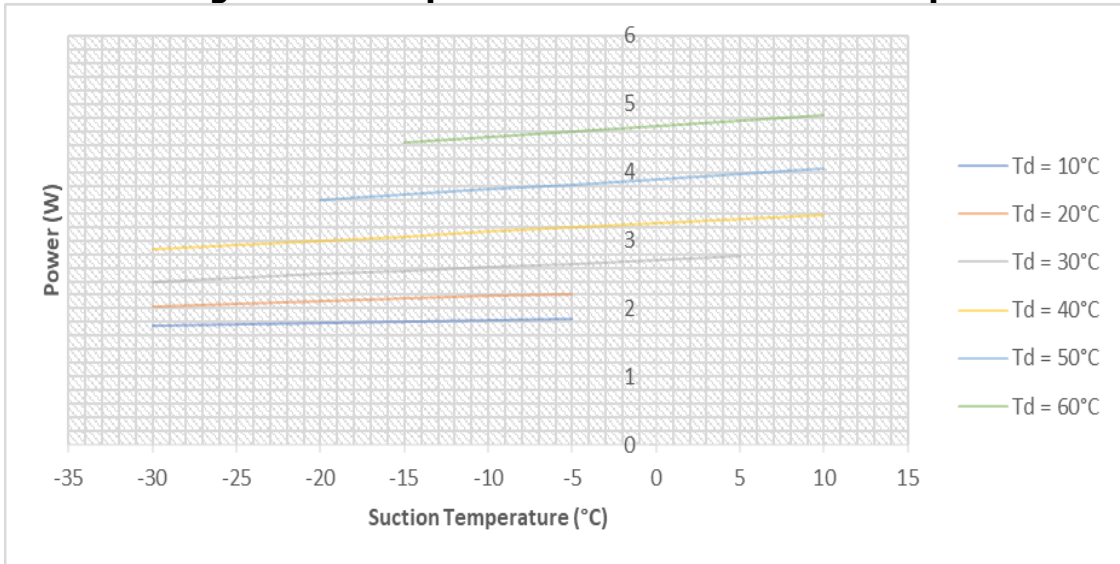
Source: Electric Power Research Institute

**Figure 56: Compressor Capacity Performance Map**



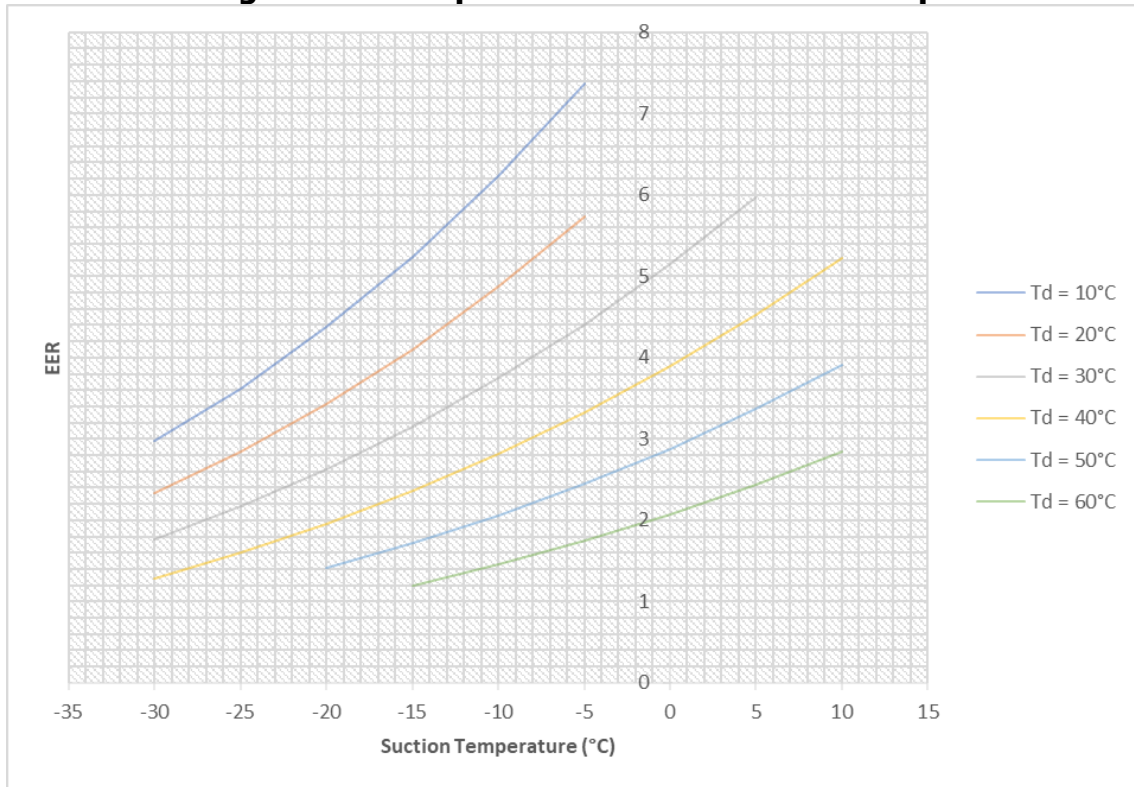
Source: Electric Power Research Institute

**Figure 57: Compressor Power Performance Map**



Source: Electric Power Research Institute

**Figure 58: Compressor EER Performance Map**



Source: Electric Power Research Institute

**Condenser**

The condenser of the Bundgaard unit is made by SWEP with model number SWEP B86HX80/IP. The specifications are shown in Figure 59.

**Figure 59: Condenser Specifications**



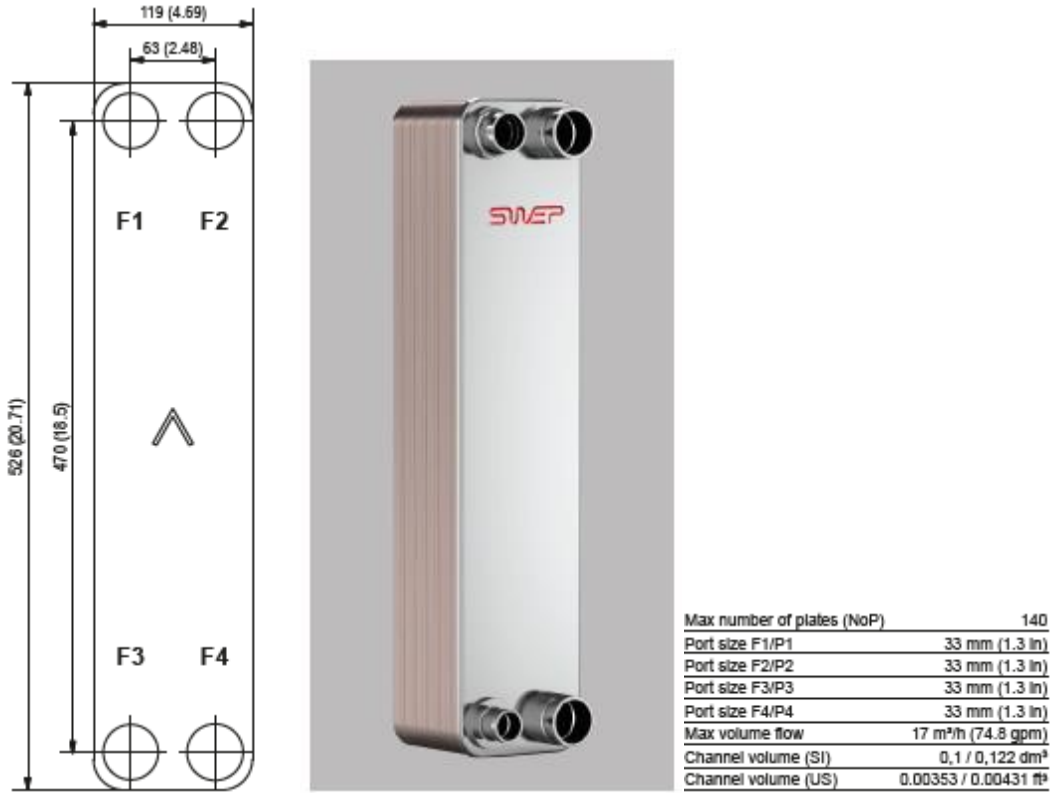
Source: Electric Power Research Institute



## Evaporator

The evaporator of the Bundgaard unit is made by SWEP with model number SWEP F80ASHX40/IP-SC-M, and the specifications are shown in Figure 60.

**Figure 60: Evaporator Specifications**



Source: Electric Power Research Institute

## Expansion valve

The expansion valve is not modeled directly in the Vapcyc model, but through setting the superheat instead.

## Results

### Modeling in EES for the Whole System (Including Indoor and Outdoor Fan Coils)

The heat exchangers are modeled based on the  $\epsilon$ -NTU method.

The heat exchanger HX1 is a glycol-to-air heat exchanger for indoor cooling. Glycol flows inside the tube while air cross flows through the coil. When the coil surface temperature at glycol outlet is lower than the entering air dewpoint temperature, dehumidification will occur.

The effective humid air mass flow ratio is

$$m^* = \frac{\dot{m}_{a,1D}}{\dot{m}_{g1} \frac{c_{p,g1}}{C_s}} \quad \text{Equation 2}$$

Where  $C_s$  is the air saturation specific heat at mean glycol temperature.

$$Ntu_{wet} = \frac{Ntu_o}{1 + m^* \frac{Ntu_o}{Ntu_i}} \quad \text{Equation 3}$$

Where

$$Ntu_i = \frac{UA_i}{\dot{m}_{g1}c_{p,g1}} \quad \text{Equation 4}$$

$$Ntu_o = \frac{UA_o}{\dot{m}_{a,ID}c_{pa,ID}} \quad \text{Equation 5}$$

and the heat transfer conductance UA is a known for a given heat exchanger.

The counterflow effectiveness can be calculated from

$$\varepsilon_{wet} = \frac{1 - \exp(-Ntu_{wet}(1-m^*))}{1 - m^* \exp(-Ntu_{wet}(1-m^*))} \quad \text{Equation 6}$$

Air outlet enthalpy can be calculated from

$$h_{a,ID,out} = h_{a,ID,in} - \varepsilon_{wet}(h_{a,ID,in} - h_{a,sat,g1in}) \quad \text{Equation 7}$$

Where  $h_{a,sat,g1in}$  is enthalpy of saturated air at glycol inlet temperature, which the lowest enthalpy it can achieve.

The cooling capacity of HX1 is

$$Q_{HX1} = \varepsilon_{wet} \dot{m}_{a,ID}(h_{a,ID,in} - h_{a,sat,g1in}) \quad \text{Equation 8}$$

The heat exchanger HX2 and HX3 are glycol-to-refrigerant plate heat exchanger inside the Bundgaard unit. The heat capacity can be calculated by

$$Q = UA\Delta t_m \quad \text{Equation 9}$$

Where  $\Delta t_m$  is log mean temperature difference (LMTD). For the evaporator HX2, assuming condensation throughout the length of the condenser and also assume the pressure drop to be negligible, the mean temperature difference is given by

$$\Delta t_m = \frac{T_{g,2in} - T_{g,2out}}{\ln \left( \frac{T_{g,out} - T_e}{T_{g,in} - T_e} \right)} \quad \text{Equation 10}$$

The heat exchanger HX4 is glycol-to-air heat exchanger, which can be calculated with the similar manner at HX1 except that HX1 is wet coil.

The system has the heat balance between the four heat exchangers and compressor with governing equations of

$$Q_{HX1} = Q_{HX2} \quad \text{Equation 11}$$

$$Q_{HX3} = Q_{HX4} \quad \text{Equation 12}$$

and

$$Q_{HX3} = Q_{HX2} + W_{comp} \quad \text{Equation 13}$$

## Calibration

First, the model was calibrated with the manufacturer reported data.<sup>6</sup> The first calibration was done with cooling performance. Since it was not mentioned in the test report, the researchers assumed the performance data was obtained at 100 percent capacity and 35°C (95°F) standard outdoor condition. The performance is shown in Table 16.

**Table 16: Bundgaard Propane System, Performance Data**

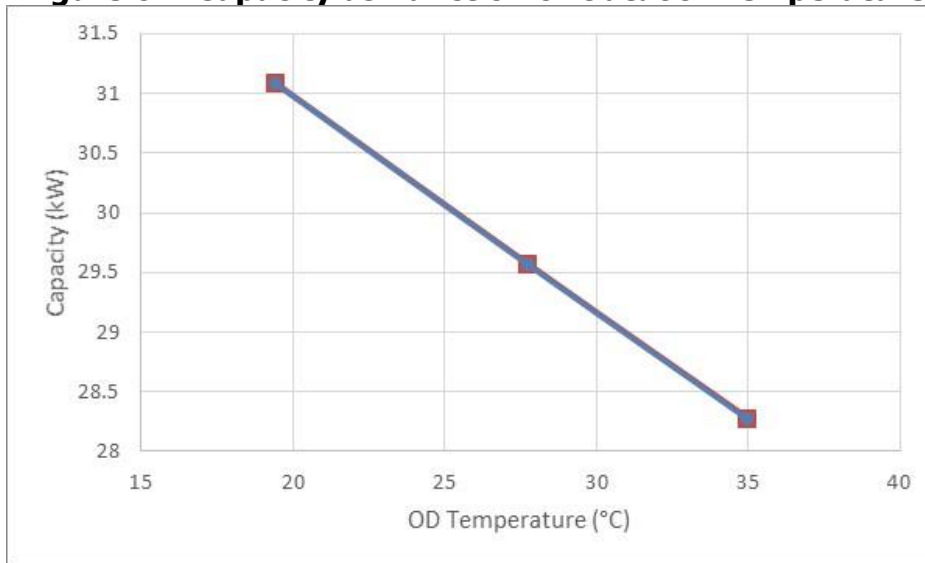
Performance Item	Data	Unit
Cooling Capacity	28.2	kW
Compressor EER (cooling COP)	3.58	
Cooling side glycol inlet temperature (Tg_1)	11	°C
Cooling side glycol outlet temperature (Tg_2)	6	°C
Glycol cooling side mass flow rate ( $\dot{m}_{g1}$ )	5.2	m3/h
Glycol high side mass flow rate ( $\dot{m}_{g1}$ )	6.3	m3/h
Indoor air entering dry bulb temperature	26.7	°C
Indoor air entering wet bulb temperature	19.4	°C
Outdoor air entering dry bulb temperature	35	°C

Source: Electric Power Research Institute

## Simulation Results

Figure 61 graphs the capacity of the Bundgaard propane system as a function of outdoor temperature.

**Figure 61: Capacity as Function of Outdoor Temperature**

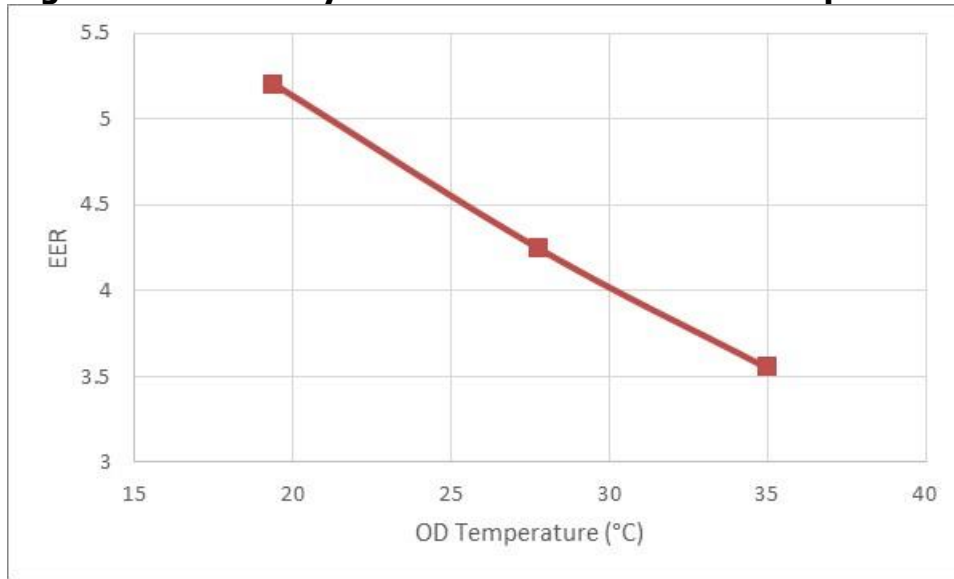


Source: Electric Power Research Institute

<sup>6</sup> Datasheet WWCXS Quotation COOLING (standard konditioner) (003)

Figure 62 graphs the efficiency of the Bundgaard propane system as a function of outdoor temperature.

**Figure 62: Efficiency as a Function of Outdoor Temperature**



Source: Electric Power Research Institute

### Performance of R410A VRF System

A typical R410A VRF system is simulated in Vapcyc. Table 17 compares the results with the Bundgaard system performance.

**Table 17: Comparison of Propane System and Simulated R410A VRF System**

	Capacity Index	OAT DB	Capacity	Power	EER
Bundgaard Propane Unit (Tested)	125%	95	<b>115,180</b>	<b>14,510</b>	<b>7.94</b>
R410A VRF (Simulated)	125%	95	115,462	14,459	7.99
ATS simulation % of test			0.24%	-0.35%	0.63%

Source: Electric Power Research Institute

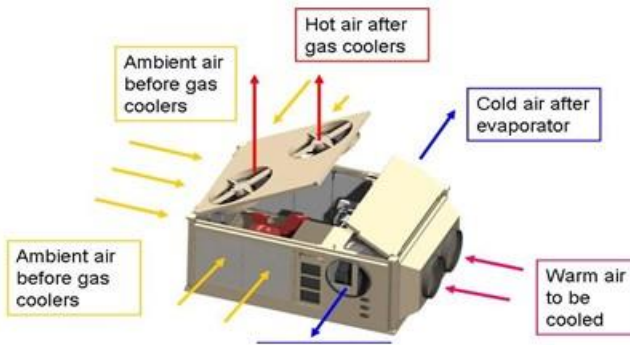
The tested performance of the propane unit closely matched the simulated R410A VRF system with respect to cooling capacity, power draw, and efficiency. This suggests that converting from standard refrigerant to the low-GWP propane refrigerant does not compromise equipment performance or efficiency.

## CTS Custom Carbon Dioxide (R744) Heat Pump

### Equipment Information

EPRI, in collaboration with Creative Thermal Solutions (CTS), custom built a CO<sub>2</sub> heat pump using R744 as refrigerant to investigate and evaluate the performance of the system and components through laboratory simulation based on predefined testing parameters. Figure 63 provides a photo of the unit after its completion and a diagram of the airflow through the unit.

**Figure 63: Carbon Dioxide Heat Pump and Air Flow Diagram**



Source: Electric Power Research Institute

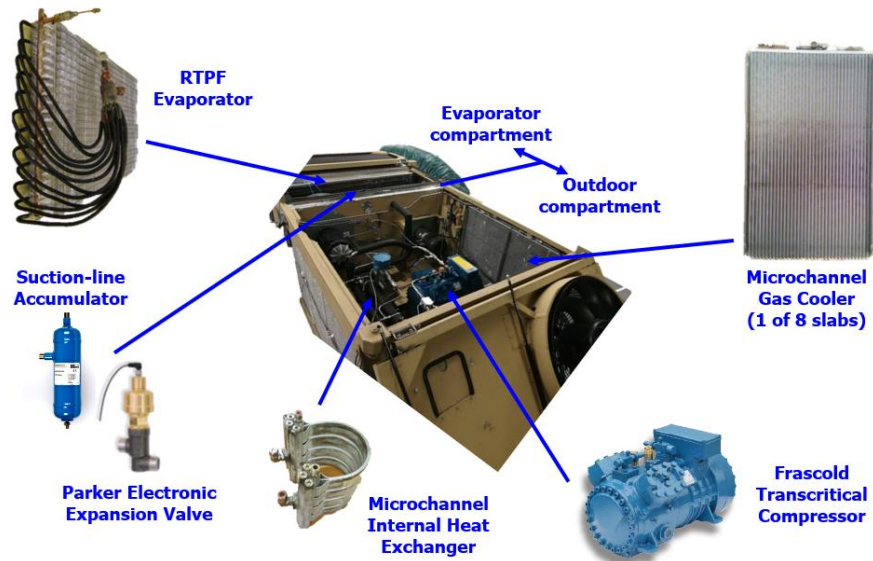
Table 18 and Figure 64 provide a further look into the exact components and locations within the unit's shell that went into the assembly of this unit.

**Table 18: List of Carbon Dioxide Heat Pump Components**

Component	Manufacturer	Model
Compressor	Frascold	Q9-6TK
Gas cooler	Modine	Microchannels: 4 x 17.2" x 22" & 4 x 13.5" x 22"
Evaporator	Modine	Round-tube-plate-fin: 1 x 22" x 44.6"
Suction-line accumulator	ESK Schultze	FA-12U-CDH
Electronic expansion valve	Parker-Sporlan	GC-20
Internal heat exchanger	Modine	Microchannel plates: 2 x 15" x 7.5"

Source: Electric Power Research Institute

**Figure 64: Diagram of Carbon Dioxide Heat Pump Component Locations**



Source: Electric Power Research Institute

The following data points were collected using the monitoring equipment installed into the system design to calculate cooling capacity, heating capacity, and coefficient of performance:

- Evaporator nozzle pressure drop
- Indoor inlet dew point
- Indoor outlet dew point
- Unit power
- Refrigerant mass flow
- Refrigerant pressure
- Refrigerant temperature

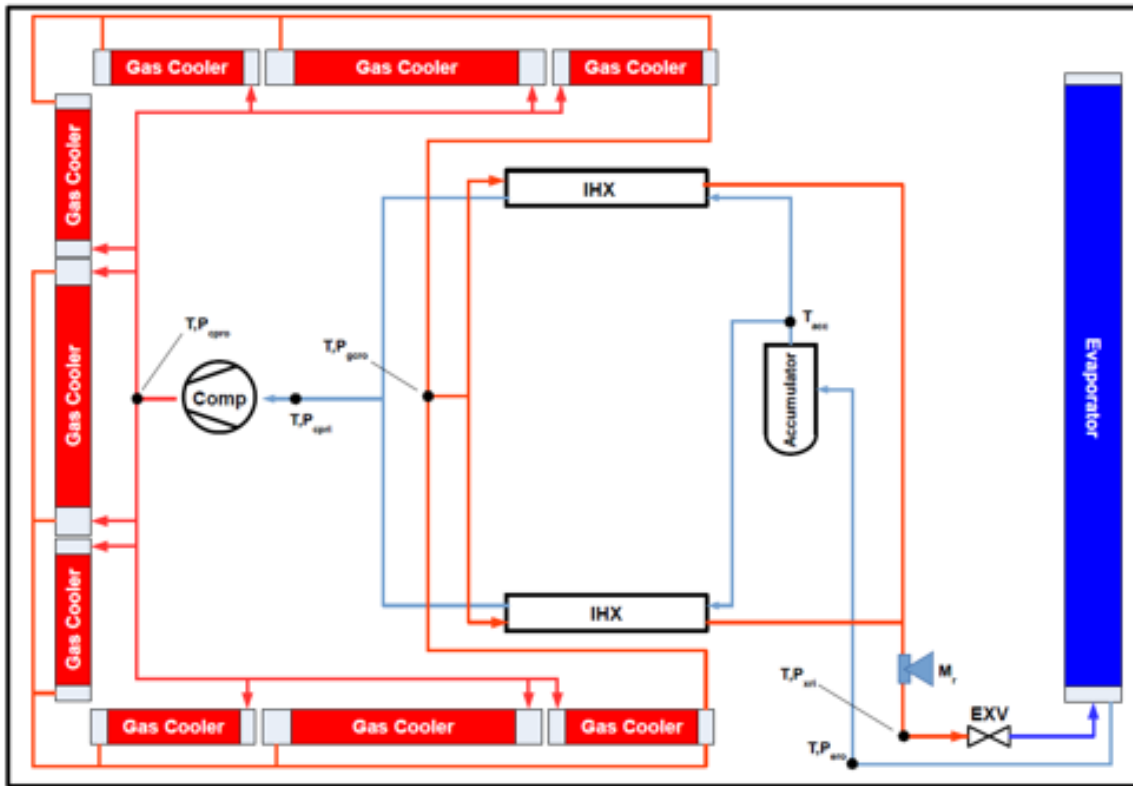
Table 19 lists the equipment responsible for collecting this information. Figure 65 shows the final schematic and instrumentation plan.

**Table 19: List of Sensors**

Sensor	Manufacturer	Model Number	Uncertainty
Evaporator Nozzle Pressure Drop	Rosemount	1151DR2F	$\pm 1.5$ Pa
Indoor Inlet Dew Point	General Eastern	1311DR-SR (sensor) Hygro-M2 (transmitter)	$\pm 0.2$ K
Indoor Outlet Dew Point	EdgeTech	S2	$\pm 0.2$ K
Unit Power	Ohio Semitronics	PC5-054E	$\pm 0.2\%$ Reading
Refrigerant Mass Flow	Micro Motion	CFM-025	$\pm 0.1\%$ Reading
Refrigerant Pressure Sensor	Rosemount	1151GP8	$\pm 0.1\%$ of Calibrated Span
Refrigerant Temperature	Omega	T-type	$\pm 0.2$ K

Source: Electric Power Research Institute

**Figure 65: Carbon Dioxide Heat Pump Schematic and Instrumentation Locations**

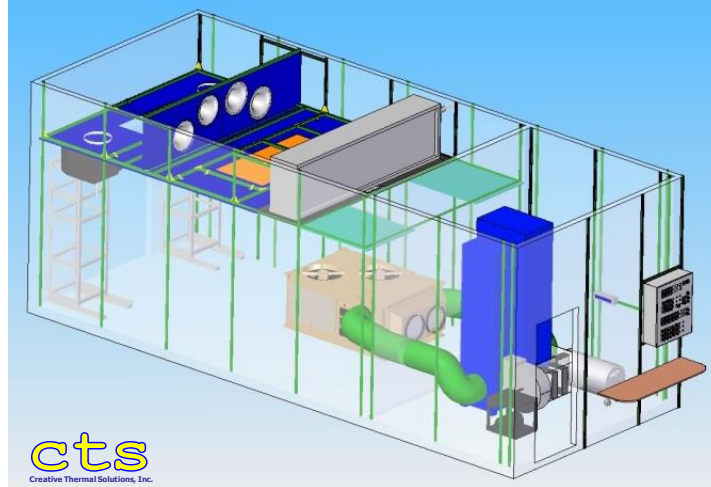


Source: Electric Power Research Institute

## Testing Plan

The laboratory testing of the custom-built CO<sub>2</sub> heat pump was performed at Creative Thermal Solutions laboratory located in Urbana, Illinois. The unit was placed in an environmental chamber to control the indoor and outdoor air conditions during multiple testing conditions and provide additional energy balance. Figure 66 shows a rendering of the final equipment locations for testing setup.

**Figure 66: Carbon Dioxide Heat Pump Testing Facility Setup**



Source: Electric Power Research Institute

To the left of the insulated divider wall separating the indoor and outdoor chambers is the heat rejection chamber where the CO<sub>2</sub> heat pump unit was located. The gray box in the rendering represents the glycol coil that helped to control temperatures by removing heat from the chamber. Figure 67 is a photo of how the heat rejection chamber currently sits today.

**Figure 67: Heat Rejection Chamber**



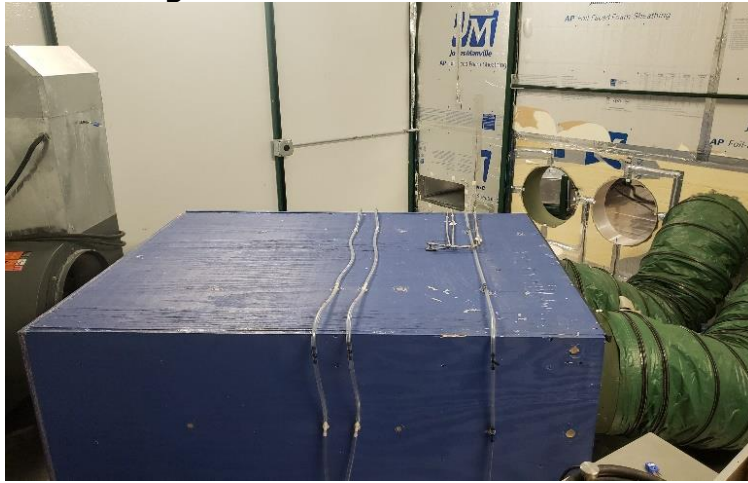
Source: Electric Power Research Institute

The heat load chamber where the air ducting and wind tunnel have been placed are to the right of the insulated divider wall.

Figure 68 shows an actual photo of the heat load chamber setup.



**Figure 68: Heat Load Chamber**



Source: Electric Power Research Institute

The testing conditions defined for the CO<sub>2</sub> heat pump follows AHRI standards for performance rating of unitary air-conditioning and air-source heat pump equipment. For cooling conditions, the standard AHRI A and C conditions for performance rating of AC units were taken from AHRI Standard 210/240. A modified B' condition with the outdoor dry bulb temperature of 109.4°F was added to evaluate the performance of the unit at a higher ambient temperature condition. The heating conditions H1, H2, and H3 heat pump performance rating conditions were taken from AHRI standard 210/240 as well. The full cooling conditions and heating temperature conditions used during testing can be referenced in Table 20 and Table 21..

**Table 20: Cooling Mode Testing Conditions**

Test	T <sub>db,id</sub> (°F)	T <sub>wb,id</sub> (°F)	T <sub>db,od</sub> (°F)
A	80.1	66.9	95.0
Modified B	80.1	66.9	109.4
C	80.1	57.0	82.0

Source: Electric Power Research Institute

**Table 21: Heating Mode Testing Conditions**

Test	T <sub>db,id</sub> (°F)	T <sub>db,od</sub> (°F)	T <sub>wb,od</sub> (°F)
H1	70.0	46.9	43.0
H2	70.0	35.1	33.1
H3	70.0	17.1	15.1

T<sub>db,id</sub> : Indoor dry-bulb temperature; T<sub>wb,id</sub> : Indoor wet-bulb temperature; T<sub>db,od</sub> : Outdoor dry-bulb temperature; T<sub>wb,od</sub> : Outdoor wet-bulb temperature

Source: Electric Power Research Institute

## Testing Results

Cooling capacity is the measure of a cooling system's ability to remove heat from the interior space it is conditioning. Inversely, heating capacity is the measure of heat to be supplied to produce a unit change in temperature. It allows one to understand a system's ability to perform heating and cooling functions. The researchers used the ASHRAE Handbook for HVAC Systems and Equipment to calculate system cooling capacity, heating capacity, and COP.

### Cooling Capacity

$$Q_{cooling} = m_r(h_{cpri} - h_{gcro})$$

Where

$Q_{cooling}$  = cooling capacity (kW)

$m_r$  = refrigerant mass flow rate (kg/s)

$h_{cpri}$  = refrigerant specific enthalpy at the inlet of the compressor (kJ/kg)

$h_{gcro}$  = refrigerant specific enthalpy at the outlet of the gas cooler (kJ/kg)

### Heating Capacity

$$Q_{heating} = m_r(h_{cpri} - h_{gcro}) + W_{cp}$$

Where

$Q_{heating}$  = heating capacity (kW)

$W_{cp}$  = compressor input power (kW)

### Coefficient of Performance

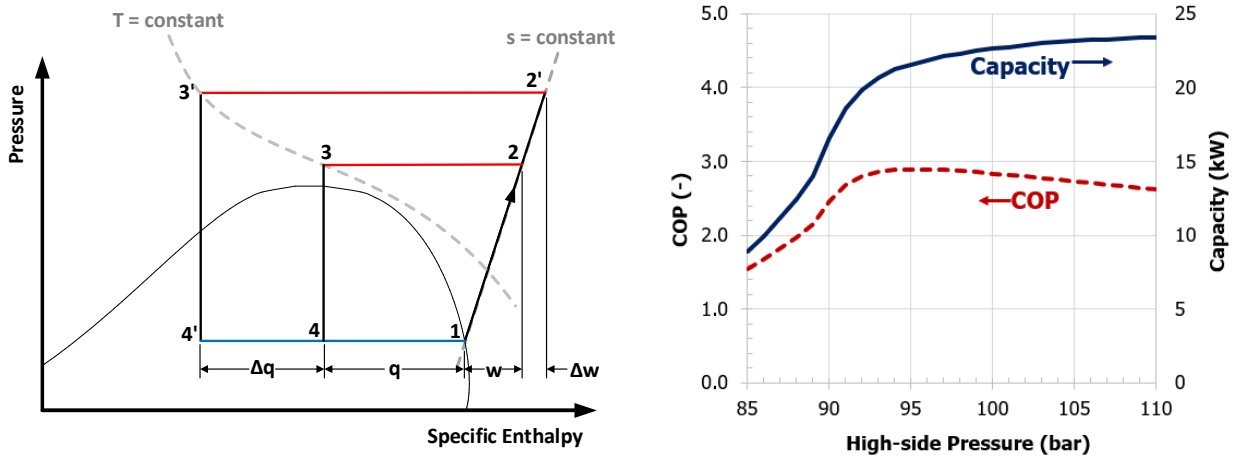
The COP is the ratio of useful heating or cooling provided to the power required by the considered system. The COP allows one to grade efficiency where a 100 percent efficient system would have a COP of 1. In the case of a heat pump, the COP can exceed a COP of 1 because it pumps additional heat to where the heat is required. The ASHRAE Handbook for HVAC Systems and Equipment, cooling capacity, heating capacity and COP were calculated through the following equations:

$$COP_{cooling} = \frac{Q_{cooling}}{W_{cp}}$$

$$COP_{heating} = \frac{Q_{heating}}{W_{cp}}$$

A simulation was performed and plotted for carbon dioxide at 95°F ambient temperature to illustrate the critical, transcritical, and subcritical points of carbon dioxide refrigerant under various pressures and the resulting performance curves. The simulation graphs can be seen in Figure 69.

**Figure 69: Pressure/Enthalpy Diagram (Left) and Performance Diagram (Right)**

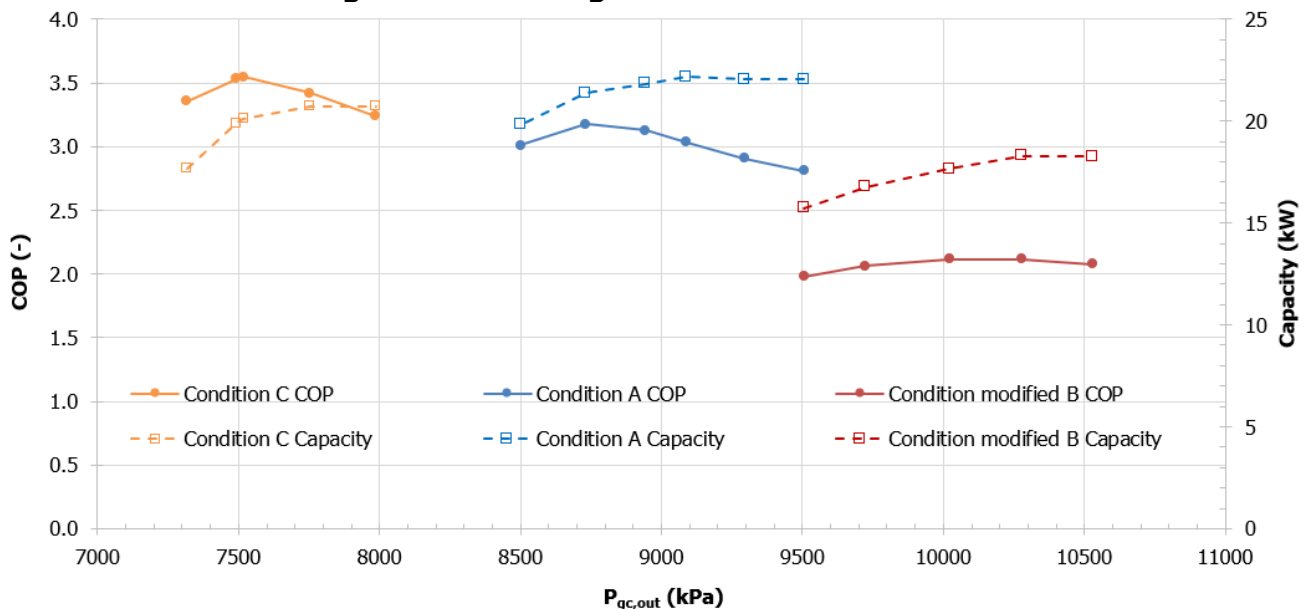


The results suggest that at greater high-side pressures, both the capacity and compressor work harder, meaning the effect on COP is not immediately clear. As high-side pressures increase, the capacity of the system will continue to increase until the COP values hit a plateau and begin to taper off because extra work is being performed to compress the system.

In fact, selecting a higher capacity system at a lower COP may be the optimal performance scenario for a given system. There is a delicate balance to reach a system’s maximum capacity and COP.

For each cooling temperature condition outlined in Table 20, experiments were performed in transcritical mode at varying pressure values to identify the optimization point where the maximum COP is obtained, beginning at high-side pressures and moving toward lower pressures to observe when the COP peaks and begins declining. The results for all tested cooling conditions can be seen in Figure 70.

**Figure 70: Cooling Conditions Test Results**



Source: Electric Power Research Institute

It was found that the optimization point was reached at a lower pressure for lower temperature conditions. This makes sense because at higher ambient conditions, in cooling

mode the system will need to operate at a higher pressure (condensing temperature) for the heat sink to reject heat into the environment. The maximum COP values obtained for all cooling and heating conditions and the resulting capacity values and temperatures can be seen in Table 22.

**Table 22: System Optimization Testing Results for Cooling and Heating**

Test	Condition				Air side		Refrigerant side		Result	
	T <sub>db,id</sub> (°F)	T <sub>wb,id</sub> (°F)	T <sub>dp,id</sub> (°F)	T <sub>db,od</sub> (°F)	T <sub>eaο</sub> (°F)	T <sub>dp,eaο</sub> (°F)	T <sub>eri</sub> (°F)	T <sub>ero</sub> (°F)	Capacity (kW)	COP
A	81.0	68.0	61.5	95.2	67.1	60.1	56.1	55.4	21.04	3.07
Modified B	80.1	66.9	60.3	109.8	68.5	59.4	57.4	56.8	17.65	2.12
C	80.1	59.2*	43.3	82.0	63.9	44.4	49.6	48.9	21.04	3.71
H1	47.3	43.2	38.5	70.0	36.7	36.0	23.4	23.2	23.24	4.23
H2	35.8	33.4	30.4	70.3	27.0	27.3	14.2	13.6	20.29	3.67
H3	19.0	16.0	7.5	69.8	14	8.1	-8.3	-8.7	13.20	2.69

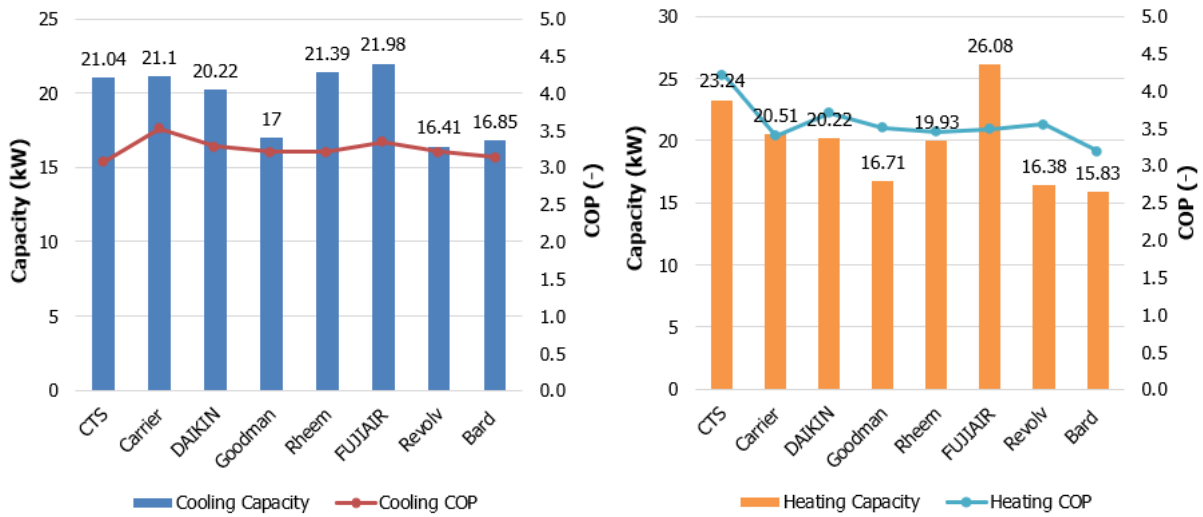
**\*Note:** For condition C, the evaporation temperature was higher than the inlet air dew point, so there was no latent load (condensation) on the evaporator, and dewpoint had no effect on the performance.

T<sub>db,id</sub> : Indoor dry-bulb temperature; T<sub>wb,id</sub> : Indoor wet-bulb temperature; T<sub>dp,id</sub> : Indoor dewpoint; T<sub>db,od</sub> : Outdoor dry-bulb temperature; T<sub>eaο</sub> : Air temperature leaving the evaporator; T<sub>dp,eaο</sub> : Air dewpoint leaving the evaporator; T<sub>eri</sub> : Refrigerant temperature at the inlet of the evaporator; T<sub>ero</sub> : Refrigerant temperature at the outlet of the evaporator.

Source: Electric Power Research Institute

The results show that at AHRI A condition, the unit can provide 21 kW of cooling capacity with a cooling COP of 3.07. At H1 heating condition, the CO<sub>2</sub> unit can provide 23 kW of heating capacity with a heating COP of 4.23. Comparison of the measured performance of the CO<sub>2</sub> heat pump system with the nominal COP of the major R410A systems on the market can be seen in Figure 71.

**Figure 71: Comparison to Other Commercially Ready R410A Systems**



Source: Electric Power Research Institute

Comparison with nominal data for commercially available R410A AC/HP systems shows the CO<sub>2</sub> heat pump system has equal or slightly lower cooling COP at equal or slightly higher cooling capacity but much higher heating capacity and the highest COP. However, further improvement to the capacity and upwards of a 20 percent increase in COP may be possible through expansion work recovery (expander, ejector, and so forth). Furthermore, the CO<sub>2</sub> heat pump unit was designed for a trailer-mounted application, meaning the unit was designed to be compact. This compact configuration for mobility does compromise system performance relative to an optimal configuration. The design and components can be further optimized for stationary application by improving cycle architecture and adding an ejector to improve the overall performance.

## Ammonia (R717) Heat Pump

In a parallel effort to this project, EPRI evaluated a first-of-its-kind, natural refrigerant-based HVAC system in its laboratory facilities in Knoxville, Tennessee for SCE’s Emerging Technology Group.<sup>7</sup> Complementing the propane refrigerant system tested in California and the CO<sub>2</sub> refrigerant system tested in Illinois, this system used ammonia (NH<sub>3</sub>, or R717 as a classified refrigerant) in a low-charge packaged chiller as the primary refrigerant for vapor compression and CO<sub>2</sub> as the convection fluid to distribute cooling to remote indoor air handlers. This configuration aligns with traditional space cooling systems that use halocarbon-based chillers coupled to chilled-water pumped loops.

In theory, this combination takes advantage of the high efficiency and favorable heat transfer properties of NH<sub>3</sub> and the high heat capacity of CO<sub>2</sub> to provide a very low GWP option for medium to large HVAC applications. Among its other advantages, ammonia is applicable across a wide range of temperatures, and its characteristic odor can serve as a warning detection for leaks. The technology concept builds on advances made in the supermarket refrigeration

<sup>7</sup> Southern California Edison. “Environmentally Friendly Advanced Refrigerant Options in Commercial HVAC Applications.” EPRI. Publication pending 2020.

sector where managing refrigeration is highly important and a shift toward zero-GWP refrigerants is already underway.

The general approach was to build a performance map of operation across a range of outdoor operating temperatures, characterized by capacity, power consumption, and efficiency over outdoor temperatures spanning approximately 70°F – 100°F. Higher outdoor ambient temperatures were accommodated by supplementing heat to the return air stream of the chiller. Indoor return air conditions were nominally held at 80°F and 50 percent relative humidity, as defined by industry rating standards like AHRI 340/360 (Performance Rating of Commercial & Industrial Unitary Air-Conditioning and Heat Pump Equipment).

The test was set up as a hybrid laboratory/field installation, with the system conditioning laboratory space with control of indoor ambient conditions in a dedicated indoor room. The chiller, CO<sub>2</sub> receiver, and CO<sub>2</sub> pump were positioned outside and were subject to the ambient conditions of the summer testing period. Figure 72 shows the outdoor installation of the system at the EPRI Knoxville laboratory.

**Figure 72: Mayekawa Sierra System at EPRI Knoxville Labs**

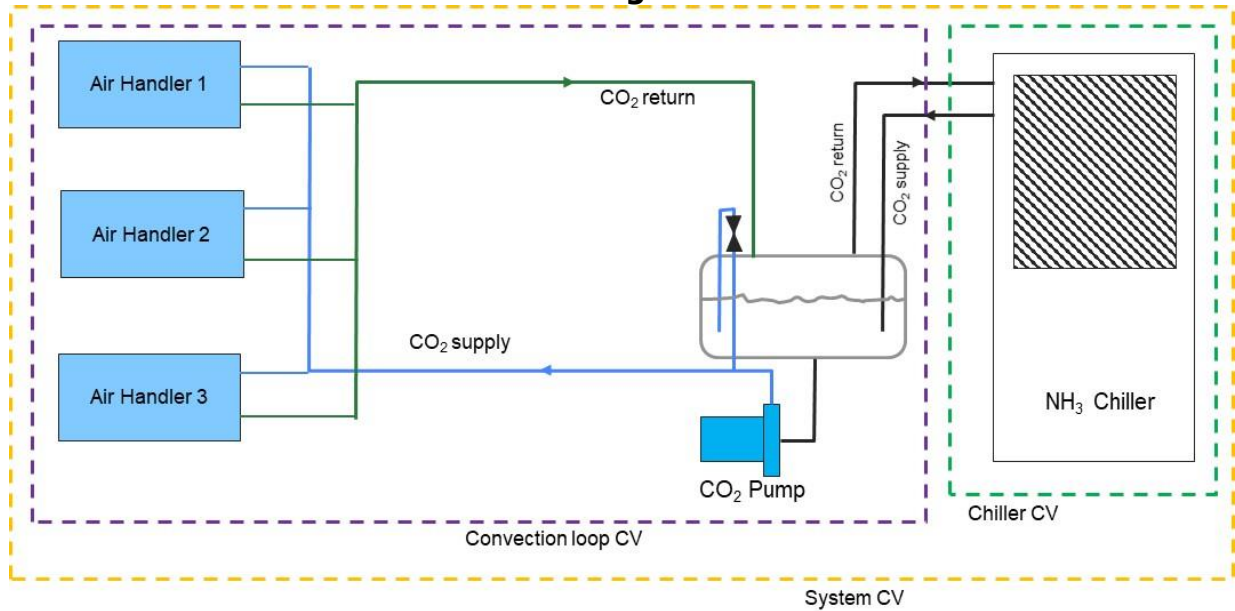


Source: Electric Power Research Institute

The system was deployed in a secondary loop configuration in which the Sierra ammonia-driven unit chills a working fluid of CO<sub>2</sub>, which pumps to provide cooling to the indoor air handling units.

Similarly, Figure 73 illustrates the CO<sub>2</sub> loops between the ammonia chiller, the CO<sub>2</sub> receiver/pump skid, and the air handling units. This configuration required two-phase CO<sub>2</sub> flow measurement, which is complex.

**Figure 73: Secondary Loop Configuration, Ammonia Chiller, and Carbon Dioxide Working Fluid**



Source: Electric Power Research Institute

Figure 74 shows the outdoor installation from the perspective of the CO<sub>2</sub> receiver and pump skid in the foreground and ammonia chiller in the background.

**Figure 74: Outdoor System Fully Installed**



Source: Electric Power Research Institute

Comparing two secondary loop configurations — the novel use of an ammonia refrigerant system with CO<sub>2</sub> as a pumped working fluid versus a traditional halocarbon refrigerant system with chilled water working fluid — reveals a number of qualitative differences, as summarized in Table 23.

**Table 23: Traditional versus Ammonia/Carbon Dioxide Refrigerant Systems**

Halocarbon/Pumped Chilled Water	NH <sub>3</sub> Chiller/Pumped CO <sub>2</sub>
Familiarity to industry and trades	High inherent NH <sub>3</sub> efficiency
Large piping, high install cost	NH <sub>3</sub> toxicity, familiarity of trades
Many products available	Lower pumping energy for CO <sub>2</sub>
GWP of refrigerants e.g. R134a	CO <sub>2</sub> pressure, familiarity of trades
Air or water source	High heat capacity of CO <sub>2</sub>
Higher pumping energy for water	Limited product availability for HVAC applications
Many configurations possible (positive displacement or centrifugal)	Air or water source
Water treatment chemicals	Limited knowledge of system lifetime issues
Scalable	Lower piping installation cost
	High operating pressure
	Near zero GWP of refrigerants
	CO <sub>2</sub> management (leaks & maintenance)

Source: Electric Power Research Institute

The main advantages of the ammonia-CO<sub>2</sub> configuration are the inherent thermal efficiency of ammonia (NH<sub>3</sub>) as a refrigerant medium, lower energy required to pump CO<sub>2</sub>, high heat capacity of CO<sub>2</sub>, and lower GWP. The heat transfer capacity of saturated CO<sub>2</sub> fluid (at a pressure of approximately 500 pounds per square in gauge) is 99.3 Btu per pound transferred (Btu/lbm), which is nearly 10 times the heat transfer capacity of water.

A fundamental challenge facing the ammonia-CO<sub>2</sub> configuration is the toxicity and corrosivity of ammonia. The toxicity risk from leakage is a primary reason why the ammonia loop is entirely outdoors to eliminate any possibility of ammonia refrigerant leaking indoors. In addition, it is important to entirely contain the ammonia refrigerant in a closed loop, indirectly exchanging heat with the CO<sub>2</sub> working fluid, to avoid impurities entering the ammonia system. The risk of impurities remains in the charging process, piping leaks, and natural chemical breakdown of ammonia. The hazards of impurities entering the ammonia system include corrosion and damage to pipes and equipment.

Due to these technical risks and limited product availability, most HVAC trades are unfamiliar with, or have no practical experience with, ammonia-CO<sub>2</sub> systems and as a result are unlikely to recommend them to a customer.

**Test Results**

Analyzing the performance of the ammonia-CO<sub>2</sub> system required design and instrumentation of both the air-side and refrigerant-side convection loop, and the refrigerant-side chiller loop.

The operative metric for measuring system performance was the combination of air-side convection loop and component power input.

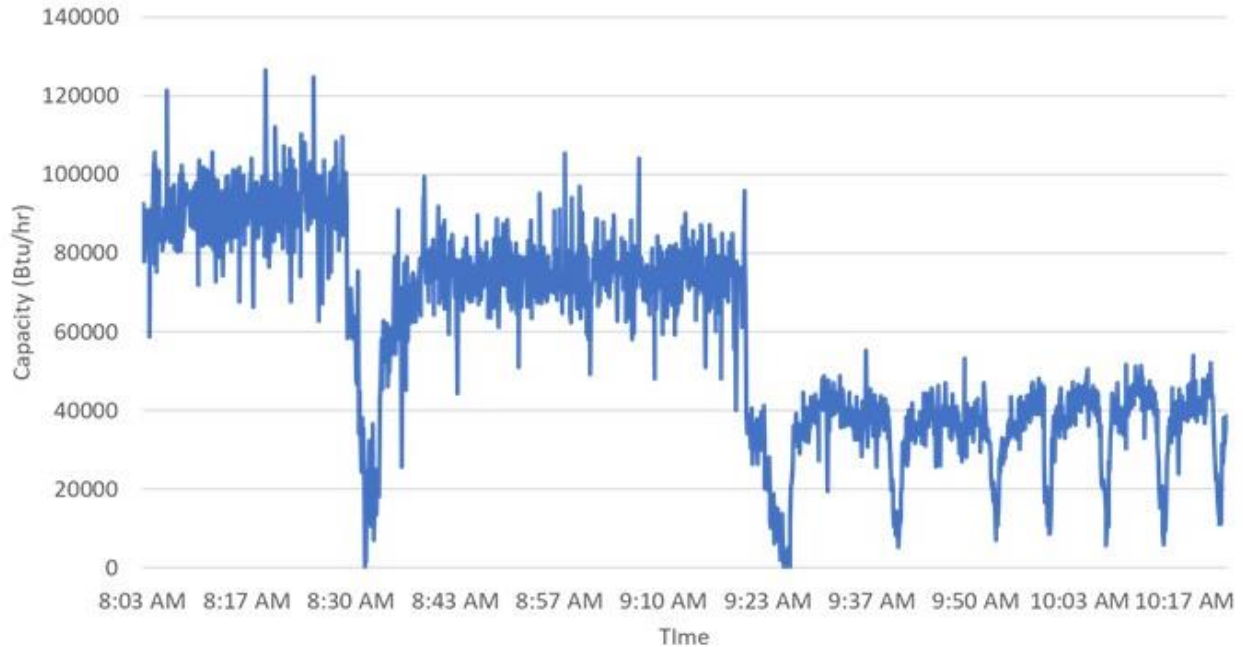


Evaluation included tests at three different ambient temperatures:

- Low Ambient ( $\sim 75\text{--}77^\circ\text{F}$ )
- Medium Ambient ( $\sim 83\text{--}87^\circ\text{F}$ )
- High Ambient ( $\sim 91^\circ\text{F}+$ )

Testing at the low ambient temperature range of  $75\text{--}77^\circ\text{F}$  was performed in steady state equilibrium with three air handlers. Figure 75 graphs the power consumption of the chiller as a function of time. The brief drop to zero capacity at the switch from three to two indoor units is a transition effect. Operating COPs ranged from 2.45 to 3.14.

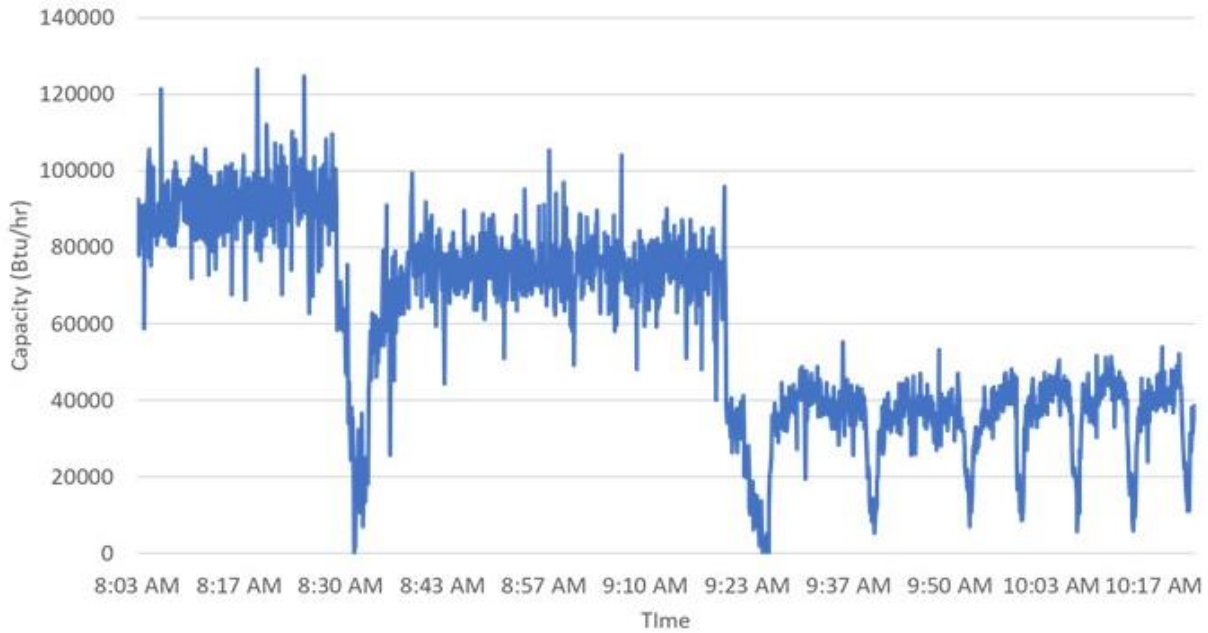
**Figure 75: Cooling Capacity vs. Time at Approximately  $75^\circ\text{F}$  Ambient Temperature**



Source: Electric Power Research Institute

Testing at the medium ambient temperature range of approximately  $86.5^\circ\text{F}$  was performed in steady state equilibrium with three air handlers and indoor return air temperature held constant at approximately  $80^\circ\text{F}$ . After reaching equilibrium and collecting data in the steady-state, two indoor units were successively turned off and the system was again allowed to reach steady-state. Figure 76 graphs the power consumption of the chiller as a function of time. Operating COPs ranged from 2.01 – 2.55.

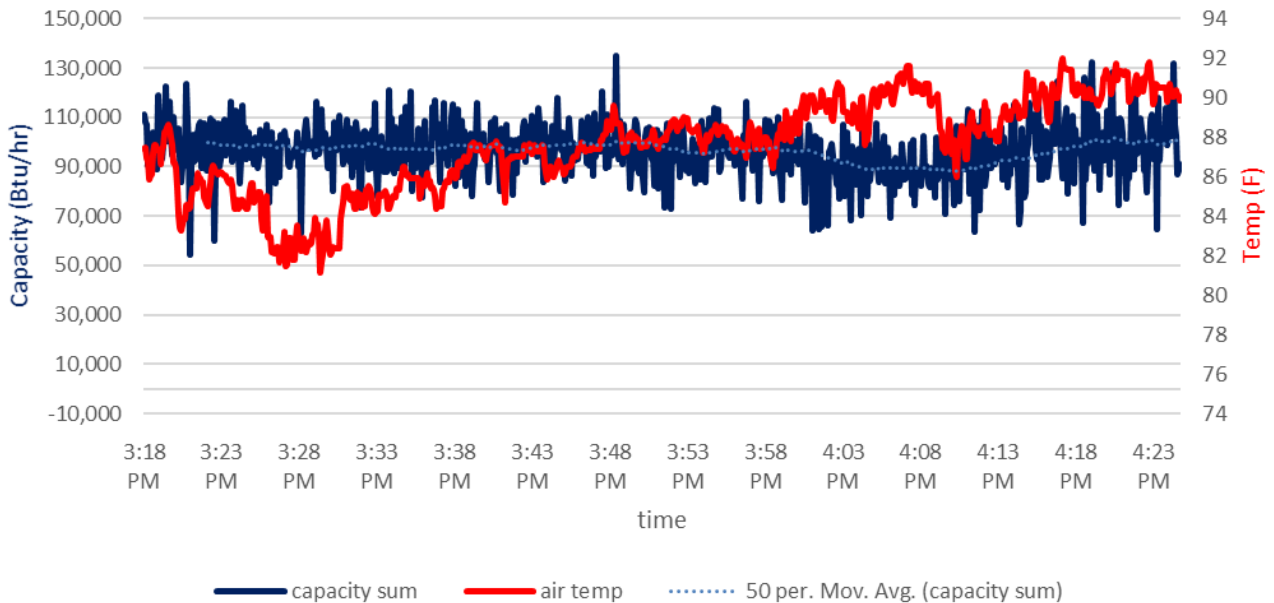
**Figure 76: Cooling Capacity vs. Time at Approximately 86.5°F Ambient Temperature**



Source: Electric Power Research Institute

High ambient testing was performed by adding supplemental electric resistance heat in stages to boost the condenser inlet air temperature to approximately 91°F. The system was operated for approximately one hour in a pseudo-steady state after equilibration, with the progression illustrated in Figure 77. At a condenser return temperature of approximately 91°F, total air-side cooling capacity was 98.4 kBtu/hr (approximately 8.2 tons), with total power consumption of 12.6kW, resulting in an overall COP of 2.14.

**Figure 77: Cooling Capacity & Outdoor Temperature vs. Time (High Ambient)**



Source: Electric Power Research Institute

This test validated a two-stage system with an ammonia chiller replacing a halocarbon chiller and a CO2 loop replacing a water loop. Considering the early-stage nature of this prototype, effectively repurposing an off-the-shelf semi-industrial chiller for an HVAC cooling application,

COPs in the range of 2.1 to 3.1 at various operating states should be considered promising. Many engineering adjustments and improvements can be made for future iterations, including more advanced CO<sub>2</sub> flow control at the air handlers, better size matching of the chiller and CO<sub>2</sub> loop components, and a more efficient pumping strategy. Therefore, target COPs for a field deployable system would be in the 3.0+ range.

Among the important procedural learnings from this test was the importance of managing the flow of the CO<sub>2</sub> working fluid. Pumping CO<sub>2</sub> near its saturated state and boiling point can cause cavitation, which poses an engineering design challenge.

A logical next step would be to design an ammonia chiller designed for higher temperature of HVAC use versus its more customary refrigeration application.

## Conclusions and Recommended Next Steps

As shown in Table 24, the test results from the three test facilities demonstrated that natural refrigerants with low to zero GWP can achieve COPs exceeding 2.0 under less than ideal test conditions with equipment not necessarily optimized for HVAC applications.

**Table 24: Summary of Refrigerant Testing Results**

Refrigerant	Tested COP Range (Cooling Mode)	Tested COP Range (Heating Mode)
Propane	2.8 – 4.0	3.4 – 4.2
CO <sub>2</sub>	2.1 – 3.7	2.7 – 4.2
Ammonia	2.1 – 3.1	NA

Source: Electric Power Research Institute

This outcome is encouraging for future tests of natural refrigerants in systems that are engineered and optimized for HVAC application where even higher COPs may be expected. These results suggest that using the natural low-GWP refrigerants propane, CO<sub>2</sub>, and ammonia does not necessarily mean a significant compromise in performance and system energy efficiency.

# CHAPTER 6:

## Knowledge Transfer Activities

---

### Variable Refrigerant Flow + Indirect Evaporative Cooling Demonstration

The demonstration sites selected for the project represent commercial buildings that are inherently appropriate candidates for the VRF+IEC hybrid system, insofar as they are small- and medium-sized offices and restaurants, typically served by incumbent packaged rooftop units, with high occupancy and therefore high ventilation requirements commensurate with an IEC system operating as a dedicated outside air system. The addressable market of small- and medium-sized commercial office buildings and restaurants in California served by rooftop units is vast and represents an opportunity for energy savings and peak load reduction through conversion to VRF+IEC systems.

By selecting a quick-serve chain restaurant, Del Taco, as one of the demonstration sites, the results are directly replicable and scalable to the other 580-plus Del Taco restaurants in California, given their similarities in size, configuration, operating hours, and occupancy patterns. This represents an immediate and sizable “warm market” for this technology, given the company’s experience with using the technology and experiencing its benefits. Corporate facility managers from different regions can review the performance data from the demonstration site and obtain first accounts from store management on the installation process and experience of staff and customers.

By extension, other quick-serve restaurant chains represent an additional addressable market. Outreach to industry trade organizations such as the California Restaurant Association can help transfer the knowledge and experience of the VRF+IEC systems. Moreover, the HVAC installation contractors that worked on this project can apply these skills and experiences to other customers. One of the aims of this project is to enable scaled field applications and programmatic incentive programs for the VRF+IEC combination. There are nearly 90,000 restaurants in California, with approximately one-third in the fast food or quick-serve segment.<sup>8</sup>

With respect to modeling, this project developed enhancements to the EnergyPlus building energy simulation tool, including updated modules for VRF, IEC, and VRF+IEC. These enhancements have been communicated to the United States Department of Energy, which funds the development of EnergyPlus through its Building Technologies Office and releases major updates each year.

The results from this project will be widely shared following the release of this report through presentations and papers at such industry outreach events as the American Council for an Energy-Efficient Economy (ACEEE) Building Summer Study, Emerging Technologies Summit, California Emerging Technology Coordination Council, Utility Energy Forum, and meetings of

---

<sup>8</sup> Ibis World. “Restaurants in California – Market Research Report. February 2020. <https://www.ibisworld.com/industry-trends/market-research-reports/california/accommodation-food-services/restaurants-in-california.html>

the California Institute for Energy and Environment, Western Cooling and Efficiency Center, and New Buildings Institute. EPRI plans to conduct similar demonstration projects in California with a greater variety of appropriate commercial buildings in different climate zones, in conjunction with utilities and other partners. Finally, EPRI intends to work with utility partners to replicate this type of technology demonstration around the country.

### **Natural Refrigerant Testing**

The results and learnings from the laboratory testing of natural refrigerant systems will be shared in research papers and articles submitted for conferences convened in the HVAC industry, including ASHRAE and ACEEE. In addition, EPRI intends to conduct follow-up research and field demonstrations with its utility clients to build upon and advance the work pioneered through this project.

# CHAPTER 7:

## Conclusions and Recommendations

---

### **Variable Refrigerant Flow + Indirect Evaporative Cooling Demonstration**

The field demonstration of VRF+IEC system at two of the three sites delivered valuable results. The performance of the VRF+IEC system at the Del Taco treatment site demonstrated energy savings relative to the nearly identical Del Taco control site using a rooftop unit (RTU) system. Since RTU is the most common default HVAC technology for the restaurant segment and a large share of the small- and medium-sized commercial buildings in California, it is most useful to measure savings of the VRF+IEC hybrid system relative to this baseline. The Del Taco results showed significant energy savings and peak demand reduction. Over the course of a six-month period spanning September 2019 through February 2020, the Del Taco treatment site with the VRF+IEC system yielded average monthly energy savings of approximately 32.4 percent compared to the RTU control site. On the summer peak day during this period, the VRF+IEC system resulted in energy savings of 20.0 percent, including a 14.7 percent reduction in peak demand during the 1:00 p.m. hour. During the winter peak day, the VRF in heating mode at the treatment site resulted in 45 percent energy savings compared to the control site heating system.

The Western Center for Cooling and Efficiency site installation provided an opportunity to observe the energy savings effect of the VRF+IEC system relative to the baseline of an incumbent VRF unit. The demonstration yielded an average energy savings of 18.7 percent beyond the previous operation of a VRF system on similar days across a variety of ambient temperatures during the cooling season. This conclusion validates the additional energy savings potential of IEC in combination with a VRF and its application to sites with pre-existing VRF systems.

EPRI plans to conduct similar demonstration projects in California with a greater variety of appropriate commercial buildings in different climate zones, in conjunction with utilities and other partners. Finally, EPRI intends to work with utility partners to replicate this type of technology demonstration around the country.

### **Natural Refrigerant Testing**

As summarized in Table 25, the test results from the three test facilities demonstrated that natural refrigerants with low to zero global warming potential can achieve coefficients of performance exceeding 2.0 under less than ideal test conditions with equipment not necessarily optimized for HVAC applications.

**Table 25: Summary of Refrigerant Testing Results**

<b>Refrigerant</b>	<b>Tested COP Range (Cooling Mode)</b>	<b>Tested COP Range (Heating Mode)</b>
Propane	2.8 – 4.0	3.4 – 4.2
CO <sub>2</sub>	2.1 – 3.7	2.7 – 4.2
Ammonia	2.1 – 3.1	NA

Source: Electric Power Research Institute

This outcome is encouraging for future tests of natural refrigerants in systems that are engineered and optimized for HVAC application where even higher coefficients of performance may be expected. These results suggest that using the natural low global warming potential refrigerants propane, CO<sub>2</sub>, and ammonia does not necessarily mean a significant compromise in performance and system energy efficiency.

EPRI intends to conduct follow-up research and field demonstrations with its utility clients to build upon and advance the work pioneered through this project.

## CHAPTER 8:

# Benefits to California Ratepayers

---

This research offers direct benefits to California ratepayers because it validated the energy savings and peak demand reduction performance of a novel HVAC configuration — a hybrid combining VRF and IEC — that has the potential to reduce energy consumption in small- and medium-sized commercial buildings by 20 – 32 percent as a replacement for the ubiquitous packaged rooftop units currently servicing this market. The project demonstrated that hybrid systems that combine IEC and vapor compression can reduce peak demand on a peak summer hour by 15 percent compared to traditional rooftop unit systems. Overall system cost can be cost competitive to rooftop replacement when the two systems are right sized using optimized economizer operation.

Greater energy efficiency and peak load reduction may obviate or defer investment in power delivery infrastructure and/or procurement of additional generation, which can avoid associated rate increases for California ratepayers.

Moreover, improved occupant comfort has been shown to enhance the productivity of workers<sup>9</sup> in office or retail buildings and the satisfaction of customers patronizing retail or restaurant establishments.

Greater energy savings also reduces emissions of carbon as well as other pollutants, which improves the carbon footprint of the state and enhances air quality goals.

The project also enhanced modeling tools and developed controls to combine VRF systems with IEC as a DOAS. The research leveraged the strengths of each technology using internet-connected controls to optimize operation of the two systems and to address the technical barriers that challenge these technologies when applied separately, resulting in more efficient operation.

The public ratepayer funding applied to this project provided a unique research and demonstration opportunity to bridge disjointed silos within the building industry. Market players focus on their particular products, design engineers focus on mitigating risk, and installers and contractors are drawn to familiar technologies. These varied interests inhibit holistic building solutions, especially for small and medium commercial buildings. VRF manufacturers are advancing technology that promises significant annual energy savings compared to conventional HVAC systems, but which only provides minor peak demand savings. IEC manufacturers are advancing technology that provides outstanding energy savings at both peak and partial loading conditions but does not provide adequate cooling capacity. While the market casts these as competing technologies, this project intended to demonstrate their complementary operation and integration to their mutual advantage.

Finally, laboratory testing results of the three natural refrigerants (propane, carbon dioxide, and ammonia) demonstrated that equipment operating on low-global warming potential natural refrigerants exhibits performance and efficiency commensurate with traditional

---

<sup>9</sup> Hedge, Alan. "Linking Environmental Conditions to Productivity". Cornell University. 2004.



synthetic refrigerants. Efficiencies in cooling mode, expressed in terms of coefficients of performance, ranged from 2.1 to 4.0 across a wide variety of ambient temperatures. This suggests that converting to low-GWP refrigerants does not compromise energy efficiency and performance efficacy. This is a significant finding to encourage further tests and scaled deployments of natural refrigerant systems to help meet California's greenhouse gas reduction goals.

The research can benefit numerous other stakeholders who are most likely California ratepayers. Energy policy makers and regulators in California can better understand the potential role of this hybrid system in achieving climate goal objectives. Utilities can inform similar demonstrations, scaled field deployments, and customer incentive programs to help attain prescribed energy efficiency goals. And the results can also bolster the confidence of HVAC contractors to offer these solutions to customers.

## LIST OF ACRONYMS

Term/Acronym	Definition
AHRI	Air Conditioning, Heating, and Refrigeration Institute
ATPL	Advanced Technology Performance Lab (at PG&E's San Ramon Technology Center)
BACnet	BACnet is a communication protocol for Building Automation and Control (BAC) networks
BTU	British Thermal Unit
CEC	California Energy Commission
CO <sub>2</sub>	Carbon dioxide
DOAS	Dedicated outside air system
EES	Engineering equation solution (programming method)
$\epsilon$ -NTU	Effectiveness – Number of Transfer Units. An equation that defines the heat transfer rate between fluids 1 and 2 in terms of an effectiveness parameter $\epsilon$
GW	Gigawatts
GWh	Gigawatt hours
GWP	Global warming potential (as applied to refrigerants)
HP	Horsepower
HVAC	Heating, ventilation and air conditioning
IDU	Indoor unit
IEC	Indirect Evaporative Cooling
MBH	Thousand British thermal units per hour
NH <sub>3</sub>	Ammonia
ODU	Outdoor Unit
R290	Propane refrigerant
R717	Ammonia (NH <sub>3</sub> ) refrigerant
R744	Carbon Dioxide (CO <sub>2</sub> ) refrigerant
RTU	Rooftop Unit
USDOE	United States Department of Energy
USEPA	United States Environmental Protection Agency
VRF	Variable Refrigerant Flow